ENGINEERING FLAVONOIDS INTO THE LIGNINS OF POPLAR

by

Elizabeth Louise Mahon

B.Sc., The University of Alberta, 2014
M.Sc., The University of Alberta, 2016

A DISSERTATION SUBMITTED IN PARTIAL FULFILLMENT OF
THE REQUIREMENTS FOR THE DEGREE OF

DOCTOR OF PHILOSOPHY

in

THE FACULTY OF GRADUATE AND POSTDOCTORAL STUDIES

(Botany)

THE UNIVERSITY OF BRITISH COLUMBIA

(Vancouver)

April 2022

The following individuals certify that they have read, and recommend to the Faculty of Graduate and Postdoctoral Studies for acceptance, the dissertation entitled:

Engineering Flavonoids into the Lignins of Poplar

submitted by Elizabeth Mahon in partial fulfillment of the requirements for

the degree of Doctor of Philosophy

in Botany

Examining Committee:

Dr. Shawn Mansfield, Wood Science, UBC
Supervisor

Dr. Lacey Samuels, Botany, UBC
Supervisory Committee Member

Dr. Harry Brumer, Michael Smith Laboratories, UBC
Supervisory Committee Member

Dr. Rob Guy, Forest and Conservation Sciences, UBC
University Examiner

Dr. Richard Hamelin, Forest and Conservation Sciences, UBC
University Examiner

Additional Supervisory Committee Members:

Dr. Simone Castellarin, Land and Food Systems, UBC
Supervisory Committee Member

Abstract

Woody feedstocks, such as poplar, willow, and eucalyptus, represent abundant and fast-growing sources of lignocellulosic biomass for use in the production of pulp and paper, biofuels, and other bio-based materials. Lignin, a polyphenolic polymer, is the second most abundant chemical constituent of plant secondary cell walls and is typically composed of three canonical monolignols: *p*-coumaryl, coniferyl, and sinapyl alcohols. Recent efforts to genetically engineer the monolignol biosynthetic pathway have led to significant changes in the content and composition of lignin, highlighting the remarkable metabolic plasticity of this major biosynthetic pathway. Moreover, a wide array of non-traditional monolignols has been found to naturally incorporate into lignins of different plant species, such as the flavonoid tricin found in the lignins of grasses. To investigate the possibility of introducing flavonoids into the lignins of poplar as novel, value-added lignin monomers, I genetically engineered poplar to accumulate flavonoids in lignifying xylem tissue and analyzed the resulting wood chemistry.

Chalcone synthase catalyzes the first committed reaction in the production of flavonoid compounds to produce naringenin chalcone which is then isomerized to naringenin. Using a lignin-specific promoter, I have genetically engineered hybrid poplar (*Populus alba* x *grandidentata*) to express a chalcone synthase gene (*MdCHS3*) derived from apple (*Malus* x *domestica*). *MdCHS3*-poplar accumulated naringenin in xylem methanolic extracts and NMR analysis revealed naringenin in the extract-free, cellulase-treated xylem tissue (enzyme lignin). *MdCHS3*-poplar displayed lower total lignin, an increase in cell wall carbohydrate content, and performed significantly better during saccharification assays compared to wild-type.

Building on these promising results, I characterized two flavonoid-modifying enzymes derived from *Brachypodium distachyon in vitro*: chrysoeriol 5'-hydroxylase (BdCYP75B4) and flavone synthase II (BdCYP93G1), both key enzymes in the production of tricin and *O*-linked tricin glycosides. I also confirmed that PaxgOMT25, an important *O*-methyltransferase in monolignol biosynthesis, can participate in tricin biosynthesis. Co-expression of *BdCYP75B4* and *BdCYP93G1* in *MdCHS3*-poplar trees resulted in stunted growth and limited plant viability, however analysis of a recoverable low-expressing line revealed accumulation of tricin in xylem

methanolic extracts not observable in controls, demonstrating that the successful production of tricin, a high value flavonoid, in poplar xylem is feasible.

Lay Summary

Xylem tissue is the vascular tissue of plants that transports water from roots to leaves. Unlike animal cells, plant cells are surrounded by cell walls which determine cell shape and provide structure to the plant. In addition to primary walls, the cells of xylem tissue are reinforced by a secondary cell wall imbued with a phenolic polymer called lignin. In all plants, but especially in trees, lignin lends the xylem tissue both the hydrophobicity and the strength required to transport water over long distances. In this thesis, I use genetic engineering to produce poplar trees that incorporate valuable phenolic compounds called flavonoids into poplar lignins. When flavonoids are produced in lignifying tissue, they are incorporated into lignin polymers making the lignin chains shorter and easier to deconstruct chemically as well as adding value to lignin waste streams when poplar are being processed to make paper or biofuels.

Preface

Portions of chapter 1 have been previously published as part of two separate review articles which I co-authored: Mahon EL, Mansfield SD (2019) Tailor-made trees: engineering lignin for ease of processing and tomorrow's bioeconomy. *Current Opinion in Biotechnology* and Chang S, Mahon EL, MacKay HA, Rottmann WH, Strauss SH, Pijut PM, Powell WA, Coffey V, Lu H, Mansfield SD, Jones TJ (2018). Genetic engineering of trees: progress and new horizons. *In Vitro Cellular & Developmental Biology-Plant*. The text from *"Tailor-made trees: engineering lignin for ease of processing and tomorrow's bioeconomy"* included in this thesis was written by Elizabeth Mahon with assistance from Dr. Shawn Mansfield. The text specifically pertaining to hemicellulose pectin taken from "*Genetic engineering of trees: progress and new horizons*" was written by Elizabeth Mahon with editing and assistance from all authors in particular Dr. Shawn Mansfield, Dr. Shujun Chang, Dr. Todd Jones.

Chapter 3 consists of text taken directly from Mahon EL, de Vries L, Jang SK, Middar S, Kim H, Unda F, Ralph J, Mansfield SD (2021). Exogenous chalcone synthase expression in developing poplar xylem incorporates naringenin into lignins. *Plant Physiology,* https://doi.org/10.1093/plphys/kiab499*.* Elizabeth Mahon conceived of the project, formulated the research plan, and wrote the article with the assistance and guidance of Dr. Shawn Mansfield. Dr. Lisanne De Vries conducted the saccharification assays. Dr. Soo-Kyeong Jang conducted the holocellulose and alpha cellulose analyses. Sandeep Middar aided Elizabeth Mahon in the isolation of the *MdCHS3* gene and performed gene expression analyses. Dr. Hoon Kim, with the assistance of Dr. John Ralph, provided the NMR analyses. Dr. Faride Unda provided assistance and technical guidance to Elizabeth Mahon. All authors participated in the editing and completion of the manuscript.

The research questions and research plan in chapter 4 was formulated by Elizabeth Mahon with assistance from Dr. Shawn Mansfield. The experiments were conducted by Elizabeth Mahon with technical support and guidance of Dr. Faride Unda, and Dr. Eliana Gonzales-Vigil. Undergraduate students Sandeep Middar, Isabelle Prince and Zachary Melo, under the supervision of Elizabeth Mahon, assisted in the isolation and characterization of

flavonoid hydroxylase genes as well as transformation and genotyping of poplar transformants. The BY4741:*PcCPR1* strain of *S. cerevisiae* used to characterized *BdCYP93G1* and *BdCYP75B4* was provided by Dr. Jörg Bohlmann. The *Brachypodium distachyon* used to isolate *BdCYP93G1* and *BdCYP75B4* was provided by Dr. Richard Sibout.

Table of Contents

List of Tables

List of Figures

List of Symbols

^{13}C	Carbon-13
cm	Centimeters
°C	Degrees Celsius
g	Grams
h	Hours
^{1}H	Hydrogen-1
kDA	Kilodaltons
m	Metres
µl	Microlitres
µM	Micromolar
mAU	Milli-absorbance units
mg	Milligrams
ml	Millilitres
min	Minutes
M	Molar
nm	Nanometres
nM	Nanomolar
mM	Nillimolar
%	Percentage
pmol	Picomoles
pH	Potential hydrogen
g	Relative centrifuge force
rpm	Rotations per minute
v/v	Volume to volume

List of Abbreviations

2-ODD	Fe2+/2-oxoglutarate-dependent dioxygenase
4CL	4-coumarate:coenzyme A ligase
4CL	4-coumarate CoA ligase
A3'H/C5'H	Apigenin 3'/chrysoeriol 5' hydroxylase
ABC	ATP binding cassette transporter
ACP	*Arabidopsis* cellulose synthase A7 promoter
AGP	Arabinogalactan-rich proteins
ARF	Auxin response factor
AtC4Hp	*Arabidopsis* cinnamate-4-hydroxylase promoter
AtCesA7p	*Arabidopsis* secondary cell wall cellulose synthase 7 promoter
C3'H	*p*-coumaroyl-shikimate/quinate-3'-hydroxylase
C4H	Cinnamate-4-hydroxylase
CA	Coniferyl alchohol
CAldOMT	Caffeoyl-CoA O-methyltransferase
CCoAOMT	Caffeoyl-CoA OMTs
CGT	*C*-glycosyl transferases
CHI	Chalcone isomerase
CHS	Chalcone synthase
COMT/CAldOMT	Caffeic acid/5-hydroxyconiferaldehyde O-methyltransferase
CSC	Cellulose synthase complex
Cu-AHP	Copper-catalysed alkaline hydrogen peroxide
CYP450	Cytochrome P450
DP	Degree of polymerization
F3'5'H	Flavonoid 3'5' hydroxylase
F3'H	Flavonoid 3' hydroxylase
F5H	Ferulate/coniferaldehyde-5-hydroxylase
FC	Fold change
FCC	Fusiform cambial cell
FMT	Ferulate monolignol transferase
FNS	Flavone synthase
GRP	Glycine-rich proteins
HCHL	Hydroxycinnamoyl-CoA hydratase-lyase
HCT	*p*-hydroxycinnamoyl-CoA shikimate/quinate *p*-hydroxycinnamoyl
HG	Homogalacturonan
HRGP	Hydroxyproline-rich glycoprotein
HSQC	^{1}H–^{13}C heteronuclear single-quantum coherence

IAA	Indole-3-acetic acid
MATE	Multidrug and toxic compound extrusion transporter
NMR	Nuclear magnetic resonance
OMT	*O*-methyl transferase
PAL	Phenylalanine ammonia-lyase
*p*CA	*p*-Coumarate conjugate
PcCPR	Lodgepole pine cytochrome P450 reductase
PCW	Primary cell wall
PRP	Proline-rich proteins
qRT-PCR	Quantitative real-time PCR
RCC	Ray cambial cells
RGI	Rhamnogalacturonan I
SCW	Secondary cell wall
SRS	Substrate recognition sequence

Acknowledgements

Firstly, I want to thank my supervisor, Dr. Shawn Mansfield, for providing me with the opportunity to carry out this research in his lab. Shawn, thank you for your unwavering support throughout my Ph.D. and your faith in me from the very beginning. You encouraged me to take risks and gave me the freedom to make my own mistakes. The independence and confidence I gained as a researcher, as a result, has been invaluable and the last five years have been the most challenging and rewarding of my life. I want to thank the Canadian Society of Plant biologists, and the Ngan Page Family Fund for their financial support during my degree. Thank you to the members of my committee, Dr. Lacey Samuel, Dr. Harry Brumer, and Dr. Simone Castellarin, for your insights and suggestions throughout my thesis research. Thank you to Dr. Faride Unda for her mentorship and guidance during my degree. Faride, you have taught me everything I know about wood chemistry and what it means to be a scientist. None of this research would have been possible without you.

Thank you to past and current lab members for their input and encouragement throughout my degree. Working every day with like-minded, curious, and intense people has been one of the great joys of my time in academia. I would also like to thank my parents, who encouraged my curiosity and provided me with the opportunity to pursue higher education. Because of them, I have had the incredible privilege to spend the last eleven years as a student of the natural world. Finally, thank you to my partner Prateek for his unwavering love and support throughout this degree. Prateek, you have shown me that I can stand up for myself when I need to, and you have always given me thoughtful, honest advice whenever I ask. I truly could not have done any of this without you in my corner.

Dedication

For my father, who came back to life. For my mother, who brought him home.

Look, the trees
are turning
their own bodies
into pillars

of light,
- *Mary Oliver*

Chapter 1: Introduction

There is a growing global need to reduce societal reliance on fossil fuels and petroleum-based plastics. One emerging alternative to traditional liquid fuels and petroleum-based polymers is biofuels/bioproducts derived from lignocellulosic biomass, the fibrous or woody components of plants. Lignocellulosic biomass is an abundant and renewable source of cellulosic fibres, fermentable sugars, and valuable phenolic compounds, all of which serve as precursors to a suite of newly emerging applications in the production of specialty biofuels, bio-based materials, and pharmaceuticals. However, plant cell walls, which form the bulk of lignocellulosic biomass, are highly recalcitrant to processing for industrial purposes, and narrow profit margins continue to limit the economic feasibility of processing lignocellulosics at the industrial scale. These limitations have motivated research efforts to modify cell walls traits of lignocellulosic feedstocks to improve processing efficiency and/or add additional value to their biomass.

1.1 Plant Cell Walls

Plant cells are surrounded by chemically and structurally complex cell walls that regulate cell volume, determine cell shape, and protect the protoplast from biochemical and/or mechanical stressors (Albersheim et al., 2010; Keegstra, 2010). Moreover, by providing the mechanical strength to withstand high levels of turgor pressure, enabling cell to cell adhesion, and supporting transpirational water flow to above-ground plant tissue, plant cell walls have played a critical role in facilitating plant colonization of land. In addition, plant cell walls have evolved to serve many specialized functions, such as protection against pests and pathogens and prevention of water loss through deposition of the hydrophobic cuticle layer, which develops on the outer side of epidermal cells (Taiz and Zeiger, 2010). Plant cell walls have long been an area of interest to researchers as they provide the raw material for many important products in human society including, textiles, paper, and lumber, and more recently, biofuel and bioproducts.

Plant cell walls are classified into primary and secondary cell walls based on the timing of their deposition during cellular development and differences in their chemical composition. Primary cell walls (PCW) are deposited to the outside of the plasma membrane in all cell types during cell division and initial stages of cell expansion. PCWs are composed of cellulose microfibrils embedded in a hydrated matrix of hemicellulosic and pectic polysaccharides (Albersheim et al., 2010). Secondary cell walls (SCW) are deposited between the plasma membrane and the PCW once a cell has finished the initial phases of expansion. The composition of SCW is specialized to cell type. The thickened SCWs of xylem vessels and fibres, which form the bulk of woody biomass in feedstocks such as poplar, contain cellulose microfibrils, SCW-specific hemicellulosic sugars, and are distinct from PCW's as they contain very little pectin and are thickened and imbued with lignin, a complex polyphenolic polymer (Albersheim et al., 2010).

1.1.1 Cell wall polysaccharides

Cell wall polysaccharides are key components in plant cell walls and exhibit distinct compositional differences between PCWs and SCWs. Pectins are a major component of PCWs, comprising up to 35% in eudicots, where they form a highly hydrated matrix surrounding cellulose microfibrils (Mohnen, 2008), but are largely absent in SCWs. Pectic polysaccharides encompass a group of heterogeneous polysaccharides rich in galacturonic acid and, in eudicots, are composed mainly of homogalacturonan (HG) and rhamnogalacturonan I (RGI), which form into a pectic-matrix surrounding the cellulosic-glycan network (Willats et al., 2001). Modifications to these pectic sugars, in particular to the degree of methylesterification of HG, play important roles in regulating morphogenesis by accommodating and regulating rapid expansion during early cellular development (Chebli and Geitmann, 2017).

Cellulose is a linear polysaccharide of (1-4) β-linked D-glucan chains that are bound together in the cell wall to form highly ordered semi-crystalline microfibril bundles that function as a load-bearing scaffolding around which other cell wall polymers assemble (Mellerowicz et al., 2001). SCWs are enriched in cellulose, comprising up to 50%, compared to only 20-30% in PCWs (McNeil et al., 1984; Meents et al., 2018). In addition, the cellulose of

SCWs exhibits a higher crystallinity and degree of polymerization compared to the cellulose of PCWs (McNeil et al., 1984). Cellulose is synthesized by complexes of cellulose synthases (CSC) moving through the plasma membrane (McFarlane et al., 2014). Imaging of fluorescently tagged CSCs shows that, in PCWs, these complexes are evenly spaced and move in linear bidirectional trajectories along the plasma membrane (Paredez et al., 2006), while in SCW, the CSCs appear to cluster together moving in a single coordinated trajectory at a higher velocity leading to larger aggregations of highly ordered and longer cellulose microfibrils compared to those of the PCW (Watanabe et al., 2015; Y. et al., 2015; Meents et al., 2018).

Hemicelluloses are a heterogeneous group of branched polysaccharides, typically characterized by a 1-4 β-linked backbone, which are thought to cross-link cellulose microfibrils contributing to the structural integrity of the wall (Scheller and Ulvskov, 2010). Hemicelluloses of eudicot PCW's consist predominantly of xyloglucan (Pauly and Keegstra, 2016), whereas the hemicellulosic fraction of the xylem SCWs in eudicots consists of xylan chains partially substituted by glucuronic acid and 4-*O*-methyl-glucuronic acid (GlcA and MeGlcA, respectively) groups (Timell, 1967). Eudicot SCWs also contain smaller quantities of glucomannan. Both xylan and glucomannan hemicelluloses can be decorated to varying degrees with acetyl groups which influence their interaction with other cell wall polymers (Terrett and Dupree, 2019).

1.1.2 Cell wall proteins

In addition to polysaccharides, cell wall proteins comprise a small fraction of both PCW and, to a lesser extent, SCWs of woody tissue. These can include glycine-rich proteins (GRPs), proline-rich proteins (PRPs), arabinogalactan-rich proteins (AGPs), and hydroxyproline-rich glycoproteins (HRGPs), as well as cell wall modifying enzymes such as expansins, endoglucanases, pectin methylesterases, laccases, and peroxidases (Showalter, 1993; Albersheim et al., 2010).

1.1.3 Lignin

While there are clear compositional differences in the polysaccharide and protein content of PCWs and SCWs of woody tissue, a key distinguishing feature of SWCs is the presence of lignin. Lignin is a polyphenolic polymer found abundantly in the SCWs of water-

conducting xylem tissue of plants, where it provides the compressive strength to transport water over long distances (Weng and Chapple, 2010). Many low lignin transgenic poplar trees exhibit collapsed xylem phenotype, reduced hydraulic conductivity, and compromised vascular integrity, highlighting the importance of lignin's role in facilitating water transport (Coleman et al., 2008b). In addition, lignin plays a vital role in supporting vertical growth and acting as a barrier against pests and pathogens. Poplar trees modified to contain severely reduced lignin exhibited reduced growth rates and increased susceptibility to pests and pathogens (Leple et al., 2007; Coleman et al., 2008a; Van Acker et al., 2014).

1.1.3.1 Structure and biosynthesis

Deposition of lignin is a defining feature of all tracheophytes. However, the products of general phenylpropanoid metabolism such as flavonoids and soluble lignans are found in bryophytes, suggesting that the metabolic scaffold responsible for monolignols evolved prior to the production of lignin and emergence of tracheophytes (Weng and Chapple, 2010). Lignin polymers are typically composed of three main hydroxycinnamyl alcohols, or monolignols: coniferyl, sinapyl, and *p*-coumaryl alcohol, which make up the G-unit, S-units, and H-units of lignin, respectively (Vanholme et al., 2010). The relative abundance of G, S, and H lignin units found in the SCW xylem elements varies between plant species, and the lignins found in poplar are composed mainly of G and S units (Stewart et al., 2009; Vanholme et al., 2010). These monolignol building blocks are typically derived from the amino acid phenylalanine, which is produced in the plastid via the shikimate pathway and, ostensibly, shuttled into the cytosol where it is deaminated by phenylalanine ammonia-lyase (PAL) to become cinnamate, thereby entering the general phenylpropanoid metabolism (Boerjan et al., 2003; Figure 1.1). Cinnamate undergoes a series of aromatic ring hydroxylations, followed by *O*-methylations, and activations to a CoA thioester followed by subsequent reductions to eventually become either G, S, or H monolignols (Boerjan et al., 2003; Figure 1.1).

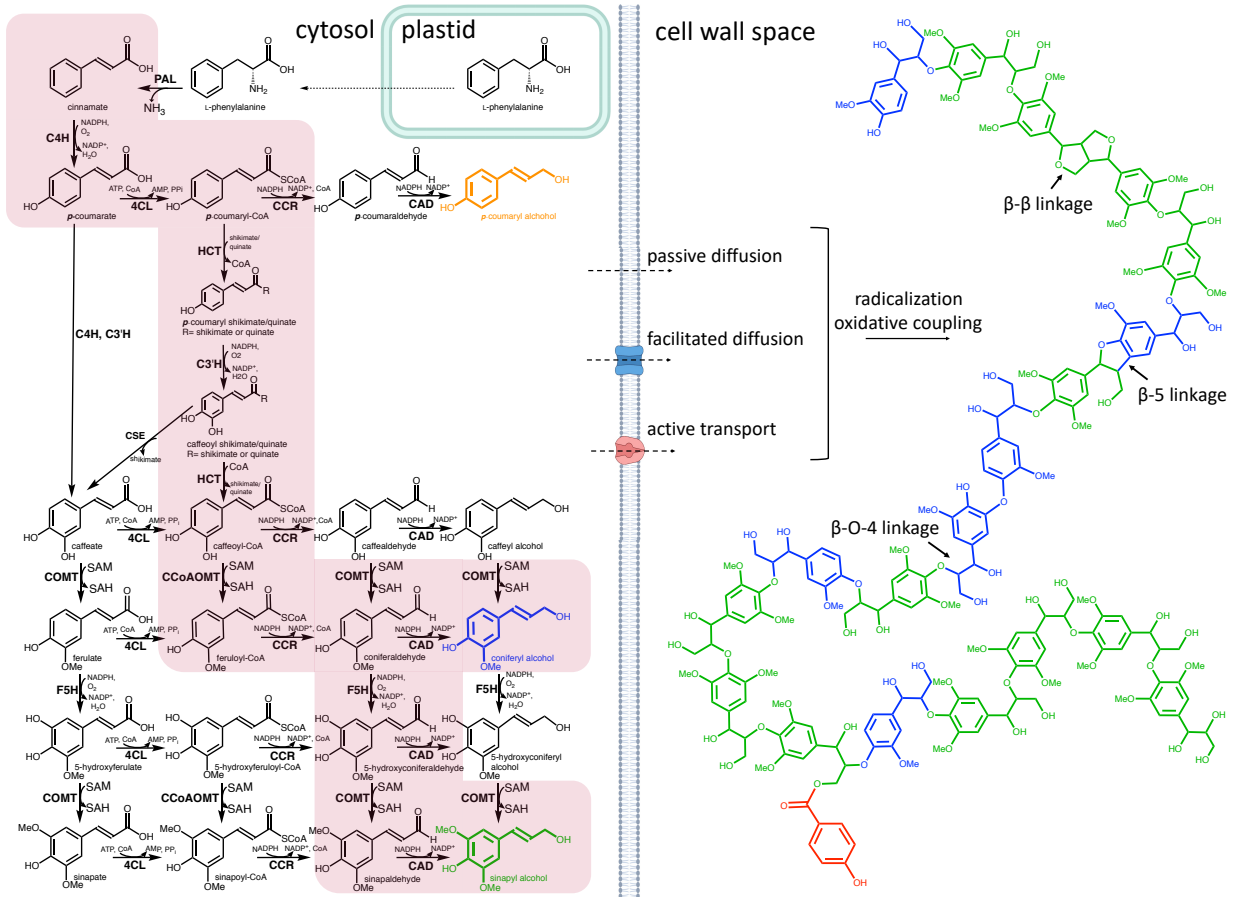

Figure 1.1: Biosynthesis, transport and assembly of canonical monolignols into poplar lignins.

Phenylalanine is produced in the plastid via the shikimate pathway and shuttled into the cytosol, where it is deaminated to cinnamate by phenylalanine ammonia-lyase (PAL), thereby entering the general phenylpropanoid pathway to produce monolignols: *p*-coumaryl, coniferyl , and sinapyl alcohol forming the H, G, and S units of lignin, respectively. Main route of carbon flux through the phenylpropanoid pathway in poplar highlighted in red. Monolignols are believed to be transported into the cell wall space through either passive diffusion, active transport and/or facilitated diffusion. *Abbreviations*: cinnamate-4-hydroxylase (C4H), 4-coumarate CoA ligase (4CL), *p*-hydroxycinnamoyl-CoA:shikimate/quinate *p*-hydroxycinnamoyltransferase (HCT), *p*-coumaroyl-shikimate/quinate-3'-hydroxylase (C3'H), caffeoyl shikimate esterase (CSE), caffeoyl-CoA *O*-methyltransferase (CCoAOMT), ferulate/coniferaldehyde-5-hydroxylase (F5H), caffeic acid/5-hydroxyconiferaldehyde *O*-methyltransferase (COMT), cinnamoyl-CoA reductase (CCR), cinnamyl alcohol dehydrogenase (CAD), inorganic phosphate (P_i), S-adenosylmethionine (SAM), and S-adenosylhomocysteine (SAH).

Each step of the monolignol biosynthetic pathway has been extensively studied through genetic perturbation and *in vitro* characterization of genes isolated from various plant species. Disruption of 4CL, C4H and HCT has typically resulted in plants with much lower lignin demonstrating the central role these early enzymes play in funnelling carbon into the phenylpropanoid pathway (Hoffmann et al., 2004; Schilmiller et al., 2009; Voelker et al., 2010; Vanholme et al., 2019). Suppression of C3H in poplar and *Arabidopsis* produced plants with lower total lignin as well as increase in the incorporation of H units, highlighting its role in the production of S and G lignin units (Franke et al., 2002; Coleman et al., 2008a). Suppression of CAD resulted in plants with lower lignins and incorporation of the non-canonical monomer, coniferaldehyde, into lignins confirming CAD's role in the dehydrogenation of hydroxycinnamaldehydes into monolignols (Lapierre et al., 2004). Suppression of CCR resulted in reduced total lignin along with buildup and incorporation of ferulic acid into lignins (Leple et al., 2007; Wadenback et al., 2008; Ruel et al., 2009). Downregulation of F5H produced plants with greatly reduced S:G ratio and, conversely, plants overexpressing F5H resulted in greatly increased S:G ratio underscoring the key role that F5H plays in the production of sinapyl alcohol (Franke et al., 2000; Franke et al., 2002; Stewart et al., 2009). Poplar and willow lignins are further distinguished by the extensive incorporation of ester-linked pHBA pendant groups, which is the result of pHBA monolignol conjugates being incorporated into lignins (Smith, 1955). While the exact metabolic steps responsible for the production of pHBA have yet to be elucidated, the monolignol transferase responsible for monolignol conjugate production has recently been identified in poplar (de Vries et al., 2021).

It was initially believed that methylation/hydroxylation steps performed by C4H, COMT, CoACOMT occur at the level of cinnamic acids prior to the sequential reduction and conversion to monolignols through action of 4CL, CAD and CCR. However, *in vitro* characterization of the core enzymes along with radiolabelled substrate feeding assays have elucidated a preferred pathway in which p-coumaryl CoA undergoes a hydroxylation/methylation through the combined action of HCT, C3'H and CCoAOMT followed by conversion to coniferyl alcohol (Boerjan et al., 2003). In angiosperms, such as poplar, coniferyl alcohol is then hydroxylated/methylated by F5H and COMT producing sinapyl alcohol (Figure 1.1). A

comprehensive predictive kinetic metabolic-flux (PKMF) model generated for the monolignol pathway poplar has further elucidated this path as the preferred route of carbon flux during monolignol biosynthesis (Wang et al., 2014). This PKMF model also helps to explain the increase in S:G ratio typically observed in plants with downregulation of PAL, C4H, HCT and C3H as coniferyl alcohol is thought to represent excess product not consumed by F5H (Gu et al., 2019).

The precise mechanism(s) responsible for the transport of monolignols from the cytosol across the plasma membrane to the apoplastic space remains unresolved (Perkins et al., 2019). One model proposes that monolignols diffuse passively across the cell membrane as a result of the concentration gradient generated between the cytosol, where monolignols are synthesized, and the cell wall space where they are rapidly incorporated into the lignin polymer, creating a significant sink (Meents et al., 2018). *Arabidopsis* mutants overexpressing *MYB58* and *MYB63*, both regulators of the phenylpropanoid pathway, accumulated substantially larger quantities of soluble phenolic compounds and exhibited a dwarf phenotype (Perkins et al., 2020). However, when *Arabidopsis* lines overexpressing the laccase, *LAC17,* were crossed with *MYB63-OX* and *MYB*58-*OX* lines, soluble phenolic glycosides returned to wild-type levels, and growth was rescued, suggesting the addition of laccases present in the cell wall space may increase consumption of excess phenolics, thereby increasing the sink strength across the cell membrane and providing further support to the mechanism of passive monolignol transport across the membrane (Perkins et al., 2020; Figure 1.1). In fact, molecular simulations estimating membrane permeability of common lignin precursors have indicated that passive diffusion alone is sufficient to support lignification (Vermaas et al., 2019).

Apart from passive diffusion, monolignols may also be exported via plasma membrane-localized transporters such as ATP binding cassette (ABC) transporters (Figure 1.1). However, candidate transporters in angiosperms that are capable of efficiently transporting sinapyl and coniferyl alcohol remain yet to be fully characterized (Meents et al., 2018; Perkins et al., 2019). Notably, coniferin, the β-glucosyl derivative of coniferyl alcohol, is thought to serve as a precursor in gymnosperm lignification (Terashima et al., 2016). It has been suggested that coniferin accumulates in the vacuoles of lignifying tracheids and is released just in advance or

coinciding with cell death (Tsuyama and Takabe, 2014; Aoki et al., 2016). Following β-glucosidase cleavage of the glucose moiety, coniferyl alcohol is released from coniferin to participate in the final stages of lignification (Meents et al., 2018). Additionally, monolignols or lignin monomers may enter the cell wall space following cell death and disintegration of the cell membrane (Perkins et al., 2019).

Once transported across the membrane and into the cell wall space, monolignols are oxidized by either peroxidase or laccase enzymes to become radicalized (Vanholme et al., 2010; Chou et al., 2018; Yi Chou et al., 2018). Lignin polymerization is initiated when two radical phenolic monomers couple to become a dimer, after which the dimer undergoes successive rounds of radical oxidation followed by combinatorial coupling to other monolignol radicals in a process called endwise coupling (Ralph et al., 2004; Vanholme et al., 2010). During polymerization, monolignol radicals favour coupling at the β position, which results in a lignin polymer composed of almost exclusively β- β, β-5, β-*O*-4 linkages (Figure 1.1; Ralph et al., 2004; Stewart et al., 2009). This non-enzymatically controlled mechanism of polymerization leads to the production of a polymer lacking ordered linkages and repeating units, making it particularly resistant to degradation or depolymerization processes, and distinct from most other biopolymers (Ralph et al., 2004). In addition to polymerization in the cell wall space, high levels of oxidative stress in the cytosol of lignifying cells is thought to cause monolignol radical formation within the cytosol, resulting in the accumulation of dimers and oligolignols, which may be either sequestered in the vacuole as oligolignol glycosides or exported to the cell wall space (Dima et al., 2015; Meents et al., 2018).

1.1.3.2 Metabolic plasticity of lignification

The monolignol biosynthetic pathway has been extensively studied and the component enzymes are well characterized (Figure 1.1). Targeted genetic manipulation of this pathway can lead to significant changes in the composition of lignins, highlighting the remarkable metabolic plasticity of lignin biosynthesis. For example, the ratio of H:S:G monomers that compose the lignin polymer can be altered by manipulating various genes within the monolignol biosynthetic pathway. RNAi-mediated suppression of *p-coumaroyl-CoA 3'-hydroxylase (C3'H)* in hybrid

poplar (*Populus alba x grandidentata*) resulted in reduced overall lignin content, as well as a substantial increase in the H units present in lignins compared to only trace amounts present in wild-type poplar (Coleman et al., 2008a). Overexpression of *ferulate 5-hydroxylase (F5H)* led to a substantial increase in S:G ratio, as much as 97.5 % in the case of hybrid poplar (*Populus tremula x alba*) compared to 68 % S:G found in their wild-type counterparts (Huntley et al., 2003; Stewart et al., 2009). Downregulation of *caffeic acid/5-hydroxyconiferaldehyde O-methyltransferase (COMT/CAldOMT)* in poplar resulted in a decrease in S units, and notably the integration of 5-hydroxyconiferyl alcohol, a non-canonical monomer, into lignins (Van Doorsselaere et al., 1995; Marita et al., 2001; Lu et al., 2010). Downregulation of *caffeoyl-CoA O-methyltransferase (CCoAOMT)* in poplar led to a significant increase in the S:G ratio, while in pine (*Pinus radiata*), down-regulation of *CCoAOMT* led to a significant increase in the H:G ratio, as well as novel integration of the caffeyl alcohol (Meyermans et al., 2000; Wagner et al., 2011).

There is also a wide diversity of non-traditional or non-conventical monolignols found naturally incorporated in the lignins of different plant species, such as monolignol ester conjugates including, *p*-coumarate, ferulate, acetate, and benzoate (Figure 1.2; del Río et al., 2020). Monolignol acetates, for example, are found ubiquitously incorporated into the lignins of angiosperms, constituting up to 80% of lignin in some specialized cases such as kenaf, sisal, and abaca (Lu and Ralph, 2002; del Río et al., 2004; del Río et al., 2007). Monolignol *p*-coumarates are commonly found in lignins of grasses (Lu and Ralph, 1999; del Rio et al., 2008), and monolignol *p*-hydroxybenzoates are found widely in lignins of poplar, willow, and palms (Smith, 1955; Lu et al., 2015). Monolignol ferulates have also been reported at low levels in some plants (Karlen et al., 2016). Some of these monolignol ester conjugates have also been strategically successfully engineered into lignin monomers into poplar and *Arabidopsis* as novel monomers. For example, expression of *p-coumaroyl-CoA monolignol transferase (OsPMT*) derived from rice (*Oryza sativa*) in hybrid poplar and *Arabidopsis* resulted in the novel incorporation of *p*-coumarate conjugates (pCA) into lignins (Smith et al., 2015). Similarly, ferulate monolignol conjugates were incorporated into the lignin backbone of hybrid poplar by expressing a *ferulate monolignol transferase* (*FMT*) from *Angelica sinensis* (Wilkerson et al., 2014). In both cases expression of *OsPMT*, driven by a universal (35S) promoter, and *AsFMT,*

driven by the SCW-specific (CesA8) promoter, resulted in incorporation of their respective monolignol conjugates into lignins, demonstrating that with appropriate spatial and temporal control, non-canonical monolignols can be produced in the cytosol and transported to the developing cell wall to participate in lignification.

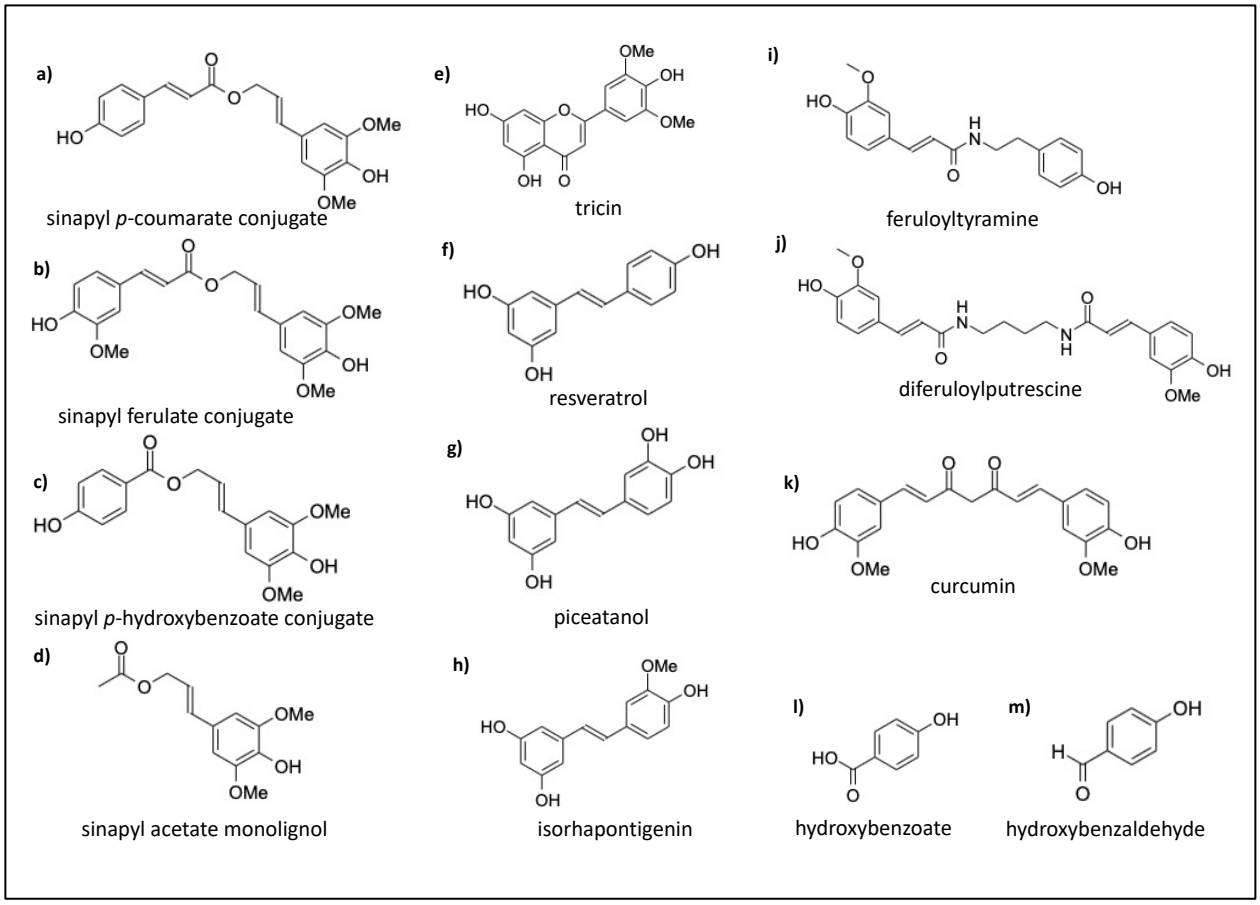

Figure 1.2: Non canonical monolignols reported to incorporate into plant lignins.

Monolignol conjugates: (a) sinapyl *p*-coumarate conjugates, (b) sinapyl ferulate conjugates, (c) sinapyl *p*-hydroxybenzoate, and (d) sinapyl acetate conjugates. Lignin monomers arising beyond the monolignol pathway: (e) tricin (f) resveratrol, (g) piceatanol, and (h) isorhapontigenin. Ferulamides: (i) feruloyltyramines and (j) diferuloulputrescine. Potential polymer initiators/terminators: (I) hydroxybenzoates, and (m) hydroxybenzaldehydes.

Phenolic compounds found beyond the monolignol biosynthetic pathway have also been found naturally incorporated into the lignins of different plant species (del Río et al.,

2020). The stilbenoid compounds resveratrol, piceatannol, and isorhapontigenin have all been identified as monomers in lignins of palm fruit endocarps (family Arecaceae; del Río et al., 2017), and their respective stilbene glycosides: piceid (resveratrol-*O*-glucoside), astringin (piceatannol-*O*-glucoside), and isorhapontin (isorhapontigenin-*O*-glucoside) have all been identified in the lignins of Norway spruce (*Picea abies*) bark (Figure 1.2; Rencoret et al. 2019). Hydroxycinnamamides, specifically ferulamides, have been shown to incorporate into plant lignins, behaving as true lignin monomers (Rencoret et al., 2019). For example, diferuloylputrescine has been identified in the lignins of corn (*Zea mays*) kernels (del Río et al., 2018), and feruloyltyramine has been identified in the lignins of tobacco (*Nicotiana tabacum*) (Figure 1.2; Ralph et al., 1998). The flavonoid tricin has been found widely incorporated into the lignins of species across the grass family and is particularly abundant in oat (*Avena sativa*), wheat (*Triticum durum*), and *Brachypodium distachyon* (Figure 1.2; Lan et al., 2016). Notably, tricin is found incorporated at the ends of lignins via β-*O*-4 ether linkages exclusively, and while biomimetic reactions demonstrate that tricin can cross couple with monolignols, no other types of cross-coupling linkages to monolignols were observed nor were tricin homodimers formed, indicating that tricin may play a role in grasses as a lignin chain initiator/terminator (Lan et al., 2015).

Finally, a suite of phenolic compounds, not yet found as naturally occurring lignin monomers, have been proposed as potential targets for introduction as novel lignin monomers in bioenergy (Lin and Eudes, 2020). Curcumin, while yet to be identified as a naturally occurring lignin monomer, has been genetically engineered into the lignins or *Arabidopsis* through co-expressing of two curcumin biosynthetic genes, *diketide CoA synthase* and *curcumin synthase 2*, derived from turmeric (*Curcuma longa*) (Figure 1.2; Oyarce et al., 2019). Disruption of flavone synthase II in rice resulted in the accumulation of naringenin, the flavanone precursor to tricin, and its novel incorporation into rice lignins (Lam et al., 2017). Ultimately, these findings highlight the metabolic plasticity of lignin biosynthesis and provide support for the hypothesis that if a chemically compatible phenolic monomer is made spatially and temporally available during lignin polymerization, it will be incorporated into the polymer.

1.2 Woody Feedstocks

1.2.1 *Populus* genus

In recent decades, poplar has emerged as a promising woody feedstock for lignocellulosic-derived biofuels and bioproducts. Poplar trees are able to grow on a wide range of marginal agricultural land, making poplar an excellent renewable and fast-growing source of lignocellulosic biomass in Canada (Yemshanov and McKenney, 2008). In addition, due to the substantial genomic and molecular resources currently available to researchers, poplar has become a model organism in the study of woody perennials (Tuskan et al., 2006; Jansson and Douglas, 2007).

Poplar trees comprise the genus of deciduous forest trees, *Populus*, found widely distributed in the northern hemisphere. These trees are short-lived and fast-growing, compared to many other forest trees, and they are often found growing in newly disturbed sites (Dickmann, 2009). The genus *Populus* is a member of the Salicaceae family and comprises approximately 30 species worldwide, 12 of which are native to North America (Dickmann, 2009). Members of the *Populus* genus are classified into six sections. White poplar (*Populus alba*) and bigtooth aspen (*Populus grandidentata*), the parent species to the P39 hybrid (*Populus alba* x grandidentata) used in this study, are both part of the *Populus* (formerly *Leuce*) section. Members of the *Populus* section characteristically grow in upland habitats, and their seeds germinate readily on ash-covered soil, allowing for rapid colonization of recently burned habitats (Dickmann, 2009).

Poplar trees are dioecious, with individual trees bearing either male or female flowers and rely on wind pollination to outcross, often reaching reproductive maturity after a prolonged juvenile phase lasting years to decades (Jansson and Douglas, 2007; Brunner, 2010). Members of the *Populus* genus are diploid, containing two sets of 19 chromosomes, and genomic analysis of willow (*Salix*) and poplar (*Populus*) revealed that both members of the *Salicaceae* family shared a common genomic duplication event prior to their evolutionary divergence (Tuskan et al., 2006; Dai et al., 2014). A useful characteristic of poplar is the ability

to undergo vegetative propagation with new shoots arising from stumps, roots, and abscised twigs. This allows poplar to be regenerated from tissue-to-plant in tissue culture, making it amenable to *Agrobacterium*-mediated genetic transformation (Dickmann, 2009). Thus, poplar is not only a promising woody feedstock but also is an excellent candidate for genetic study of wood formation in dicots.

1.2.2 Wood formation in dicots

Secondary xylem tissue forms the bulk of woody biomass in poplar. The formation and resulting physiological function of specialized cell types within secondary xylem tissue are both important considerations when altering lignin characteristics of woody tissue. Formation of secondary xylem tissue is initiated in the vascular cambium, a radially arranged ring of meristematic tissue from which secondary xylem arises to the interior and secondary phloem arises to the exterior (Mellerowicz et al., 2001; Larson, 2012). The term “cambial cells” encompasses the cambial initial cell, the phloem mother cell, and xylem mother cell. The cambial initial regulates the number of radial files as the tree grows and expands radially through anticlinal divisions, setting the pattern of meristem organization (Mellerowicz et al., 2001). Xylem and phloem tissue arise from periclinal divisions of the respective mother cell (Mellerowicz et al., 2001; Larson, 2012). Cambial initials may be further classified into fusiform cambial cells (FCC), which are axially elongated and ray cambial cells (RCC) and are isodiametric in shape. In poplar xylem, FCCs give rise to vessel elements, fibres, and axial xylem parenchyma, whereas RCCs give rise to ray parenchyma (Larson, 2012). Vessel elements and fibres both undergo programmed cell death during development and are dead at maturity. Vessel elements are characteristically larger in diameter than xylem fibres and are joined end-to-end by perforated plates forming vessels that facilitate bulk water transport throughout the plant (Mellerowicz et al., 2001; Baas et al., 2004). Xylem fibres are narrower in diameter with tapered ends and are thought to provide structural support (Baas et al., 2004). Finally, axial xylem parenchyma, which elongate along the vertical axis, and ray parenchyma, which elongate along the radial axis, remain alive at maturity and form a network of living tissue within the dead fibres and vessels, where they are reported to improve radial strength (Reiterer et al., 2002), aid in defence response and pathogen containment (Morris et al., 2016) and facilitate

lignification of neighbouring vessel elements, and fibres following cell death (Smith et al., 2013). Ray parenchyma may be further divided into contact ray cells, which contain pits and face vessel elements, and isolation ray cells, which contain fewer pits and face xylem fibres. Poplar wood is reported to contain 33% v/v vessel elements, 53-55% (v/v) fibres, 11-14% (v/v) ray parenchyma and 1% (v/v) axial parenchyma (Mellerowicz et al., 2001).

During the initial stages of xylogenesis, the xylem mother cells undergo cell expansion, with fibres and axial parenchyma undergoing some radial expansion and fibres further elongating beyond the length of their FCC (Larson, 2012). Vessel elements undergo radial and tangential expansion, and ray cells elongate radially via uniaxial elongation (Mellerowicz and Gorshkova, 2012). The degree and direction during initial enlargement of these cells is regulated by modifications to the pectin and hemicellulose component of the primary cell wall, which facilitate cell wall loosening and expansion in controlled directions (Mellerowicz et al., 2001; Chebli and Geitmann, 2017). Xylem cells begin forming secondary cell walls once radial expansion is complete, while the orientation of cellulose microfibrils in PCWs is random or longitudinal (Funada, 2008). In SCWs, cellulose microfibrils are arranged in a denser helical array which prevents further radial expansion (Funada, 2008). In fibres, three successive layers of secondary cell walls are deposited with ordered cellulose microfibrils. Lignin is first deposited in the middle lamella at cell corners once the cell has completed deposition of the cell wall polysaccharides composing the first S1 layer (Mellerowicz et al., 2001; Keegstra, 2010). Lignification progresses inward from the cell corners during formation of the S2 layer, and deposition of lignin becomes most prolific when the S3 layer is formed as it progresses towards the cell lumen until all secondary layers are lignified (Mellerowicz and Gorshkova, 2012). Once lignification is complete cells, vessel elements, and fibres undergo programmed cell death. Although lignification may continue due to the presence of living xylem parenchyma providing monolignol precursors (Smith et al., 2013; Meents et al., 2018).

1.2.3 Hormonal regulation of wood development

Auxin, derived from the shoot apical meristem, is a key hormone signal in the initiation of xylogenesis from the vascular cambium and is required for lateral growth. The exogenous

application of auxin to cambial tissue is sufficient to stimulate differentiation of intact xylem cells (Björklund et al., 2007), and repression of auxin signalling typically results in fewer periclinal divisions (Nilsson et al., 2008). Auxin accumulates in a radial pattern across wood forming tissue with the highest concentrations found in the cambium and lower concentrations diffusing outwards in a bilateral pattern as cells develop into secondary xylem tissue (Immanen et al., 2016; Brackmann et al., 2018; Xu et al., 2019). Differential regulation of auxin transport, perception and/or production is thought to play an important role in the maintenance of cambial characteristics (Sanchez et al., 2012).

Auxin also plays an important role in the formation of tension wood, which forms on the upper side of gravistimulated stems, pulling the stem upward by generating tension (Mellerowicz and Gorshkova, 2012). Tension wood is produced by an increase in the rate of cell division at the vascular cambium and is characterized by a reduced number of vessels, smaller and specialized G-fibres, which contain a cellulose-rich, low lignin, tertiary cell wall layer termed the G layer (Mellerowicz and Gorshkova, 2012). It has been proposed that tension wood in aspen is induced by the downward re-localization of the auxin transport protein PIN3 in starch-filled amyloplasts, resulting in auxin transport towards the cambium on the upper side of a tilted stem and away from the cambium on the bottom surface (Gerttula et al., 2015) Moreover, exogenous application of auxin to developing poplar xylem resulted in the formation of tension wood in upright trees (Yu et al., 2017). Flavonoids are known inhibitors of polar auxin transport (Jacobs and Rubery, 1988; Peer and Murphy, 2007). The relationship between wood development, auxin signalling, and flavonoid concentrations is significant when considering the impact of ectopic production of flavonoid compounds in developing xylem tissue. Flavonoids have been shown to inhibit auxin transport and impact architecture of shoot and root development in *Arabidopsis* (Besseau et al., 2007; Buer et al., 2013; Yin et al., 2014), as well as alfalfa (*Medicago sativa*) (Laffont et al., 2010) and tomato (Maloney et al., 2014). Notably, flavonoids scutellarin and scutellarein were found to promote primary root growth in *Arabidopsis,* as well as induce expression of auxin transport mediators, and the authors speculate that the unique presence of a 6-hydroxyl group may have an opposing effect on auxin transport when compared to other previously reported flavonoid auxin transport inhibitors

(Zhang et al., 2021). Thus, depending on the structure, ectopic production of flavonoids in the cambial meristems of poplar may inhibit transport of auxin derived from the shoot apical meristem and impact hormonal regulation of developing xylem.

1.2.4 Reducing cell wall recalcitrance of poplar

The overall chemical and structural complexity of lignocellulosic biomass hinders extraction of fermentable sugars; however, lignin specifically is thought to contribute to cell wall recalcitrance by limiting access of hydrolytic enzymes to cellulose and competitively binding cellulolytic enzymes (Mooney et al., 1998; Berlin et al., 2005). Genetically modified trees with reduced lignin content display drastically improved rates of saccharification (Leple et al., 2007; Mansfield et al., 2012a; Sykes et al., 2015), but significant reductions in total lignin are commonly associated with reduced overall biomass yield either from growth impairments or greater susceptibility to environmental conditions (Leple et al., 2007; Coleman et al., 2008a). The agronomic penalty incurred by reduced total lignin content has therefore motivated research efforts to alter composition rather than total content of lignin in woody feedstocks.

Several modifications to cell wall characteristics in poplar have improved processing efficiency. Strategically driving the monomer ratio in favour of S-subunits inherently increases the frequency of β-ether bonds, which are the most labile bonds in native lignin polymers and are therefore the primary 'target' of established delignifying pretreatments, such as kraft pulping. Moreover, forcing the balance of monomers towards a S-rich lignin content, through over expression of *F5H* in poplar resulting in higher levels of β-ether bonds, concurrently decreases the frequency of 5–5 and β–5 bonds, ultimately producing a more easily extractable lignin polymer (Figure 1.3; Huntley et al., 2003; Mansfield et al., 2012a). Incorporation of ferulate monolignol conjugates into lignins resulted in significantly improved saccharification yields after several different pretreatments, as the incorporation of these conjugates introduces chemically labile ester bonds into the polymer backbone facilitating its depolymerization under mild alkaline conditions (Wilkerson et al., 2014). The incorporation of these conjugates into poplar lignins significantly improved the efficacy of other pretreatments, including ionic liquid and copper-catalysed alkaline hydrogen peroxide (Cu-AHP) treatments

(Kim et al., 2017a; Bhalla et al., 2018). These same poplar lines also performed better than their wild-type counterparts during alkaline kraft pulping (Zhou et al., 2017).

The frequency of crosslinking and intermolecular associations between lignin and carbohydrate polymers is thought to limit accessibility to carbohydrates during enzymatic hydrolysis. Relatively little is known about the nature of lignin crosslinking to hemicelluloses in dicots (Terrett and Dupree, 2019). It has been proposed that alcohol and carboxylic acid moieties found in hemicelluloses may form covalent linkages to lignin by acting as nucleophiles, quenching the quinone intermediate formed as an intermediate during oxidative coupling of monolignols at the β position (Figure 1.3; Ralph et al., 2004; Terrett and Dupree, 2019). Recently, the removal of the methylglucuronic acid (MeGlcA) branching groups native to the xylan backbone has been shown to substantially increase the release of both xylose and glucose during enzymatic hydrolysis in *Arabidopsis* (Lyczakowski et al., 2017). This may be a consequence of altered interactions between xylan and lignin via an ester linkage to GlcA xylan moieties, which has been proposed as a mechanism of covalent insertion between these two secondary cell wall constituents (Figure 1.3; Giummarella and Lawoko, 2016).

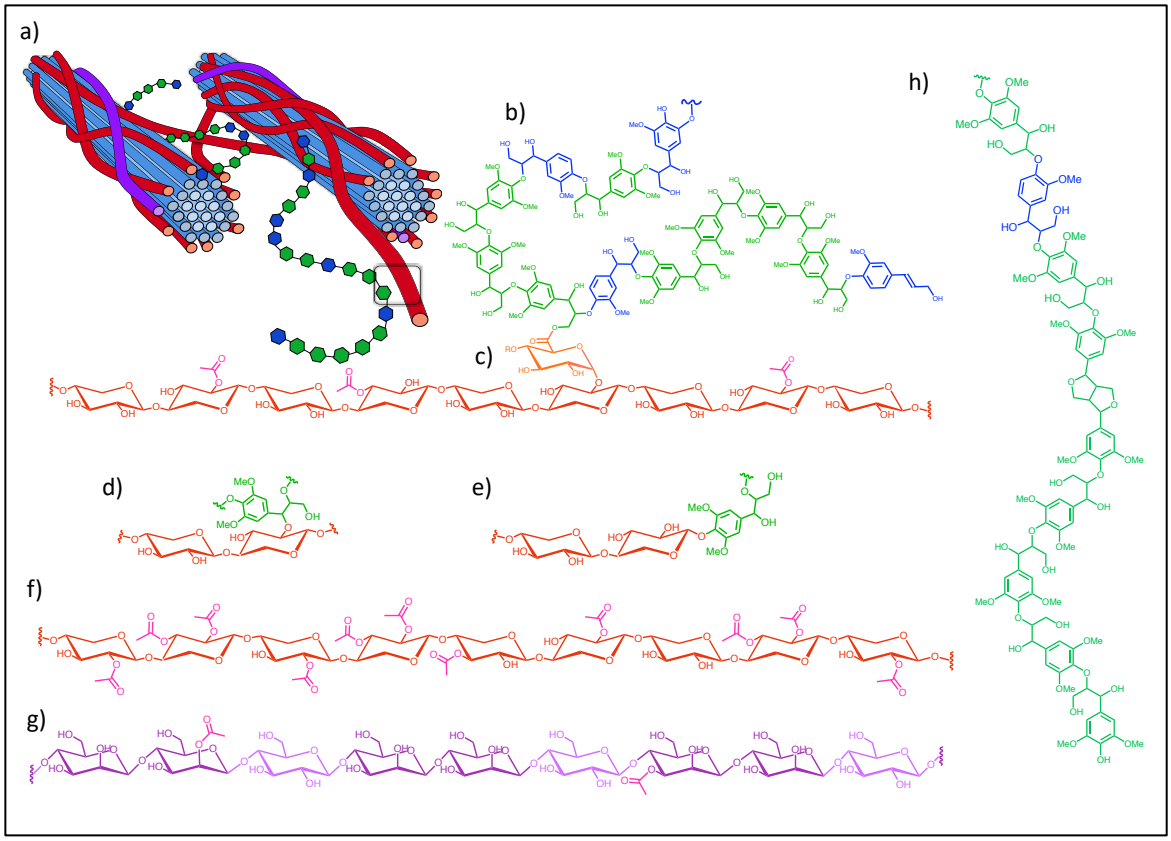

Figure 1.3: Proposed mechanisms of interaction between macromolecules in secondary cell walls of eudicots.

(a) Cellulose microfibrils are embedded in a dehydrated matrix of hemicellulosic carbohydrates (xylan and glucomannan) and lignin (G-units derived from coniferyl alcohol monomers and S-units derived from sinapyl alcohol monomers). (b) Partial lignin polymer modelled from poplar. Three possible covalent linkages proposed to occur between hemicelluloses and lignins: (c) ester linkage between lignin and a glucuronic acid branching group found decorating the xylan backbone (Lyczakowski et al., 2017), (d) benzyl ether linkages between C2 or C3 hydroxyls on xylan and lignin, and (e) phenyl glycosides between C1 of xylose and lignin (Giummarella et al., 2016). (f) Proposed model of highly acetylated xylan in which endogenous acetate groups hydrolyze to acetic acid, improving efficiency of pretreatment (Johnson et al., 2017). (g) Glucomannan, a relatively minor hemicellulosic component of cell walls of woody dicots that may also be acetylated. (h) Model of lignin enriched in syringyl moieties (Steward et al., 2009).

Finally, reducing the degree of lignin polymerization has been shown to improve the extractability of lignin during pulping and enhance the efficiency of pretreatment before enzymatic hydrolysis. For example, targeted expression of a *hydroxycinnamoyl-CoA hydratase-lyase (HCHL)* in *Arabidopsis* resulted in the accumulation of hydroxybenzaldehyde and

hydroxybenzoate derivatives adorning lignin polymer ends, consequently reducing the degree of lignin polymerization (Figure 1.2). Moreover, these plants showed clear and marked improvement in saccharification yield (Eudes et al., 2012).

Most currently employed biochemical pretreatments have been developed with the aim of separating lignin from carbohydrates in an attempt to improvine the release of fermentable sugars from cell wall carbohydrates or extracting cellulosic fibres for pulp and paper. Typically, the lignin recovered during these processes (e.g., kraft pulping, sulphite pulping, dilute acid pretreatment) is burnt to provide process energy for the upstream processes, and in some cases, the excess energy produced may be sold back to the grid as a revenue source. Current models exploring the economic feasibility of using poplar as a source of cellulosic biomass for biofuels continue to indicate narrow profit margins for Canadian growers even in ideal locations such as Western Prairie Provinces (Yemshanov and McKenney, 2008; Shooshtarian et al., 2018). Therefore, modifications to lignin that add intrinsic value to the polymers themselves offer the potential for complete biomass utilization and for the incorporation of value into 'waste streams', thereby elevating the economic feasibility of processing lignocellulosic residues. Moreover, incorporation of a high-value phenolic monomer capable of only single coupling reactions, such as the flavonoid tricin, would add additional value to lignin waste streams while simultaneously shortening polymers by acting as a chain initiator/terminator (Lan et al., 2015).

1.3 Flavonoids

Beyond the non-canonical monolignols described above, both flavonoid and stilbenoid compounds have been found naturally incorporated into lignins of grasses and the endocarp of palm fruit, respectively, demonstrating that phenolic compounds found outside the monolignol biosynthetic pathway can also be incorporated into lignins (del Rio et al., 2012; Rencoret et al., 2013; del Río et al., 2017). Of particular interest is the high-value pharmaceutical compound tricin, a flavonoid found widely incorporated as a monomer into the lignins isolated from grasses and other monocots (del Rio et al., 2012; Lan et al., 2016).

1.3.1 Role in plants

Flavonoids represent a highly diverse group of over 9000 unique phenolic compounds found across all orders of land plants, including some non-lignified bryophytes (Winkel-Shirley, 2001; Williams and Grayer, 2004; Yonekura-Sakakibara et al., 2019). Flavonoids are classified based on chemical structure and the major classes include flavanones, flavones, flavonols, isoflavones, anthocyanidins, and proanthocyanidins (condensed tannins) (Figure 1.4; Rausher, 2006). While flavonoids were previously thought to occur exclusively in land plants, they have recently been identified in distinct lineages of microalgae, suggesting that the ability of green algae to produce flavonoids was either lost in most lineages or developed independently multiple times (Goiris et al., 2014; Yonekura-Sakakibara et al., 2019).

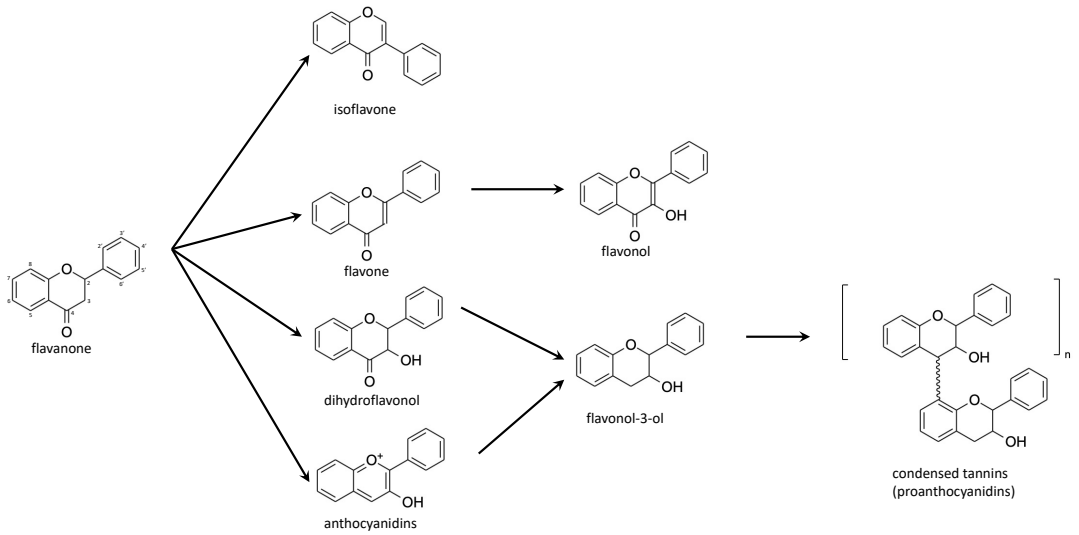

Figure 1.4: Basic chemical structures of the major classes of flavonoid compounds.

Chalcone synthase performs the first committed step in flavonoid biosynthesis producing flavanones, such as naringenin, which may be converted into isoflavones, flavones, or dihydro-flavonols and anthocyanins. Flavones may then be converted to flavonols. Dihydro-flavonols and anthocyanins may both be converted to flavon-3-ols, which may then condense to form condensed tannins (Winkel, 2006). The diverse array of flavonoids observed in nature arises from terminal modifications such as hydroxylations, methylations, and glycosylation of these chemical backbones. Carbon numbering system applied to flavonoids indicated on the flavanone compound.

In general, flavonoids are thought to play a universal role as UV protectants; however, flavonoids often play highly specialized roles in processes such as pathogen defence, microbial interactions, insect attraction and pollination, floral colouration, male fertility, auxin transport, and response to abiotic stress (Winkel-Shirley, 2001; Rausher, 2006). In poplar, flavonoids have been reported to play a variety of specific roles. For example, the flavanol quercetin and its glycoside form, rutin, are exuded from roots and are found to induce expression of the effector protein *MiSSP* in the ectomycorrhizal fungus *Laccaria bicolor*, facilitating establishment of a mutualistic relationship between plant and microbe (Plett and Martin, 2012). Anthocyanins contribute to the red colouration of poplar anthers and autumn leaves, where they are thought to act as photoprotectants, shielding senescing leaves and facilitating recovery of foliar prior to leaf abscission (Hoch et al., 2003; Alcalde-Eon et al., 2016). Proanthocyanindins, or condensed

tannins, are polymers of flavan-3-ols and are linked to herbivore resistance in poplar (Figure 1.4; Barbehenn and Constabel, 2011).

The chemical structure of specialized flavonoid groups often informs function within a plant. For example, polymethoxylated flavones such as tricin are highly lipophilic and are often exuded in their aglycone (un-conjugated) form onto the surface of leaves and buds, where they potentially serve as UV protectants, antimicrobial agents, or feeding deterrents (Berim and Gang, 2015; Li et al., 2016). Tricin is also exuded from the roots and seed hulls of rice in the form of *O*-linked glycosides where it is reported to prevent the spread of seedling rot disease and other soil borne pathogens (Kong et al., 2007; Kong et al., 2010). Tricin is found in grasses as well some of orders of eudicots, but historically only tricin precursors, apigenin and luteolin, have been previously reported in poplar (Morreel et al., 2006; Lan et al., 2016; Li et al., 2016). Interestingly trace amounts of tricin 4'-*O*-syringic acid and tricin-*O*-glucuronic acid were reported in poplar trees that have been artificially cultivated for red colouration of leaves and accumulate high levels of the anthocyanin pelargonin along with several anthocyanidin-based pigments in leaf tissue (Tian et al., 2021). The occurrence of trace quantities of tricin in cultivated poplar varieties could indicate a degree of biosynthetic flexibility at the flavone level.

1.3.2 General Biosynthesis of flavonoids in plants

Flavonoids are characterized by a C6-C3-C6 carbon structure and are derived from the amino acid phenylalanine, sharing a central biosynthetic pathway with phenylpropanoids in which phenylalanine is converted to *p*-coumaroyl-CoA through the combined action of PAL, cinnamate-4-hydroxylase (C4H), and 4-coumarate CoA ligase (4CL) (Figure 1.4 & 1.5). Next, *p*-coumaroyl-CoA enters either monolignol biosynthesis or is catalysed to naringenin chalcone by CHS. Naringenin chalcone is then isomerized to naringenin by CHI, thereby committing the carbon to flavonoid biosynthesis (Winkel, 2006; Figure 1.5). In poplar, CHS can also act on cinnamoyl-CoA and caffeoyl-CoA to produce pinocembrin chalcone and eriodictyol chalcone, respectively (Morreel et al., 2006).

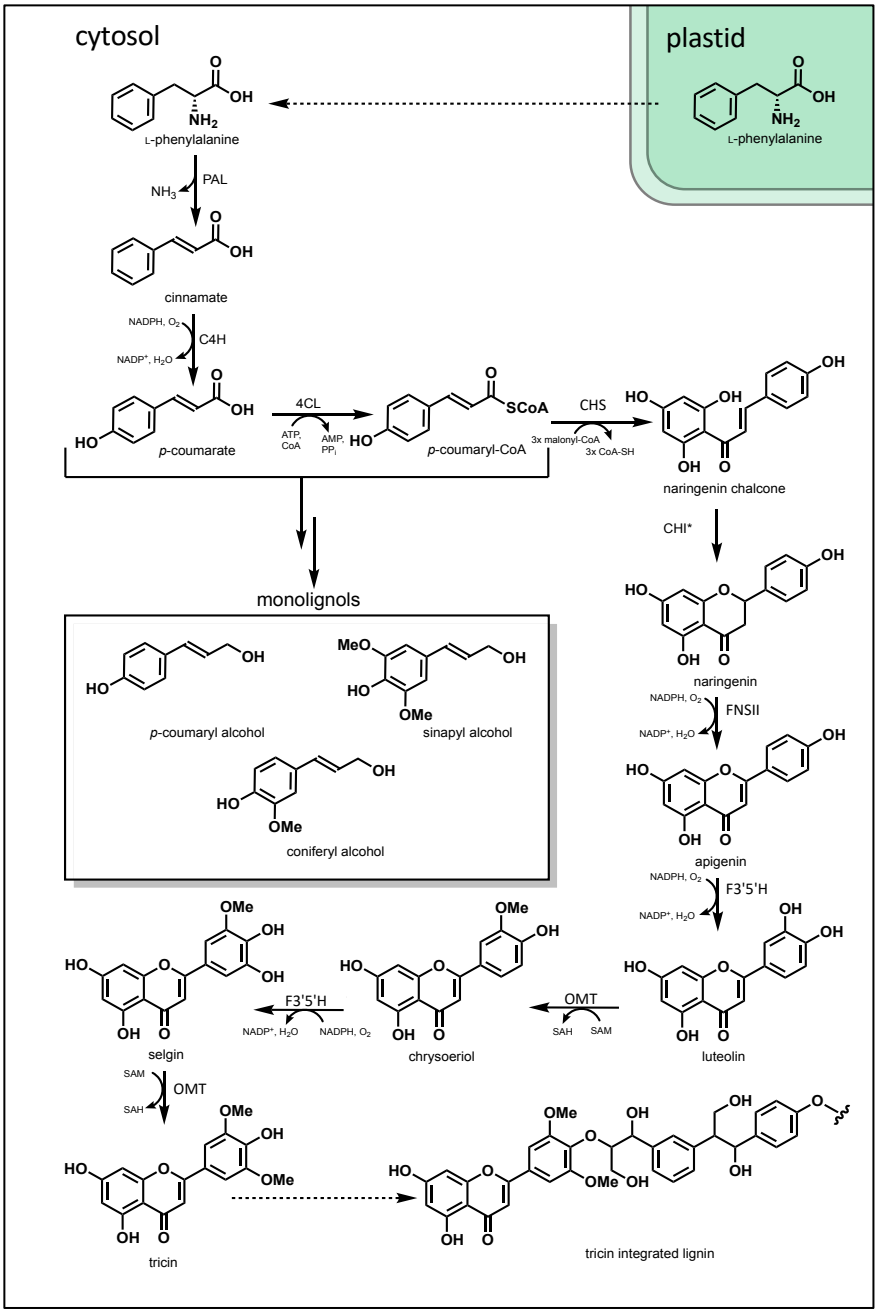

Figure 1.5: Tricin biosynthetic pathway elucidated in rice.

Flavonoids share a central biosynthetic pathway with phenylpropanoids. Chalcone synthase (CHS) combines three molecules of cytosolic malonyl-CoA with one molecule of *p*-coumaroyl-CoA, produced via the phenylpropanoid pathway, producing naringenin chalcone which is isomerized into naringenin (Austin and Noel, 2003). Naringenin is converted to apigenin by a flavone synthase II specific to the production of *O*-linked tricin glycosides (Lam et al., 2014). Apigenin undergoes a series of stepwise hydroxylation/methylation steps through the combined action of flavonoid 3'5'hydroxylase (F3'5'H) and a SAM dependant *O*-methyltransferase (OMT) to produce tricin (Lam et al., 2015).

The phenylpropanoid and flavonoid biosynthetic pathways are tightly linked, and alterations that disrupt monolignol biosynthesis are often associated with increased accumulation of flavonoids (Figure 1.5). For example, RNAi-mediated silencing of *p*-hydroxycinnamoyl-CoA shikimate/quinate *p*-hydroxycinnamoyltransferase (HCT) in *Arabidopsis* leads to the accumulation of flavonoids (Hoffmann et al., 2004). Overexpression of *ZmMYB31* in corn, a transcription factor involved in the regulation of phenylpropanoid biosynthesis, also resulted in reduced lignin and redirection of metabolic flux towards flavonoids, leading to the accumulation of anthocyanins (Fornale et al., 2010). Similarly, downregulation of *CCoAOMT* in alfalfa resulted in accumulation of isoflavonoids, the predominant class of flavonoids found in legumes (Gill et al., 2018).

It has been previously proposed that accumulation of flavonoids in response to disruption of monolignol biosynthesis may, in part, contribute to the dwarf phenotype observed in reduced lignin plants through inhibition of auxin transport (Besseau et al., 2007). RNAi-mediated silencing of both HCT and CHS in *Arabidopsis* was reported to alleviate the dwarf phenotype observed in HCT downregulated only plants (Besseau et al., 2007). However, further investigation revealed no difference between the dwarf phenotype observed in both wild-type and CHS null mutant (tt4-2) *Arabidopsis* lines subjected to RNAi-mediated silencing of HCT (Li et al., 2010). Moreover, the growth phenotype of low lignin C3'H mutant (ref8) was indistinguishable from ref8 tt4-2 double mutants suggesting that growth inhibition may be independent of flavonoid accumulation in lignifying tissues (Li et al., 2010).

Conversely, silencing of CHS in corn resulted in drastically reduced levels of the flavonoids apigenin and tricin, yet a significant increase in total lignin content (Eloy et al., 2017). Taken together, these results indicate that CHS plays a central role in directing carbon flux between phenylpropanoid and flavonoid pathways. Furthermore, poplar (*Populus tremula* x *Populus alba*) overexpressing a petunia (*Petunia hybridata*) derived *CHS* gene was reported to accumulate flavonoids in its stem tissue indicating that introduction of non-endogenous *CHS* gene into poplar can successfully channel carbon flux toward flavonoid production (Nicolescu et al., 1996).

1.3.3 Biosynthesis of tricin

The tricin biosynthetic pathway has recently been fully elucidated in rice (Figure 1.5; Lam et al., 2015). Following the production of naringenin chalcone by CHS, CHI catalyses a ring closure step to produce the flavanone naringenin, which is then converted to the flavone apigenin. Flavanones are converted to flavones through the introduction of a double bond between C-2 and C-3. This reaction can be catalysed by either FNSI, a soluble $Fe^{2+/2-}$ oxoglutarate-dependent dioxygenases (2-ODDs), or, in most higher plants, by FNSII an oxygen- and NADPH-dependent cytochrome P450 (CYP450) membrane-bound monooxygenases (Figure 1.5; Jiang et al., 2016). Apigenin then undergoes a series of hydroxylations carried out by membrane-bound cytochrome P450 enzymes and methylations carried out by *O*-methyltransferases to finally produce tricin (Figure 1.5; Lam et al., 2015).

1.3.3.1 Flavonoid hydroxylases in tricin biosynthesis

In rice, OsCYP75b4 alone catalyses the hydroxylation of chrysoeriol at the 5' position to produce selgin, a key step in the production of tricin (Figure 1.5; Lam et al., 2015). Phylogenetic analysis of the flavonoid 3'/5' hydroxylase (F3'5'H) *CYP75* gene family, composed of CYP75A and B subfamilies, reveals that *OsCYP75B4* is a member of a highly conserved subclade of genes occurring in the *CYP75B* subfamily and found only in monocots, corresponding to reports of tricin's wide-ranging occurrence in a number grass species (Lan et al., 2016; Lam et al., 2017). While the major CYP450 domains are highly conserved between all members of the *CYP75* subfamily, members of this distinct *F3'5'H CYP75B* subclade carried a single amino acid change at position eight in substrate recognition site six (SRS6), a key motif in substrate determining specificity (Lam et al., 2019a). Biochemical characterization of OsCYP75B4 homologues in sorghum (*Sorghum bicolor*), SbCYP75B97, and switchgrass, PvCYP75B11, has also demonstrated that these enzymes are capable of converting chrysoeriol to selgin and apigenin to luteolin (Lui et al., 2020). However, similar to OsCYP75B4, they do not convert luteolin further to tricetin, nor do they accept tricetin as a substrate, indicating that these enzymes participate in tricin biosynthesis exclusively through sequential hydroxylation-methylation steps (Lui et al., 2020). Interestingly, tricin and tricin-lignins have also been reported in alfalfa, a dicot found outside the Poaceae family (Lan et al., 2016). Phylogenetic analysis of the CYP75B subfamily in the dicot

alfalfa, revealed a subgroup of flavonoid hydroxylases in the CYP75B subfamily specific to the *Medicago* genus capable of performing both 3'/5' hydroxylations *in vitro* and shown *in planta* to be necessary for tricin biosynthesis (Lui et al., 2020). Further *in vitro* analysis of MtCYP75B (MtFBH-4) revealed high substrate specificity for chrysoeriol over tricetin, indicating that, similar to grasses, tricin biosynthesis in alfalfa occurs through sequential hydroxylation followed by *O*-methylations performed by *O*-methyltransferases (Lam et al., 2015; Lui et al., 2020). Researchers propose that similar to grasses, the replacement of a Thr residue with Gly at position eight in SRS6 is likely responsible for the 5' chrysoeriol hydroxylase activity of MtCYP75b (MtFBH-4; Lam et al., 2015; Lui et al., 2020). Taken together, these results demonstrate that while the tricin biosynthetic pathway arose in grasses and *Medicago* genus independently, the sequence of biochemical steps remain largely the same, and a single amino acid change to SRS6 in *CYP75B* genes may be sufficient to facilitate both 3' and 5' activity.

Both dicot and monocot members of the CYP75A subfamily are reported to have F3'5'H activity, while most dicot members of the CYP75B subfamily have been traditionally reported to only have F3'H activity, with the exception of the *Medicago* genus and some members of the Asteraceae family (Seitz et al., 2006; Yonekura-Sakakibara et al., 2019; Lui et al., 2020). Three putative *CYP75* gene members have been identified within the poplar genome: *PtCYP75A12, PtCYP75A13*, and *PtCYP75B12* (Nelson et al., 2008; Tanaka and Brugliera, 2013). While these putative flavonoid hydroxylases have yet to be characterized, overexpression of proanthocyanidin positive regulator, *PtMYB115*, in poplar resulted in increased expression of *PtCYP75A12* and *PtCYP75B12* as well as an increase in accumulation of the tri-hydroxylated flavonol dihydromyricetin in leaves, indicating that one or both likely accepts 3' hydroxylated dihydroflavonols/flavones as substrates (James et al., 2017). Considering the single amino acid change attributed to a member of the CYP75B subfamily in grasses and alfalfa gaining 5' hydroxylation capacity, it is possible that the member of the CYP75B family in poplar played a role in the trace production of tricin observed in artificially cultivated, red-leafed, *Populus deltoides* (Tian et al., 2021).

Current models propose that flavonoid biosynthesis occurs in the cytosol through the action of a multi-enzyme complex, or metabolone, that assembles near the surface of the endoplasmic reticulum through protein-protein interactions with ER-associated CYPP450 membrane-bound proteins such as C4H, F3'Hs, and F3'5'Hs (Winkel, 2006; Petrussa et al., 2013). The coordination of enzymes into an organized complex allows for metabolic channelling, or the rapid transfer of biosynthetic intermediates between catalytic sites while preventing diffusion of toxic or unstable intermediates into the cell (Winkel, 2006). Flavones are found most often in their glycosylated form, which aids in increasing the stability and solubility of a compound within the cell (Jiang et al., 2016). In grasses, tricin is found predominantly as *O*-linked glycosides, *O*-linked flavonolignans, and lignin-integrated tricin (Lam et al., 2014; Lan et al., 2016). While *O*-linkages are the most common form of glycosylation, flavones can also be found C-glycosylated, which occurs through the direct linkage of carbons in the flavonoid and sugar backbones (Jiang et al., 2016). Two independent metabolic pathways are responsible for the production of *O*-linked and C-linked flavone conjugates (Jiang et al., 2016), and in rice, two distinct *FNS* genes, OsCYP93G1 and OsCYP93G2, are responsible for channelling flavonoids between these two pathways (Lam et al., 2014; Jiang et al., 2016). OsCYP93G1 is an FNSII that channels the flavone pathway towards the production of tricin *O*-linked conjugates (Lam et al., 2014). Alternatively, OsCYP93G2 channels flavonoids towards the production of the C-glycosylated tricin precursors; C-glycosylapigenin, C- glycosylluteolin, and C-glycosylchrysoeriol (Du et al., 2010). Disruption of OsCYP93G2 in rice does not impact the accumulation of tricin conjugates; however, disruption of OsCYP93G1 results in the depletion of *O*-linked tricin glycosides and flavonolignans, as well as lignin-integrated tricin (Du et al., 2010; Lam et al., 2014; Lam et al., 2017). Furthermore, expression of *OsCYP93G1* in *Arabidopsis* resulted in the production of flavone *O*-glycosides not naturally present in wild-type *Arabidopsis*, and co-expression of *OsCYP93G1* with *OsCYP75b4*, the flavonoid hydroxylase critical to the production of tricin in grasses, resulted in the accumulation of *O*-linked tricin conjugates in *Arabidopsis* (Lam et al., 2015). Taken together, these results highlight the importance of pairing specific flavone biosynthetic genes with the appropriate upstream partner enzymes when engineering novel flavonoid pathways.

1.3.3.2 Flavonoid *O*-methyltransferases

In grasses, the biosynthesis of tricin and monolignols are linked by COMT/CAldOMT, which play a dual role in the biosynthesis of monolignols and tricin (Figure 1.1 & 1.5). Rice deficient in *OsCAldOMT*, which displays similar substrate affinity for both 5-hydroxyconiferaldehyde and selgin *in vitro,* contained significantly lower quantity of both S-lignin and tricin-lignin units and displayed a substantial reduction in accumulation of soluble tricin glycosides, along with increased accumulation of soluble luteolin and selgin glycosides (Kim et al., 2006; Lam et al., 2015; Lam et al., 2019b). In sorghum, SbCOMT/Bmr12 mutants not only display the characteristic brown midrib phenotype but also contain lower tricin-lignin units and lower soluble tricin glycosides (Eudes et al., 2017). Moreover, when *Arabidopsis tt6/tt7* double mutants, deficient in both flavanone 3-hydroxylase and flavonoid 3'-hydroxylase activity, were transformed with co-expressing rice derived *OsCYP75b4* and *OsFNSII* (*OsCYP93G1*) genes, they were able to accumulate tricin, suggesting that the endogenous OMT's in *Arabidopsis* were able to participate in the sequential methylation steps involved in tricin biosynthesis (Lam et al., 2015). Considering the dual role played by COMT/CAldOMT's in grasses and the capacity of endogenous OMT's in *Arabidopsis* to participate in *O*-methylation of tricin precursors, it is likely that the endogenous COMT/CAldOMT's of other dicots, such as poplar, are also capable of participating in tricin biosynthesis.

Plant OMTs represent a large family of plant enzymes that function by catalysing the transfer of a methyl group from *S*-adenosylmethionine (SAM) to the oxygen atom of a broad range of small phenolic molecules, including phenylpropanoids, simple phenols, flavonoids, and some alkaloids (Lam et al., 2007). Plant OMTs have been traditionally divided into two groups based on molecular weight and catalytic activity (Joshi and Chiang, 1998; Lam et al., 2007). Group I contains CCoAOMTs which range in weight between 26 and 30 kDa and are catalytically dependent on divalent ions. Group II contains COMT/CAldOMT's, which can accept both phenylpropanoid and flavonoid substrates, range in weight from 40 to 43 kDa, and do not require divalent ions to function (Lam et al., 2007; Kim et al., 2010a; Jiang et al., 2016). In total, 26 COMT/CAldOMT's sequences have been identified in the poplar genome, nine of which are found to cluster into a subclade with other previously characterized OMTs, which are functional

on both flavonoid and monolignol substrates (Barakat et al., 2011; Lam et al., 2015). Included in this cluster are *PtOMT7 (PtrCOMT4)*, a poplar gene previously shown to function on flavonoids *in vitro* (Kim et al., 2006), and *PtOMT25 (PtrCOMT2)*, a COMT/CAldOMT which participates in monolignol biosynthesis and is very highly expressed in xylem tissue (Van Doorsselaere et al., 1995; Jouanin et al., 2000; Marita et al., 2001; Lu et al., 2010; Shi et al., 2010). Interestingly, PtOMT25 (PtrCOMT2) also clusters most closely with *OsCAldOMT* and *AtOMT1* both of which have been shown to act on monolignol and flavonoid substrates (Muzac et al., 2000; Kim et al., 2006; Lam et al., 2015; Lam et al., 2019b). It is therefore likely that PtOMT25 (PtrCOMT2) can facilitate tricin biosynthesis in lignifying tissue of transgenic poplar as it is highly expressed in developing xylem tissue and clusters closely with other OMTs shown to have activity on flavonoids.

1.3.4 Subcellular transport of flavonoids

Flavonoids are found throughout the cell, and flavones are typically reported to accumulate in the vacuole in their glycosylated form (Zhao and Dixon, 2010). Two non-mutually exclusive hypotheses have been proposed as mechanisms for flavonoid transport from the flavonoid biosynthetic complex to the vacuole. One model proposes that flavonoids are transported via membrane-bound vesicles, based on observations of the movement of membrane-bound inclusion bodies carrying anthocyanins from the ER to the vacuole (Zhao and Dixon, 2010; Zhao, 2015). The second model proposes that flavonoids are transported in and out of the vacuoles via membrane-bound transporters such as ABC transporters and multidrug and toxic compound extrusion (MATE) transporters (Zhao and Dixon, 2010; Zhao, 2015). To date, most studies examining subcellular trafficking of flavonoids have focused on the accumulation of anthocyanins and proanthocyanidins in the vacuole. However, one study examining transport of the flavone glucosides sparonin and isovitexin in barley (*Hordeum vulgare*) reported uptake into the vacuole by a proton antiporter (Frangne et al., 2002). The same study reports that in *Arabidopsis*, which does not naturally synthesize sparonin and isovitexin, uptake into the vacuole was characteristic of an ABC transporter (Frangne et al., 2002). The authors suggest the apparent difference in transport mechanisms may be due to the development of specialized transporters for endogenous flavonoid glucosides in barley, in

comparison to a more general transport mechanism employed by *Arabidopsis* to transport foreign glycosylated flavonoids (Frangne et al., 2002). The occurrence of high levels of tricin-integrated lignin in grasses suggests that tricin may undergo transport to the cell wall space in a mechanism similar to monolignols. In fact, molecular simulations estimating membrane permeability of tricin have indicated that similar to monolignols, tricin is also capable of passive diffusion across the membrane (Vermaas et al., 2019).

1.4 Research Objectives

Lignification of xylem tissue is highly plastic, and tricin's natural incorporation into the lignins of grass species indicates that tricin is chemically compatible with lignification. Furthermore, the recent elucidation of the tricin biosynthetic pathway in rice and other grass species (Lam et al., 2015; Lui et al., 2020) has made the exogenous production of tricin in woody feedstock such as poplar through genetic manipulation eminently feasible. If tricin can be made available during lignin polymerization in the developing xylem of poplar, it will likely be incorporated as an end group onto lignins, thereby limiting the degree of lignin polymerization while simultaneously adding a high-value compound to industrial lignin waste streams. To that end, the objective of my thesis project is to genetically engineer P39 hybrid poplar (*Populus alba x grandidentata*), a fast-growing and ecologically important woody feedstock, to produce lignin-integrated tricin. To achieve this, I aimed to accomplish three main objectives:

1. Redirect carbon flux away from monolignol biosynthesis and towards flavonoid production in developing xylem cells.
2. Characterize putative tricin biosynthetic enzymes derived from *Brachypodium distachyon,* and poplar *in vitro.*
3. Determine if engineering the production of tricin, and tricin-integrated lignin, in the developing xylem tissue of poplar is possible.

In Chapter 3, I address the first objective by expressing *MdCHS3*, a previously characterized chalcone synthase derived from apple (*Malus domestica*) in poplar using a lignin-specific promoter. I then present my analysis of the resulting poplar lines displaying changes in the soluble phenolic profile of xylem tissue, alterations to wood chemistry such as lignin content, S:G ratio, cell wall acetate content, and structural sugars as well as improvements in saccharification rates.

In Chapter 4, I address my second objective and describe the successful characterization of *Brachypodium* derived chrysoeriol 5' hydroxylases (BdCYP75B4) and flavone synthase II (BdCYP93G1*).* I examined the activity of both enzymes independently and together as a

bicistronic construct (*BdCYP75B4-2A-BdCYP93G1*) in yeast expressing a plant-specific NADPH-dependent cytochrome P450 reductase, using both isolated microsomal fractions and substrate feeding assays. Next, I describe the successful *in vitro* characterization of the endogenous poplar OMT, PtrCOMT2, using recombinant protein produced in *E.coli* and isolated with a Ni-NTA His-tagged protein purification system. I also present an enzyme kinetic analysis comparing the activity of PtrCOMT2 activity with luteolin vs. caffeic acid. Finally, I show that expression of *BdCYP75B4* and *BdCYP93G1 MdCHS3*-poplar results in the novel production of tricin xylem tissue. I also investigate the negative impact on growth that expression of *BdCYP75B4-2A-BdCYP93G1* using secondary cell wall promoters has in both wild-type and *MdCHS3*-poplar. I then assess the growth and viability of wild-type and *MdCHS3*-poplar expressing only *BdCYP75B4* or *BdCYP93G1* to better understand contribution of each gene to the reduced plant growth and viability of poplar expressing *BdCYP75B4-2A-BdCYP93G1.*

Chapter 2: Materials and Methods

2.1 Generation of Constructs

2.1.1 Gene isolation from plant material

MdCHS3 (*NM_001328985*) was isolated from golden delicious apple seedlings (*Malus domestica* x Borkh.). Seeds were collected from locally purchased apples, stratified at 4°C in the dark for two weeks, and germinated in soil under long day conditions. Xylem tissue of mature P39 hybrid poplar *(Populus alba* x *grandidentata)* was freshly scraped, flash-frozen and ground in liquid N_2 in order to isolate *PaxgOMT25.* Wild-type *Brachypodium distachyon* (line Bd21-3) seeds were vernalized in soil at 4°C for four days and transferred to growth chambers under long-day conditions (16 hours light/ 8 hours dark). After four weeks of growth stem tissue from the last internode was collected from plants then pooled, flash-frozen, and ground in liquid N_2 to isolate *BdCYP75B4* (*Bradi4g16560*) and *BdCYP93G1* (*Bradi5g02460*). RNA was extracted from plant materials using the Purelink plant RNA extraction kit (Invitrogen, Carlsbad, CA). Contaminating DNA was removed from RNA samples using the TURBO DNA Free kit (Invitrogen, Carlsbad, CA) and 1 µg of RNA was used to synthesize cDNA with the iScript cDNA Synthesis Kit (Bio-Rad Laboratories, Hercules, CA). The coding region of *MdCHS3* was amplified using BestTaq polymerase (Applied Biological Materials, Richmond, BC, Canada*)* from 1 µl of cDNA with primers modified to include Gateway *attB1* and *attB2* cloning sites at the 5' and 3' positions, respectively (Table 2.1). *MdCHS3* was cloned into the Gateway entry vector pDONR221 (Invitrogen, Carlsbad, CA) by BP clonase recombination. The coding region of *PaxgOMT25* was amplified using coding sequence (cds) targeted primers (Table 2.1) and cloned into the Blunt II TOPO vector using the Zero Blunt TOPO PCR cloning kit (Invitrogen, Carlsbad, CA). The coding regions of *BdCYP75B4* and *BdCYP93G1* were amplified using BestTaq polymerase (Applied Biological Materials, Richmond, BC, Canada*)* from 1 µl of cDNA with primers modified to included Gateway *attB1* and *attB2* cloning sites at the 5' and 3' positions, respectively (Table 2.1). PCR amplicons were cloned into the Gateway entry vector pDONR221 (Invitrogen, Carlsbad, CA) by BP recombination (Table 2.2).

2.1.2 ph7WGY2-*AtC4Hp::MdCHS3* plant expression construct

The *35S* promoter sequence contained in the ph7WGY2 Gateway (Invitrogen, Carlsbad, CA) plant expression vector was replaced with a 2900bp section of the *Arabidopsis thaliana C4H* promoter sequence (*AtC4Hp*) using digestion/ligation cloning method. Briefly, *AtC4Hp* was amplified from the pTkan-*pC4H::schl::qsuB* plasmid (Eudes et al., 2015) by PCR using primers: AtC4HP + SacI FWD and AtC4HP + XbaI REV (Table 2.1) producing a PCR amplicon with SacI and XbaI restriction digestions sites at 5' and 3' positions respectively. The ph7WGY2 vector and *AtC4Hp* PCR amplicon were then digested with SacI/SpeI and SacI/XBaI respectively, using the FastDigest protocol (Thermo Fisher Scientific, Waltham, MA). Fragments were separated using gel electrophoresis, purified using the PureLink gel extraction kit (Invitrogen, Carlsbad, CA), and ligated together with T4 DNA ligase (Thermo Fisher Scientific, Waltham, MA) to generate the *AtC4Hp*-ph7WGY2 vector. *MdCHS3* was transferred from pDONR221-*MdCHS3* gateway entry vector via LR recombination into the ph7WGY2-*AtC4Hp* vector generating the ph7WGY2-*AtC4Hp*::*MdCHS3* plant expression construct (Table 2.2).

2.1.3 pDONR221-*CYP75B4-2A-BdCYP93G1*

The *CYP75B4-2A-BdCYP93G1* bicistronic construct, containing two tandem viral 2A cleavage peptides, P2A and F2A, was produced using the three nucleotide (TNT) cloning system (De Paoli et al., 2016). Briefly, *BdCYP75B4* and *BdCYP93G1* were amplified from their respective pDONR221 Gateway vectors (Invitrogen, Carlsbad, CA) with primers modified to contain the 3 nt signatures 1 and 2 (De Paoli et al., 2016) at the 5' and 3' ends, respectively, and modified to exclude the stop codon at the 3' end of *BdCYP75B4* (Table 2.1). A *P2AF2A* sequence with signatures 1 and 2 at the 5' and 3' was obtained synthetically as a gblock sequence (Integrated DNA Technologies, Coralville, IA). Then the modified fragments were cloned into TNT pStart vectors using a one-pot digestion/ligation reaction. *BdCYP75B4, P2AF2A,* and *BdCYP93G1* sequences were transferred into α1A, αB, and αC TNT vectors respectively, and assembled into an Ω2 vector using a one-pot TNT digestion/ligation reaction. Once assembled, the bicistronic sequence *CYP75B4-P2AF2A-BdCYP93G1* was PCR amplified with *attB1-BdCYP75B4-FWD* and *attB2-BdCYP93G1-REV* modified primers and cloned into *pDONR221* Gateway vector via BP clonase reaction (Invitrogen, Carlsbad, CA; Table 2.2).

2.1.4 pYES-DEST52 yeast protein expression constructs

BdCYP75B4, BdCYP93G1, and *CYP75B4-P2AF2A-BdCYP93G1* were transferred from their respective pDONR-221 entry vectors into pYES-DEST52 Gateway yeast expression vector (Invitrogen, Carlsbad, CA) by LR recombination (Table 2.2).

2.1.5 *BdCYP75B4-P2AF2A-BdCYP93G1, BdCYP75B4* and *BdCYP93G1* plant expression constructs

The *BdCYP75B4-P2AF2A-BdCYP93G1, BdCYP75B4,* and *BdCYP93G1* fragments were each transferred from pDONR221 into the plant expression vector pk7WG2 modified to contain the *Arabidopsis* CesA7 promoter (pk7WG2-*AtCesA7p*) (Smith et al., 2015) via LR recombination. The *BdCYP75B4-P2AF2A-BdCYP93G1* fragment was also transformed into the pk7WGY2-*AtC4Hp* plant expression vector described above (Table 2.2).

2.1.6 Pet28MHL-*PaxgOMT25 E. coli* protein expression construct

PaxgOMT25 (*Potri.012G00640*) was transferred from the Blunt II TOPO vector to the Pet28MHL protein expression vector (Structural Genomics Consortium, Toronto, ON, Canada) using a restriction digestion/ligation reaction. *PaxgOMT25* was PCR amplified from the Blunt II TOPO vector using primers modified to produce a PCR amplicon with NdeI and XhoI restriction sites at the 5' and 3' ends, respectively (*NdeI-PaxgOMT25-FWD* and *XhoI-PaxgOMT25-REV*) (Table 2.1). The Pet28MHL vector (Structural Genomics Consortium, Toronto) and *PaxgOMT25* PCR amplicon were then digested with NdeI and XhoI using the FastDigest protocol (Thermo Fisher Scientific, Waltham, MA). Fragments of appropriate size were separated using gel electrophoresis, purified using the PureLink gel extraction kit (Invitrogen, Carlsbad, CA), and ligated together with T4 DNA ligase (Thermo Fisher Scientific, Waltham, MA) to generate the Pet28MHL-*PaxgOMT25* vector (Table 2.2).

2.2 In vitro Enzyme Assays

2.2.1 Substrate feeding assays with *BdCYP93G1* and *CYP75B4-P2AF2A-BdCYP93G1* expressing yeast

BdCYP93G1 and *CYP75B4-P2AF2A-BdCYP93G1* were transferred from their respective pDONR221 entry vectors into the pYESDEST52 Gateway yeast expression vector (Invitrogen, Carlsbad, CA) by LR recombination. The pYESDEST52-*BdCYP7593G1* and pYESDEST52-*BdCYP74B4-2A-BdCYP7593G1* constructs (Table 2.2) were then transformed into the *Saccharomyces cerevisiae* LpCPR strain (Geisler et al., 2016). As a control, β-glucuronidase (GUS) was inserted into pYESDEST52 and transformed into LpCPR yeast. Cultures were grown for 24 hours shaking at 30 °C in 5 ml SC (-uracil) 2% glucose liquid media (pH 5.6) supplemented with 200 μg/ml of geneticin G418. Cells were then concentrated via centrifugation, supernatant was discarded, and cells were resuspended in 5 ml induction SC (- uracil) 2% galactose liquid media (pH 5.6) supplemented with 350 μM flavonoid substrate and shaken for 20 hours at 30 °C.

2.2.2 In vitro characterization of *BdCYP75B4* expressing microsomes

pYESDEST52-*BdCYP75B4* was transformed into LpCPR yeast (Geisler et al., 2016). 30 ml starter cultures were grown for 24 hours shaking at 30 °C in 5 ml SC (-uracil) 2% glucose liquid media (pH 5.6) supplemented with 200 μg/ml geneticin G418. Cells were then concentrated via centrifugation, the supernatant was discarded, and cells were resuspended in 200 ml of SC (-uracil) 2% galactose liquid media (pH 5.6) supplemented with 200 μg/ml geneticin and incubated for 16 hours shaking at 30 °C geneticin G418. Cells were then concentrated again via centrifugation, the supernatant was discarded, and cells were incubated in resuspension buffer (50 mM Tris-HCl, pH 7.4, 2 mM EDTA, and 100 mM fresh 2-mercaptethanol) for 30 min at 30 °C. Microsomal preparations were performed as described in Urban et al., 1994, with some alterations. Briefly, cells were pelleted via centrifugation and washed twice with wash buffer (Tris-HCl, pH 7.4, 2 mM EDTA, 100 mM KCl), then resuspended in lysis buffer (50 mM Tris-HCl, pH 7.4, 2 mM EDTA, 0.6 M sorbitol) and shaken vigorously with glass beads. Crude extracts were centrifuged for 3 min at 3500g and then for 10 min at 10000g, the supernatant was

collected and incubated on ice with PEG 4000, 0.1 g for 1 ml of extract, and 1 M NaCl to 0.15 M concentration for 15 min. Precipitated microsomes were pelleted by centrifugation at 10000g at 4 °C for 20 min and resuspended in storage buffer (50 mM Tris-HCl, pH 7.4, 2 mM EDTA, and 20% (v/v) glycerol). Microsomal protein concentration was measured using the Bio-Rad Bradford protein assay (Bio-Rad laboratories, Hercules, CA) using bovine serum albumin as a standard protein. *In vitro* reactions were performed by incubating 500 μg microsomal protein in 100 mM potassium phosphate buffer (pH 7.0) containing 100 μM flavonoid substrate, 5mM fresh NADPH, and 2 mM *L*-glutathione for 1 hour at 30 °C.

2.2.3 Purification and *in vitro* characterization of recombinant PaxgOMT25

The Pet28MHL-*PaxgOMT25* vector was transformed into chemically competent BL21(DE3) *E. coli.* Cultures were grown overnight in 5 ml LB (kanamycin 50 μg/ml, chloramphenicol 25 μg/ml) media with shaking at 37 °C, and then transferred into 200 ml LB broth (kanamycin 50 μg/ml, chloramphenicol 25 μg/ml, 1mM IPTG) and left to shake at room temperature for 30 hours. Following incubation, cultures were centrifuged at 5000 rpm for 5 min, the supernatant discarded, and cells were resuspended in lysis buffer (20mM NaH_2PO_4, 500 mM $NaCl_2$, 10 mM imidazole). Cells were sonicated on ice using a needle sonicator set to 10% amplitude for 30 seconds for three repetitions. Lysed cells were centrifuged at 4°C and 14000rpm for 20 min, and the supernatant collected as the soluble fraction. The soluble fraction was incubated at 4°C with Ni-NTA resin (Qiagen, Hilden, Germany) for 1 hour, and the slurry was transferred to columns packed with glass wool and rinsed with wash buffer (20mM NaH_2PO_4, 500 mM $NaCl_2$, 20 mM imidazole). Eluent fractions were collected and tested for protein content using a Bradford reagent (Bio-Rad laboratories, Hercules, CA). Once eluent fractions were determined to contain no protein, PaxgOMT25 was eluted from the column using elution buffer (20mM NaH_2PO_4, 500 mM $NaCl_2$, 100 mM imidazole). Protein was concentrated using Vivaspin 30kDA protein concentrators (GE Healthcare, Chicago, IL), and the elution buffer was exchanged for a 10 mM Tris-HCl buffer (pH 7.4). Protein fractions were analysed at all stages of the purification using SDS-PAGE gel electrophoresis and stained with Coomassie Brilliant Blue (R-250). Final protein concentrations were determined with the Bio-Rad Bradford protein assay (Bio-Rad laboratories, Hercules, CA) using bovine serum albumin as

a standard protein. *In vitro* enzyme reactions were performed using 50 µM phenolic substrate, 40 µM AdoMet, 2 mM DTT, and 5 µg purified protein in 500 µl 10 mM Tris-HCl buffer (pH7.4). Reactions were incubated at 37 °C for 1 hour and stopped with the addition of 5 µl 6 M HCl. Enzyme kinetic analyses were performed using a time stop assay. The time stop of 5 min was determined from enzyme progress curve generated at 10 µM substrate concentration. V_0 was measured in reactions incubated for 5 min at 37 °C with substrate concentration ranging from 10 µM to 350 µM and replicated in triplicate. Vmax and Km were calculated using Prism7 (GraphPad Software), which generates a non-nonlinear regression model of V_o vs substrate concentration.

2.2.4 Analysis of *in vitro* assay products

Phenolic reaction products of *in vitro* enzymatic assays were analysed by adding 5 µl *o*-anisic acid (2-3 mg/ml) to either microsomal reactions or to cultures from yeast substrate feeding assays for use as an internal standard. Soluble phenolics were then extracted twice using an ethyl acetate phase extraction, evaporating ethyl acetate to dryness and resuspending in 100% MeOH for UPLC-UV analysis. Samples were analysed on a Agilent 1290 Infinity II UPLC with a1290 Infinity II Diode Array Detector (DAD) with an EclipsePlus C18 column (Agilent, Santa Clara, CA). Phenolic substrates and products were eluted from the column at 0.3 ml/min, using a gradient transition from 95% water (0.1% TFA): 5% acetonitrile to 60% water (0.1% TFA) :20% MeOH: 20% acetonitrile over 2 min, followed by a gradient transition to 50% MeOH: 50% acetonitrile over 6 min and 2 min wash of 5% water (0.1% TFA): 95% acetonitrile. Reaction products were identified by comparison to standards and when used for relative quantification, peak area was normalized across reaction samples to an internal standard.

2.3 Poplar Transformations

2.3.1 Agrobacterium-mediated transformation

Transformations performed as outlined in Wilkerson et al., 2014. Briefly leaf discs were harvested from six-week-old P39 hybrid poplar plants and co-cultivated with an *Agrobacterium tumefaciens* (EAH105) containing the plant expression construct. Following co-cultivation with *Agrobacterium* (OD_{600nm}=0.12) in woody plant media (WPM) for 30 min at 28°C in a gyratory shaker (100 rpm), the discs were blotted dry on sterile filter paper and placed abaxially on WPM (0.1, NAA, 0.1 BA, and 0.1 TDZ µM) culture medium. Plates were incubated in the dark for two days and transferred on the third day to WPM media (0.1 NAA, 0.1 BA, and 0.1 TDZ µM) containing 250 mg l^{-1} cefotaxime and 500 mg l^{-1} carbenicillin to eliminate any residual *Agrobacterium.* Plates were incubated in the dark for two subsequent days then transferred to WPM (0.1 NAA, 0.1 BA, and 0.1 TDZ µM) selection media containing 250 mg l^{-1} cefotaxime, 500 mg l^{-1} carbenicillin, and the appropriate antibiotic (20 mg l^{-1} hygromycin or 50 mg l^{-1} kanamycin) to select for transformants. After five weeks, discs were transferred to new WPM selection media (0.01 µM BA), and after emergence, shoots (one shoot per leaf disc) were transferred to WPM selection media (0.01 µM NAA). Plants were genomically screened after six weeks of growth. Transgenic plants were sub-cultured, multiplied (minimum eight replicates per transformation event), and transferred to antibiotic-free WPM media (0.01 µM NAA). After four weeks of growth, the tops of clonally propagated lines were excised and transferred to new antibiotic-free WPM media and grown in tissue culture. After six weeks of growth, leaves were collected from tissue culture, and quantitative real-time PCR (qRT-PCR) was used to determine transcript abundance of the transgene.

2.3.2 Genomic screening

Genomic DNA was extracted using a cetyltrimethylammonium bromide (CTAB) (Sigma-Aldrich Co., San Louis, MO) DNA extraction method and quantified using a spectrophotometer ND1000 (NanoDrop Technologies LLC, Wilmington, DE). DNA was stored at -20°C. Target genes were detected using PCR screening of genomic DNA with gene-specific primers (Table 2.1).

2.3.3 Gene expression analysis

RNA was extracted from tissue culture leaves using TRIzol RNA extraction (Thermo Fisher Scientific, Waltham, MA) and from freshly scraped poplar xylem tissue and mature expanded leaves using a modified CTAB RNA extraction method to account for high quantities of phenolics present in xylem tissue of *MdCHS3*-poplar (Chang et al., 1993). cDNA was produced from extracted RNA as described above. Relative expression levels of putative poplar *CHS* genes (*Potri.014G145100, Potri.003G176700, Potri.003G176800, Potri.003G176900, Potri.001G051500, Potri.001G051600*) were quantified using BlasTaq 2X qPCR MasterMix (Applied Biological Materials, Richmond, BC). Reactions consisted of 5 µl 2X master mix, 20 pmol of primers, 1 ul of cDNA, and nuclease-free water to a volume of 10 µl. Relative expression levels were determined using qRT-PCR expression primers (Table 2.1). qRT-PCR was performed using the following cycling parameters: 1 cycle of 5 min at 94°C, 39 cycles of 94°C for 10 s, and 58°C for 30 s, 1 cycle of 94°C for 10 s, followed by a melt curve cycle of 56°C to 95°C at 0.5°C increments for 5 s to ensure amplification of only one product. Reactions were performed in triplicate. Fold change ratio of gene targets to reference *PtEF1*- β (*Potri.009G018600*) was determined with correction for primer efficiency. Relative expression levels of *BdCYP75B4, BdCYP93G1,* and *BdCYP75B4-2A-BdCYP93G1* were determined using BlasTaq 2X qPCR MasterMix (Applied Biological Materials, Richmond, BC) with the same reaction parameters previously described. Target Cq values were normalized to the average expression of *PtrTIFF (Potri.006G185000)* and *PtrUBQ (Potri.001G418500)* reference genes across all samples. Then each sample's normalized target Cq was subtracted from the sample with the highest reported target gene Cq and converted to fold-change difference relative to the lowest-expressing tree. Relative expression levels of *MdCHS3* were quantified using SsoFast Eva Green® Supermix (Bio-Rad Laboratories, Hercules, CA). qRT-PCR reactions consisted of 5 µl of SsoFast Eva Green® Supermix (Bio-Rad Laboratories, Hercules, CA) 20 pmol of primers, 0.3 µl of cDNA, and nuclease-free water to a total volume of 10 µl. qRT-PCR was performed on a CFX 96 System® (Bio-Rad Laboratories, Hercules, CA). The 88 bp fragment of the *MdCHS3* transcript was amplified with *MdCHS3*-qPCR primers following the cycle parameters previously described. Reactions were performed in triplicate. Relative transgene transcript levels were determined

using the sample analysis described above for *BdCYP75B4, BdCYP93G1,* and *BdCYP75B4-2A-BdCYP93G1* expression analysis.

2.4 Plant Phenotyping

2.4.1 Growth conditions and measurements

Six-week-old plants, grown from transferred plant apical meristems, were transferred from WPM media into two-gallon pots containing perennial soil mix (50% peat, 25% fine bark, and 25% pumice; pH 6.0) and grown under 16h supplemental light and watered daily on flood tables at the UBC greenhouse. After four months of growth, height was recorded by measuring the distance from root collar to tree apex; stem diameter was determined using digital calipers 10 cm above the root collar. Weight of fresh biomass of the whole tree cut 10 cm above the root collar collected immediately after cutting.

2.4.2 Phenolic metabolite profiling

For analysis of sixteen-week-old trees, a section of fresh stem 10 cm from the root collar of each tree was cut, lyophilized for 24 h, and ground using a Wiley Mill (Thermo Fisher Scientific, Waltham, MA) to pass through a 40-mesh screen and used in all downstream analysis. For analysis in tissue culture, whole stem pieces were ground in using liquid nitrogen and freeze-dried to remove all moisture. Five µl *o*-anisic acid (2-3 mg/ml) was added to 25 mg of ground tissue as an internal standard. Two extractions were performed per sample. Tissue was incubated with 700 µl of 50% MeOH (0.01% trifluoroacetic acid (TFA)) at 70°C for 15 min and centrifuged for 5 min at 13000 rpm. Supernatant was collected, and tissue was extracted consecutively with 80% MeOH (0.01% TFA) and 100% MeOH (0.01% TFA). Supernatants from all three washes were pooled together, and a 500 µl aliquot was taken for hydrolysis and combined with 25 µl 0.2 M NaOH. Samples were evaporated down to 10 µl in volume in a SpeedVac concentrator (Thermo Fisher Scientific, Waltham, MA), mixed with 300 µl of 1 M HCl, and incubated at 95°C for 3 h. Phase extraction of phenolic compounds was performed by mixing with 400 µl of ethyl acetate, and the upper organic phase was collected, evaporated to dryness, and resuspended in 100% MeOH (0.01% TFA). Samples were analysed on a Agilent 1290 Infinity II UPLC with a 1290 Infinity II Diode Array Detector (DAD) with an EclipsePlus C18 column (Agilent, Santa Clara, CA). Naringenin was eluted from the column at 0.3 ml/min, using a gradient transition from 95% water (0.1% TFA):5% acetonitrile to 60% water (0.1% TFA):20%

MeOH:20% acetonitrile over 2 min, followed by a gradient transition to 50% MeOH:50% acetonitrile over 6 min and 2 min wash of 5% water (0.1% TFA):95% acetonitrile. Naringenin was quantified using a standard curve generated from a dilution series of an external standard, and calculations were normalized to an internal standard, *o*-anisic acid. Naringenin was not detectable at levels >0.70 µg/g xylem tissue.

2.4.3 Cell wall composition analysis

The ground lyophilized mature stem xylem samples were Soxhlet extracted with acetone for 24 h. The extractive-free material was used for all further cell wall analysis. Total lignin content was determined using a modified Klason lignin analysis as previously described (Coleman et al., 2006). Dried extractive-free tissue (200 mg), two reactions per sample, was treated with 3 ml 72% H_2SO_4 for 2 h, diluted to 3% H_2SO_4 with 112 ml of distilled water, then autoclaved at 121°C for 60 min. The mixture was filtered through a dry, pre-weighed medium coarseness crucible; the retentate dried overnight at 105°C, and acid-insoluble lignin was determined by weighing the retentate. The filtered aliquot was collected, and absorbance at 205 nm using a UV spectrophotometer was measured to determine acid-soluble lignin content. Carbohydrate content was determined by HPLC analysis of filtered aliquots as previously described (Huntley et al., 2003). Glucose, xylose, mannose, galactose, arabinose, and rhamnose were analysed using a Dx-600 anion-exchange HPLC (Dionex, Sunnyvale, CA) on a CarboPac PA1 column at a flow rate of 1 ml/min with post-column detection. Concentration of sugars was determined using standard curves generated from a dilution series of external standards. Calculations were normalized to an internal standard, fucose. Lignin (S:G) monomer ratio was determined using thioacidolysis (Robinson and Mansfield, 2009) and analysed using gas chromatography on a Thermo Trace 1310 instrument (Thermo Fisher Scientific, Waltham, MA), equipped with an autosampler, FID detector, and a TG-5MS (30 m x 0.32 mm x 0.25 µl) capillary column. Injections of 1 µl separated with helium as a carrier gas (1ml/min) with inlet and detector temperatures set to 250°C. Initial temperature of the oven was set to 130°C for 3 min, ramping up in temperature by 3°C per minute for 40 min ending at a 250°C hold for 5 min, followed by a cool down. Peaks were identified consistent with analysis presented in (Robinson and Mansfield,2009).

Holocellulose and alpha cellulose fractions were obtained using the methods described in Porth et al., 2013. Briefly, 150mg of dried Soxhlet-extracted wood powder was combined with 3.5 ml of solution A (60 ml glacial acetic acid and 1.3 g/l NaOH) and 1.5 ml of 20% sodium chlorite solution (20 g $NaClO_2$ in 80 ml distilled water) and shaken at 50°C for 16 h. Reactions were quenched by placing tubes in an ice bath, the supernatant was removed, and the procedure was repeated. Reacted wood meal was filtered through pre-weighed coarse sintered crucibles and washed with 50 ml of 1% glacial acetic acid, followed by 10 ml of acetone under applied vacuum. Crucibles were dried overnight at 50°C and weighed to determine holocellulose content. Alpha cellulose was obtained by reacting 2.5 ml of 17.5% NaOH with 30 mg holocellulose for 30 min, followed by the addition of 2.5 ml distilled water was left to react for 30 min. Reaction mixtures were filtered through a fresh set of pre-weighed course sintered crucibles and washed with 3x 50 ml distilled water. The crucibles were then soaked in 1.0 M acetic acid for 5 min and washed with distilled water. Crucibles were dried overnight at 50°C and weighted to determine alpha cellulose content.

2.4.4 Acetyl content analysis

Cell wall acetyl content was determined via saponification of extractive-free xylem tissue. Extract free tissue (30 mg) was combined with 100 µl of butyric acid (1:20 dilution), used as an internal standard, and 1 ml of 2 M NaOH. Two reactions were performed for each sample. Samples were incubated at 30°C for 24 hours with shaking at 500 rpm. Reactions were acidified by adding 100 µl of 72% H_2SO_4 and placed on ice for 5 min. Samples were centrifuged at 13000 rpm for 2 min, and the supernatant was collected and filtered through a 0.45 µm filter in preparation for HPLC analysis. Acetic acid released from saponification was determined on a Summit HPLC analytical system (Dionex, Sunnyvale, CA) fit with an Aminex Ion exclusion HPX-87H column (Bio-Rad Laboratories, Hercules, CA). Samples were eluted with 5% H_2SO_4 at a flow rate of 0.6 ml/min.

2.4.5 NMR analysis

Dried stems were ground, extracted, and ball milled as previously described (Mansfield et al., 2012b). Ground tissue was extracted sequentially using sonication in 80% ethanol (3x 20

min), acetone (1x 20 min), chloroform-methanol (1:1 v/v, 1 x 20 min). Extract-free biomass was ball milled for 10 min followed by 10 min of rest for three hours per 500 mg of sample using a PM100 ball mill (Retsch, Newtown, PA) vibrating at 600 rpm in zirconium dioxide vessels (50 ml) containing ZrO_2 ball bearings (20 × 6.5 mm diameter). Ball-milled samples were digested four times over three days at 50 °C using the commercial enzyme cocktails Cellic CTec3 and HTec2 (Novozymes, Bagsværd, Denmark) 30 mg/g sample in 50 mM sodium citrate buffer (pH 5.0). The residual enzyme-lignin (EL) preparations were washed three times with deionized water and lyophilized overnight. Ball-milled whole cell wall, enzyme lignin, and 80% ethanol extracts were analysed by 2D $^{1}H–^{13}C$ heteronuclear single-quantum coherence (HSQC) nuclear magnetic resonance (NMR) spectroscopy (Kim and Ralph, 2010; Mansfield et al., 2012b; Kim et al., 2017b).

2.4.6 Limited saccharification assay

Pretreatment and limited saccharification assays were performed as previously described (Van Acker et al., 2013), with several modifications**.** Samples of ground, lyophilized xylem powder (15 mg) were subjected to either no pretreatment or a mild acid pretreatment, with two technical replicates per treatment. Samples subjected to mild acid pretreatment were incubated in 2% sulphuric acid at 80°C for 2 h. After incubation, the samples were neutralized and washed four times with water. The aliquots for saccharification without pretreatment were similarly washed four times with water. Both sets of samples were dried for 4 days at 50°C. Briefly, 1 ml of 0.1 M acetic acid buffer solution (pH 4.8) was added to washed samples and incubated at 50°C, shaking at 300 rpm. The enzyme Cellic® CTec3 (Novozymes, Bagsværd Denmark) was diluted 100 times, and 100 µl was added to each sample. After 4, 24, 48, and 72 h, 20 µl of aliquots were taken from the saccharification sample and diluted 10, 20, 20, and 20 times respectively. The concentration of glucose and xylose at each timepoint determined with a Dx-600 anion-exchange HPLC (Dionex, Sunnyvale, CA) as described above.

2.4.7 Microscopy

Stem samples from four-month-old *MdCHS3*-poplar and WT poplar were soaked overnight in distilled water. Samples were cut into 30 µm cross-sections with a Spencer AO860

hand sliding microtome (Spencer Lens Co., Buffalo, NY). Sections were treated with 0.01% Calcoluor-white in 1X PBS for 3 min, then washed 3 X 5 min in 1X PBS for cellulose staining (Falconer and Seagull 1985). To calculate average vessel diameter and number, three trees from the highest expressing line, *MdCHS3-poplar* line *2,* and WT were analysed; pictures were taken from five different zones of each section. Vessels were counted in three separate images per tree at 2.5x magnification; vessel area and width of 25 vessels per tree were measured at 12.5x magnification. Sections were mounted and visualized with UV at 20x magnification with a Leica DRM microscope (Leica Microsystems, Wetzlar, Germany). Photos were taken with a QICam camera (Q-imaging, Surrey, BC) and analysed with OpenLab 4.0Z software (PerkinElmer Inc., Waltham, MA). Multiphoton imaging of stems in tissue culture was completed using hand sectioned stems pieces, incubated with DPBA (Diphenylboric acid 2-aminoethyl ester) for 5 mins and mounted immediately with water. Images were taken using a 380-560nm filter at 810nm laser excitation with 25X magnification on an Olympus FV1000 Laser Scanning/Two-Photon Confocal Microscope.

2.4.8 Statistical analysis

Cell wall analyses, gene expression analysis, phenolic extractions, and saccharification analyses in chapter 3 were carried out in technical duplicates across five biological replicates from each line. Data sets were assessed for normality and equality of variance, and significant difference compared to WT was determined using two-tailed *t*-test at 95% confidence ($p<0.05$). A mixed-effect model was used to account for batch variation in Klason hydrolysis of cell wall carbohydrates. A significant linear relationship between naringenin produced in developing xylem and exogenous expression of *MdCHS3* was determined using Pearson's correlation coefficient for significance ($p<0.05$). Significant effect of transgene expression on vessel/fibre area was determined using a 2-way ANOVE. Pariwise differences determine with post hoc Tukey's t-tests with a Bonferroni correction for multiple comparisons.

Table 2.1: Primer sequences used in this study.

Primer	Sequence
AttB1-MdCHS3	5'-GGGGACAAGTTTGTACAAAAAAGCAGGCTATGGTGACCGTCGAGGAAGTT-3'
AttB2-MdCHS3 REV	5'-GGGGACCACTTTGTACAAGAAAGCTGGGTTCAAGCAGCCACACTGTGAAGCAC-3'
MdCHS3-cds-FWD	5'-ATGGTGACCGTCGAGGAAGTT-3'
MdCHS3-cds-REV	5'-GCAGCCACACTGTGAAGCAC-3'
PtCHS-Potri.014G145100-qPCR-FWD	5'-TGATACTCACTTGGATTCAA-3'
PtCHS-Potri.014G145100-qPCR-REV	5'-TGGAAGTGTCAGGATCAG-3'
PtCHS-Potri.003G176800/ Potri.003G176700-qPCR-FWD	5'-CGATACCCATCTTGATAGCC-3'
PtCHS-Potri.003G176800/Potri.003G176700-qPCR-REV	5'-CTCCTACCACTGGGTCAG-3'
PtCHS-Potri.001G051600- qPCR-FWD	5'-TGACACTCACCTTGATAGCC-3'
PtCHS-Potri.001G051600-qPCR-REV	5'-CCCCCAGCACAGGATCCG-3'
PtCHS-Potri.001G051500-qPCR-FWD	5'-TGACACCCACCTCGATAGTC-3'
PtCHS-Potri.001G051500-qPCR-REV	5'-CCCCCAGCACAGGATCCG-3'
PtCHS-Potri.003G176900-qPCR-FWD	5'-CGATACTCATCTTGATAGCC-3'
PtCHS-Potri.003G176900-qPCR-REV	5'-CTCCTATCACTGGATCAG-3'
PtEF1-β- qPCR-FWD	5'-AACCTGGTCGTGATTTCCCT-3'
PtEF1-β- qPCR-REV	5'-ATCACCAGCAGCCTCCTTG-3'
MdCHS3-qPCR-FWD	5'-TGTCAAGTGCGTGTGTCTTG-3'
MdCHS3-qPCR-REV	5'-TCCAGTCCTTCTCCAGTTGTT-3'
PtUBQ-qPCR-FWD	5'-TCACTTGGTGCTGCGTCTC-3'
PtUBQ-qPCR-REV	5'-GATCTTGGCCTTCACGTTGT-3'
P39AldOMT2-FWD	5'-ATGGGTTCGACAGGTGAAACTCAGA-3'
P39AldOMT2-REV	5'-TTAGTTCTTGCGGAATTCAATGACA-3'
NdeI-P39AldOMT2-FWD	5'-GTTAcatatgGGTTCGACAGGTGAA-3'
XhoI-P39AldOMT2-REV	5'-ACTGctcgagTTAGTTCTTGCGGAAT-3'
attB1-BdCYP75B4-FWD	5'-GGGGACAAGTTTGTACAAAAAAGCAGGCTATGGAGCTCCTCGACG-3'
attB2-BdCYP75B4-REV	5'-GGGGACCACTTTGTACAAGAAAGCTGGGTCTACACAATCTCATA-3'
attB1-BdCYP93G1-FWD	5'-GGGGACAAGTTTGTACAAAAAAGCAGGCTATGGCAATGGCGGC-3'
attB2-BdCYP93G1-REV	5'-GGGGACCACTTTGTACAAGAAAGCTGGGTTTAGACGACGGCCGG-3'
CYP75b-TNT-FWD	5'-GCTCTTCCACCATGGAGCTCCTCGACG-3'
CYP75b-TNT-REV	5'-GCTCTTCCATCGACAATCTCATATGCC-3'
CYP93G1-TNT-FWD	5'-GCTCTTCCACCATGGCAATGGCGGCG-3'
CYP93G1-TNT-REV	5'-GCTCTTCCATCTTAGACGACGGCCGG-3'
BdCYP75B4-qPCR-FWD	5'-GATGATGCAGGAGGAGAAG-3'
BdCYP75B4-qPCR-REV	5'-CGAATAGGTTCAGGACGAG-3'
BdCYP93G1-qPCR-FWD	5'-GAGAGGATGGGAAGAAGAAGG-3'
BdCYP93G1-qPCR-REV	5'-GTACCCGCCACGAATAGG-3'
TIF-qPCR-FWD	5'-CTGATAACACAAGTTCCCTGC-3'
TIF-qPCR-REV	5'-GACGGTATTTTAGCTATGGAATTG-3'
AtC4HP + SacI FWD	5'-GTGAGCTCTCCCATATGGTCGACGGAATGAGAGACGAGAGC-3'
AtC4HP + XbaI REV	5' -GCTCTAGAGCGGCCGCCTGCAGGTCGACCTAGGGGGCGAGAGTAATTG-3'

Table 2. 2: Constructs employed in this study.

Construct name	Vector type	Backbone	Insert
pDONR 221-*MdCHS3*	entry	pDONR 221	*MdCHS3*
pDONR 221-*BdCYP75B4*	entry	pDONR 221	*BdCYP75B4*
pDONR 221-*BdCYP93G1*	entry	pDONR 221	*BdCYP93G1*
Blunt II TOPO-*PaxgOMT25*	entry	Blunt II TOPO	*PaxgOMT25*
TNTpSTART-*BdCYP75B4*	entry	TNTpSTART	*BdCYP75B4*
TNTpSTART-*BdCYP93G1*	entry	TNTpSTART	*BdCYP93G1*
TNTpSTART-*2A*	entry	TNTpSTART	*2A*
TNTα1A-*BdCYP75B4*	entry	TNTα1A	*BdCYP75B4*
TNTαB-*2A*	entry	TNTαB	*2A*
TNTαC-*BdCYP93G1*	entry	TNTαC	*BdCYP93G1*
TNTΩ2-*BdCYP75B4-2A-BdCYP93G1*	entry	TNTΩ2	*BdCYP75B4-2A-BdCYP93G1*
Pet28MHL-*PaxgOMT25*	bacterial expression	Pet28-MHL	*PaxgOMT26*
ph7WGY2-*AtC4Hp::MdCHS3*	plant expression	ph7WGY2	*MdCHS3*
pk7WGY2-*AtCesA7p::BdCYP975B4*	plant expression	pk7WGY2	*BdCYP975B4*
pk7WGY2-*AtCesA7p::BdCYP93G1*	plant expression	pk7WGY2	*BdCYP993G1*
pk7WGY2-*AtCesA7p::BdCYP75B4-P2AF2A-BdCYP93G1*	plant expression	pk7WGY2	*BdCYP75B4-P2AF2A-BdCYP93G*
pk7WGY2-*AtC4Hp::BdCYP75B4-P2AF2A-BdCYP93G1*	plant expression	pk7WGY2	*BdCYP75B4-P2AF2A-BdCYP93G*
pYesDEST52-*BdCYP975B4*	yeast expression	pDEST52	*BdCYP975B4*
pYesDEST52-*BdCYP93G1*	yeast expression	pDEST52	*BdCYP993G1*
pYesDEST52-*BdCYP75B4-P2AF2A-BdCYP93G1*	yeast expression	pDEST52	*BdCYP75B4-P2AF2A-BdCYP93G*

Chapter 3: Exogenous chalcone synthase expression in developing poplar xylem incorporates naringenin into lignins

3.1 Introduction

Lignin, a major chemical constituent of lignocellulosic biomass, poses a significant barrier to the efficient industrial processing for the production of pulp and paper, specialty chemicals and fibres, and liquid biofuels. However, this complex polyphenolic polymer may serve as a chemical precursor in the development of new bio-based materials, high-value polymers, and chemicals. Although fast-growing woody feedstocks, such as poplar and eucalyptus, represent abundant and renewable sources of lignocellulosic biomass, narrow profit margins continue to limit the economic feasibility of employing them as dedicated energy crops at an industrial scale (Yemshanov and McKenney, 2008; Shooshtarian et al., 2018).

Lignin is typically composed of three canonical monolignols: *p*-coumaryl, coniferyl, and sinapyl alcohols, which undergo oxidative coupling in the developing cell wall to form polymeric lignin. Efforts to genetically engineer the core monolignol biosynthetic pathway have led to significant changes in both content and composition of lignin, highlighting the remarkable metabolic plasticity of this biosynthetic pathway (Ralph et al., 2004; Leple et al., 2007; Coleman et al., 2008a; Sykes et al., 2015; Chanoca et al., 2019). Moreover, a wide array of non-canonical monolignols has recently been found to naturally incorporate into lignins of different plant species (Vanholme et al., 2019). For example, the stilbenoid compounds, resveratrol, piceatannol, and isorhapontigenin, have all been identified as monomers in lignins of palm fruit endocarps (del Río et al., 2017), and their respective stilbene glycosides have also been identified in the lignins of Norway spruce bark (Rencoret et al., 2019). Hydroxycinnamamides, specifically ferulamides, have been shown to incorporate into plant lignins, behaving as true lignin monomers (Negral et al., 1996; del Río et al., 2020). Also, the high-value flavonoid tricin, reported to have a wide variety of potential pharmaceutical applications (Li et al., 2016), was found incorporated at the ends of lignins in many monocots (Del Río et al., 2012; Lan et al., 2015). Recently, disruption of a *flavone synthase II* (*fnsII*) in rice resulted in the accumulation of

naringenin, a flavanone precursor to tricin and the subsequent occurrence of naringenin in the lignin-enriched cell wall fraction, indicating that other flavonoids could be engineered into grass lignins as well (Lam et al., 2017).

Chalcone synthase catalyzes the first committed reaction in the production of flavonoid compounds by combining *p*-coumaroyl-CoA, a precursor in the monolignol biosynthetic pathway, with three malonyl-CoA units to produce naringenin chalcone, which is then cyclized to naringenin (Figure 3.1). Previous genetic manipulations in plants have shown that the flavonoid and monolignol biosynthetic pathways are tightly linked. For example, RNAi-mediated silencing of an important monolignol biosynthetic gene, *hydroxycinnamoyl-CoA:shikimate hydroxycinnamoyl transferase* (*HCT*), in *Arabidopsis* has led to the accumulation of flavonoids (Hoffmann et al., 2004). Similarly, downregulation of a monolignol biosynthetic gene, *caffeoyl-CoA O-methyl transferase* (*CCoAOMT*), in alfalfa (*Medicago sativa* L.) resulted in the accumulation of isoflavonoids, the predominant class of flavonoids in legumes (Gill et al., 2018). Conversely, silencing of *CHS* in corn resulted in drastically reduced levels of the flavonoids apigenin and tricin, yet caused a significant increase in total lignin content of leaves (Eloy et al., 2017). Taken together, these results indicate that CHS plays an important role in directing carbon flux between monolignol and flavonoid pathways. In poplar, transgenic down regulation of *4-coumarate:coenzyme A ligase* (4CL), another key monolignol biosynthetic gene, resulted in a reduction of lignin and led to the accumulation of the naringenin and kaempferol in stem extractives of transgenic trees (Voelker et al., 2010). Notably, naringenin and kaempferol were not observed in extractives of WT stem tissue, indicating that *CHS* expression may be low in stem tissue (Voelker et al., 2010). To confirm this, we examined expression of all six previously identified putative poplar *CHS* genes (Zavala and Opazo, 2015) in WT hybrid poplar used for genetic transformation (*Populus abla x grandidentata*). We determined that expression levels were considerably lower in xylem tissue compared to leaf tissue, where flavonoids are known to accumulate (Figure 3.2; Tian et al., 2021). Thus, overexpression of *CHS* in lignifying tissues of poplar, which does not appear to contain high levels of flavonoids, may serve to reduce lignin by redirecting carbon flux away from monolignol biosynthesis while simultaneously producing

high-value flavonoids that could be incorporated into the lignins of important potential bioenergy crops such as poplar, adding further value to woody feedstocks.

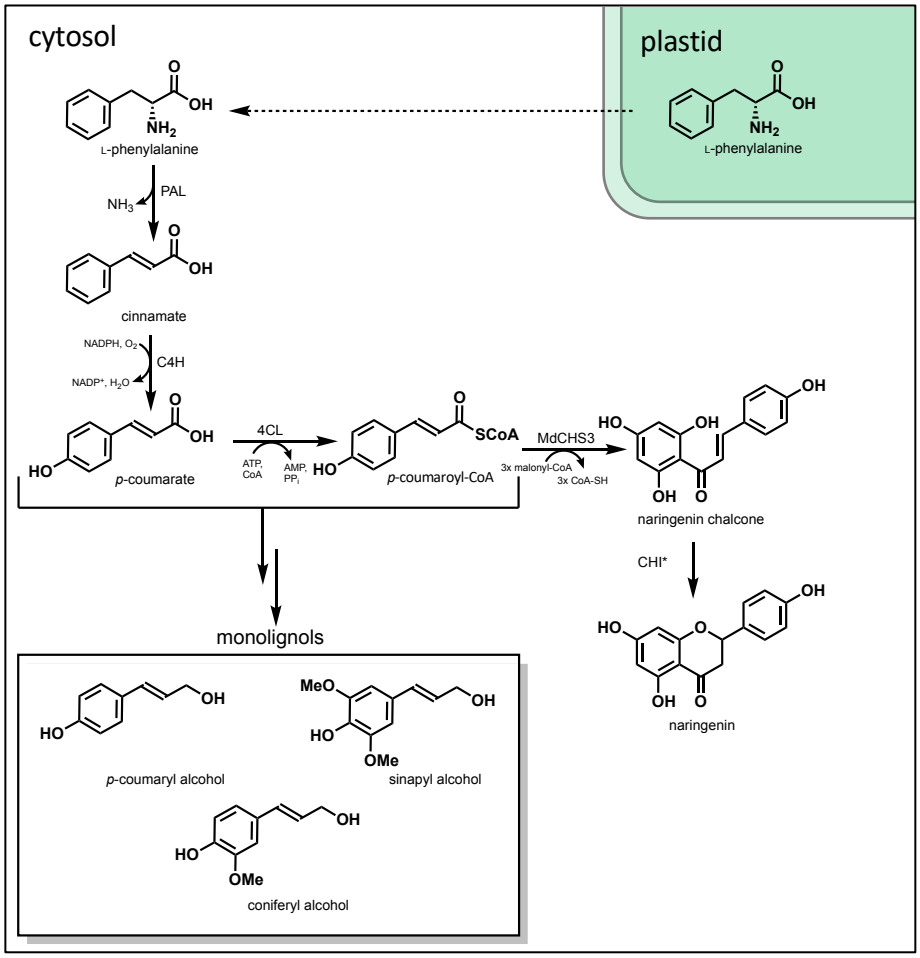

Figure 3.1: Biosynthesis of naringenin in xylem tissue.

Phenylalanine is produced in the plastid via the shikimate pathway and transported into the cytosol where it is deaminated by phenylalanine-ammonia lyase (PAL) to produce cinnamate, which is then hydroxylated by cinnamate-4-hydroxylase (C4H) producing *p*-coumarate. *p*-Coumarate is converted to *p*-coumaroyl-CoA by 4-coumarate CoA ligase (4CL). Chalcone synthase (CHS) then combines three molecules of malonyl-CoA with *p*-coumaroyl-CoA producing naringenin chalcone, which is isomerized to (2*S*)-naringenin by chalcone isomerase (CHI). *p*-Coumaroyl-CoA and *p*-coumarate are both important precursors in the biosynthesis of monolignols: *p*-coumaryl alcohol, coniferyl, alcohol, and sinapyl alcohol.

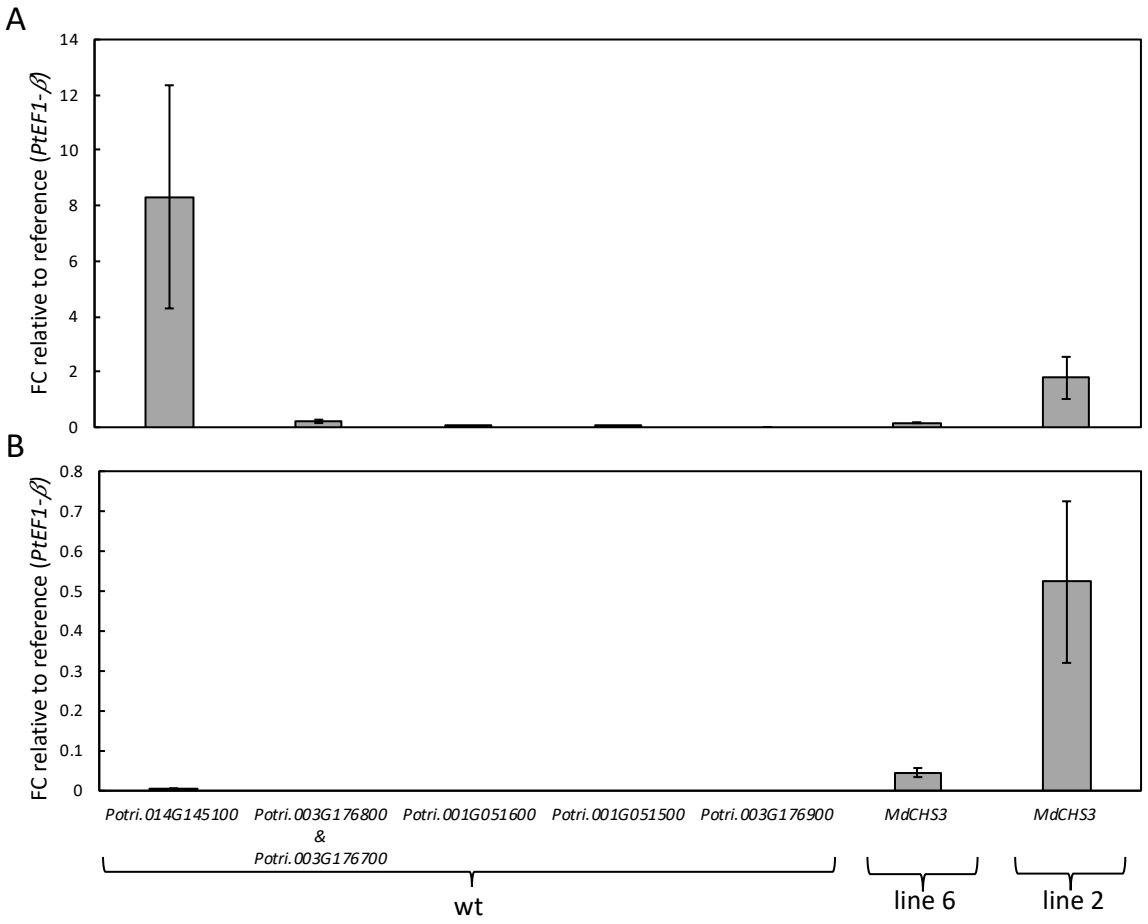

Figure 3.2: Relative expression of six putative endogenous poplar *CHS* genes.

Relative expression in leaves (A) and xylem (B) tissue of WT poplar.Expression of *MdCHS3* in the lowest (line 6) and highest (line 2) expressing transgenic poplar shown for comparison. Relative expression determined by qRT-PCR and shown as fold change (FC) relative to the reference gene (*PtEF1-β)*. Error bars represent standard error across four biological replicates.

To this end, we have genetically engineered hybrid poplar (*Populus alba* x *grandidentata*) to express a previously characterized chalcone synthase gene (*MdCHS3*) derived from apple (*Malus* x *domestica*) using a lignin-specific promoter (Yahyaa et al., 2017). *MdCHS3* (accession number NM_001328985) was selected for expression in lignifying tissues as it shows high substrate affinity for *p*-coumaroyl-CoA relative to reported Km values for competing poplar enzymes in the lignin biosynthetic pathway (Wang et al., 2018). MdCHS3 was also reported to display greater substrate specificity for *p*-coumaroyl-CoA over cinnamoyl-CoA

making it a good candidate for expression in poplar xylem (Yahyaa et al., 2017). Poplar expressing *MdCHS3* in xylem tissue (hereafter referred to as *MdCHS3*-poplar) clearly displayed an accumulation of naringenin in xylem methanolic extracts, not inherently observable in WT, and NMR analysis revealed the novel incorporation of this flavonoid compound (a flavanone) into polymeric lignins. In addition, the highest expressing *MdCHS3*-poplar lines displayed reduced total lignin, increased cell wall carbohydrate content, yet displayed no changes in growth or biomass compared to their WT counterparts and significantly improved saccharification efficiency after dilute acid pretreatment.

3.2 Results

3.2.1 Generation of transgenic poplar expressing *MdCHS3*

MdCHS3 was previously characterized and shown to display greater substrate specificity for *p*-coumaroyl-CoA compared to cinnamoyl-CoA, as well as high catalytic efficiency (Yahyaa et al., 2017). As such, *MdCHS3* was selected to drive production of naringenin in the developing xylem of poplar. *MdCHS3* was isolated from golden delicious apple seedlings and inserted into a plant expression vector under control of a lignin-specific promoter, *AtC4Hp*. The *AtC4Hp::MdCHS3* expression construct was then transformed into hybrid poplar using *Agrobacterium*-mediated transformation as previously outlined (Wilkerson et al., 2014). Successful transformants were confirmed by genomic screening, and expression levels in leaves were subsequently determined by quantitative real-time PCR (qRT-PCR). The five highest-expressing lines were then clonally propagated and transferred to the greenhouse for growth in soil (Figure 3.3).

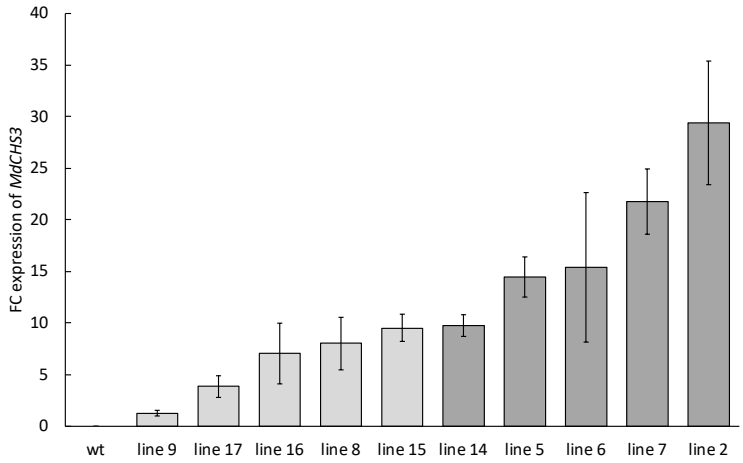

Figure 3.3: Relative expression of MdCHS3 in ten independently transformed poplar.

Tissue collected from leaves in tissue culture. The five highest expressing individuals (dark grey) were selected for clonal propagation and growth in a greenhouse. Relative expression was determined by qRT-PCR and shown as fold change (FC) relative to the lowest expressing plant (line 9), error bars represent variation across three technical replicates.

MdCHS3-poplar accumulate naringenin in developing xylem tissue

Trees were harvested after sixteen weeks of growth, and expression of *MdCHS3* in mature xylem tissue was again confirmed via qRT-PCR analysis (Figure 3.4a). UPLC-DAD analysis of methanolic extracts from *MdCHS3*-poplar xylem tissue clearly revealed the accumulation of naringenin in its aglycone form, as well as multiple unknown compounds, accumulating in *MdCHS3*-poplar xylem and not observed in WT trees (Figure 3.5). Subsequent hydrolysis of the methanolic extracts resulted in the release of additional naringenin aglycone, ostensibly freed from *O*-glycosylated forms (Figure 3.5). We detected a total of 2.49 to 9.94 μg naringenin/g dried xylem tissue in the hydrolysed methanolic extracts derived from *MdCHS3*-poplar lines, in which variability was directly correlated with the expression level of *MdCHS3* (Figure 3.4b). In comparison, no naringenin was detectable in the methanolic extracts of WT xylem after hydrolysis. *MdCHS3*-poplar displayed no significant differences in stem diameter or biomass compared to WT trees. Most transgenic lines also displayed no significant differences in height, with the exception of trees from line 14, which were significantly taller than their WT counterparts (Table 3.1; Figure 3.6).

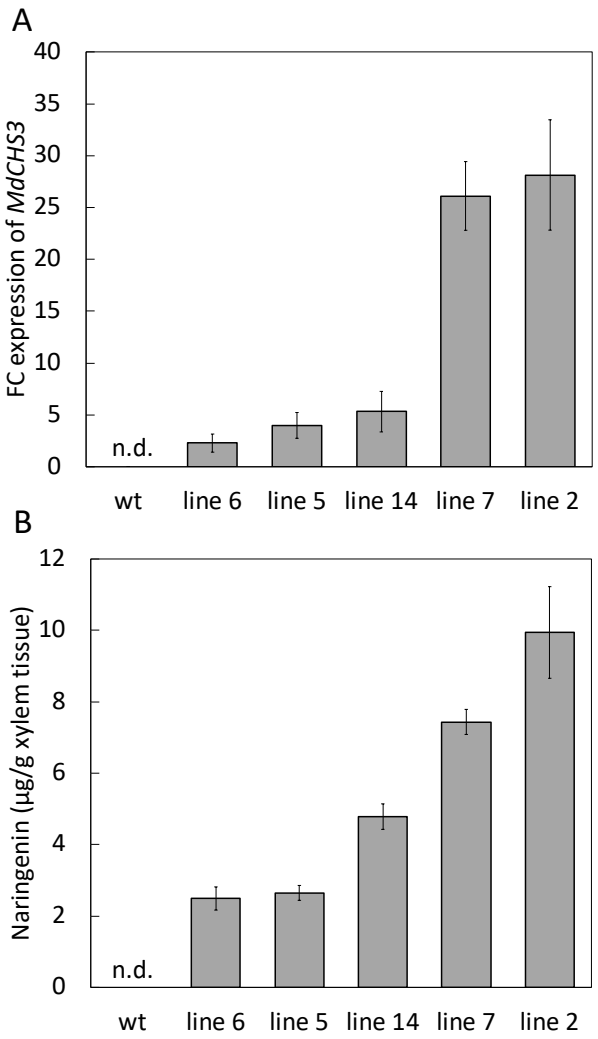

Figure 3.4: Expression of MdCHS3 in poplar xylem tissue correlated to soluble naringenin.

(A) Relative expression levels of *MdCHS3* in transgenic poplar xylem tissue determined by qRT-PCR gene expression analysis are shown as fold change (FC) relative to the lowest expressing tree, originating from *MdCHS3*-poplar line 6. Expression of *MdCHS3* was not detectable in WT poplar. Expression levels represent the mean across five biological replicates, standard error indicated by error bars. (B) Naringenin released after hydrolysis of methanolic extracts of *MdCHS3*-poplar xylem tissue. No naringenin was detectable in WT extracts (detectable levels >0.70 µg/g xylem tissue). Values represent the mean across five biological replicates for line 5, line 14, line 7, and line 2. Naringenin was detectable in only four of five biological replicates in line 6 (n=4). Standard error indicated by error bars.

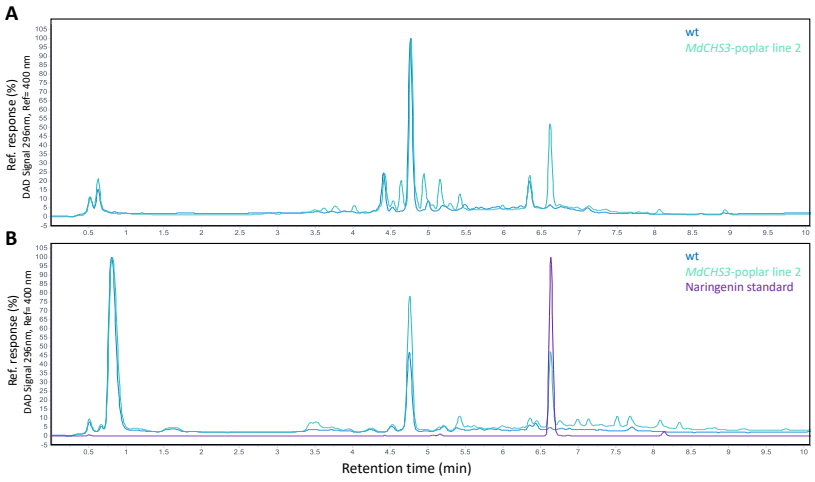

Figure 3.5: UPLC analysis of xylem methanolic extracts from *MdCHS3*-poplar.

Naringenin glycosides are present in xylem extracts of the highest expressing MdCHS3-poplar line, but are not observed in wild-type lines. UPLC analysis of xylem methanolic extracts display clear differences between wild-type (blue) and the highest expressing *MdCHS3*-poplar line 2 (green). Xylem methanolic extracts (A), hydrolysed methanolic extracts (B), naringenin standard (purple).

Table 3.1: Mean growth measurements of wild-type and *MdCHS3*-poplar.

Values represent the mean growth across five biological replicates per line after sixteen weeks. Standard error is represented in brackets. Significant differences ($p<0.05$) compared to wild-type are bolded and were determined using Student's t-test.

Poplar line	Height (cm)	Stem diameter (cm)	Fresh biomass (g)
wt	174.6 (4.87)	3.708 (0.18)	472.8 (48.36)
line 6	174.2 (9.69)	3.352 (0.28)	409.4 (71.27)
line 5	182.2 (5.01)	3.302 (0.11)	393.2 (38.09)
line 14	**192.6 (2.66)**	3.708 (0.29)	471.8 (28.52)
line 7	183.0 (3.55)	3.556 (0.16)	413.4 (20.76)
line 2	179.4 (8.70)	3.200 (0.21)	375.8 (54.05)

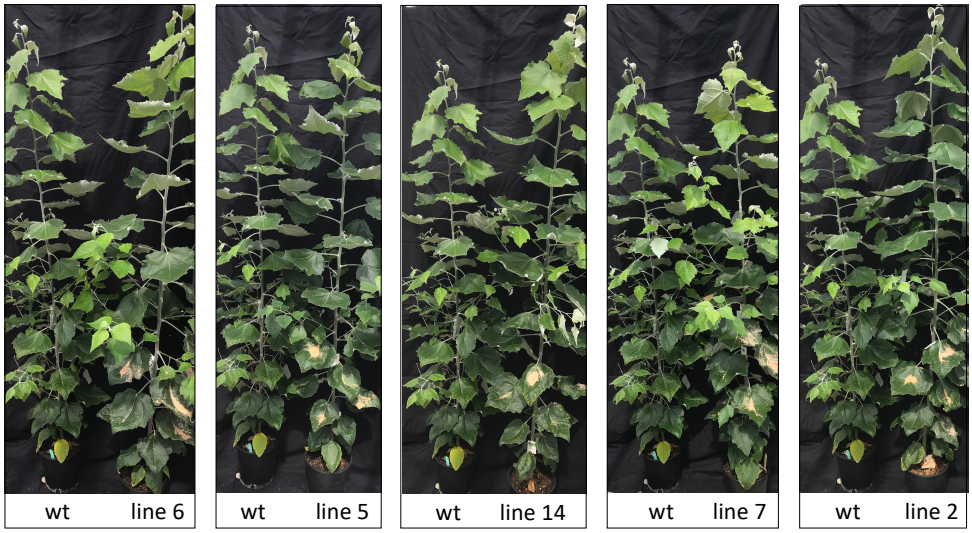

Figure 3.6: MdCHS3-poplar displays no obvious growth penalties.

Photos of individuals representing each of the five *MdCHS3*-poplar lines next to a WT tree after sixteen weeks of growth.

3.2.2 MdCHS3-poplar exhibit changes to cell wall composition

Ectopic *MdCHS3* expression draws carbon away from the monolignol biosynthetic pathway by combining *p*-coumaroyl-CoA with three molecules of malonyl-CoA to produce naringenin chalcone (Figure 3.1). To further investigate the impact of *MdCHS3* expression on lignin biosynthesis, we performed Klason lignin analysis and thioacidolysis on dried, extract-free xylem tissue. The higher-expressing *MdCHS3*-poplar lines (lines 5, 14, 7, and 2) displayed significant reductions in acid-insoluble lignin, as low as 14.87% total cell wall content, compared to 16.72% in WT whereas no differences in acid-soluble lignin were observed (Table 3.2). The three highest expressing *MdCHS3*-poplar lines (lines 2, 7 and 14) also contained significantly less total lignin, as low as 18.16% total cell wall content compared to 20.2% observed in WT trees (Table 3.2). Thioacidolysis indicated no significant differences in lignin S:G ratio (Table 3.2).

Table 3.2: Cell wall composition of WT and MdCHS3-poplar xylem.

Total lignin content measured in extract free whole cell wall material of WT control and *MdCHS3*-hybrid poplar xylem determined using Klason lignin analysis. Lignin monomeric composition was determined by thioacidolysis and relative % carbohydrate cell wall content determined by holocellulose and alpha cellulose reactions. Values represent the mean across five biological replicates per line, standard error in brackets. Statistical significance compared to WT are bolded ($p<0.05$) and were determined using Student's t-test.

	Lignin content (mg/100 mg)			Monomer	% holo-	% alpha cellulose
Poplar	Acid-soluble	Acid-insoluble	Total Lignin	S:G ratio	cellulose	
WT	3.47 (0.23)	16.72 (0.12)	20.19 (0.30)	2.79 (0.05)	63.77 (0.62)	35.90 (0.36)
line 6	3.56 (0.12)	16.04 (0.36)	19.60 (0.38)	2.71 (0.10)	**66.75 (1.00)**	37.20 (1.39)
line 5	4.01 (0.15)	**16.15 (0.19)**	20.16 (0.20)	2.71 (0.09)	65.42 (0.69)	33.02 (1.53)
line 14	3.35 (0.10)	**15.70 (0.17)**	**19.05 (0.22)**	2.74 (0.02)	**66.74 (0.98)**	37.53 (1.30)
line 7	3.22 (0.21)	**14.94 (0.39)**	**18.16 (0.47)**	2.77 (0.03)	64.70 (0.76)	**36.24 (0.60)**
line 2	3.42 (0.12)	**14.87 (0.27)**	**18.27 (0.30)**	2.65 (0.05)	64.50 (0.29)	**38.77 (1.06)**

Reductions in lignin are often associated with changes to cell wall carbohydrate content (Coleman et al., 2008a; Van Acker et al., 2013; Sykes et al., 2015). HPLC analyses of the individual cell wall carbohydrates released during secondary acid hydrolysis revealed a significant increase in glucose, as well as increases in galactose and rhamnose in the highest-expressing line (line 2) compared to WT (Table 3.2 & 3.3). In order to ascertain if the increased glucose content is derived from cellulose or hemicellulose, alpha cellulose was determined. Significant increase in alpha cellulose was observed in three of the transgenic lines (Table 3.2). An examination of acetic acid released from the cell wall following saponification demonstrated a slight but significant reduction in the cell wall acetate content of the highest-expressing *MdCHS3*-poplar line 2 compared to WT (Table 3.4). Together these results indicate that expression of *MdCHS3* led to not only the production of naringenin in developing xylem tissue but also to significant alterations in cell wall composition.

Table 3.3: Structural cell wall carbohydrates in xylem MdCHS3-poplar.

Values represent the mean (μg/mg extracted tissue) across five biological replicates per line. Standard error is represented in brackets. Means were estimated from a mixed-effect model controlling for differences across four separate hydrolysis batches of twenty four reactions each. Significant differences compared to wild-type are bolded ($p<0.05$).

	Structural carbohydrates (μg/mg)						
Poplar line	Arabinose	Rhamnose	Galactose	Glucose	Xylose	Mannose	Total carbohydrates
wt	3.35 (0.13)	4.18 (0.14)	7.53 (0.76)	432.97 (8.49)	174.45 (5.89)	10.05 (1.12)	638.22 (12.59)
line 6	3.36 (0.14)	4.62 (0.14)	8.98 (0.76)	434.87 (7.76)	170.62 (5.89)	11.97 (1.16)	643.53 (12.59)
line 5	3.58 (0.14)	4.69 (0.14)	8.58 (0.77)	450.41 (7.93)	175.69 (5.95)	13.39 (1.13)	656.05 (11.85)
line 14	3.51 (0.13)	4.51 (0.14)	8.56 (0.76)	442.91 (7.76)	172.95 (6.20)	9.68 (1.12)	646.85 (11.65)
line 7	3.95 (0.14)	4.67 (0.15)	9.00 (0.81)	444.28 (8.48)	182.55 (6.20)	9.00 (1.16)	653.27 (12.58)
line 2	3.54 (0.13)	**4.91 (0.14)**	**10.51 (0.76)**	**466.58 (7.75)**	198.47 (5.89)	11.21 (1.12)	670.00 (11.64)

Table 3.4: Cell wall acetate content in xylem tissue of MdCHS3-poplar.
Values represent the mean % acetate released from extract free cell wall material by saponification across five biological replicates per line. Standard error is represented in brackets. Significant differences were detected between *MdCHS3*-poplar line 2 and wild-type poplar, as determined by Student's t-test ($p<0.05$).

Poplar line	% Acetate
wt	5.88 (0.13)
line 6	5.90 (0.04)
line 5	5.69 (0.13)
line 14	5.77 (0.20)
line 7	5.64 (0.21)
line 2	**5.59 (0.11)**

Naringenin, along with other flavonoids, is reported to inhibit auxin transport, resulting in tissue-specific accumulation of auxin (Brown et al., 2001; Peer et al., 2004; Peer and Murphy, 2007). This accumulation of auxin in cambial tissue and developing xylem could potentially initiate tension wood formation, which in-turn could manifest itself in altering the cell wall carbohydrate profile (Gerttula et al., 2015). To investigate this possibility, we examined stem sections from the highest-expressing *MdCHS3*-poplar line 2 for evidence of tension wood formation; however, transgenics exhibited no differences in vessel number, area, or width

compared to WT trees, nor was there a notable increase in cellulose staining with calcofluor white in cross sections, suggesting that the change to cell wall carbohydrates is not the result of tension wood formation (Table 3.5: Figure 3.7).

Table 3.5: Vessel count and area in cross-sections of sixteen-week-old MdCHS3-poplar (line 2).

Values represent the mean across three biological replicates with standard error represented in brackets. A total of fifteen vessels per biological replicate were measured for area and width. No significant differences were detected between *MdCHS2*-poplar line 2 and wild-type, as determined by Student's test.

Line	Area per vessel (μm^2)	Width (μm^2)	Vessel count (per 100 000 μm^2)
wt	1531.37 (324.14)	47.01 (6.18)	15.91 (1.85)
line 2	1578.64 (335.17)	50.01 (6.14)	14.74 (1.23)

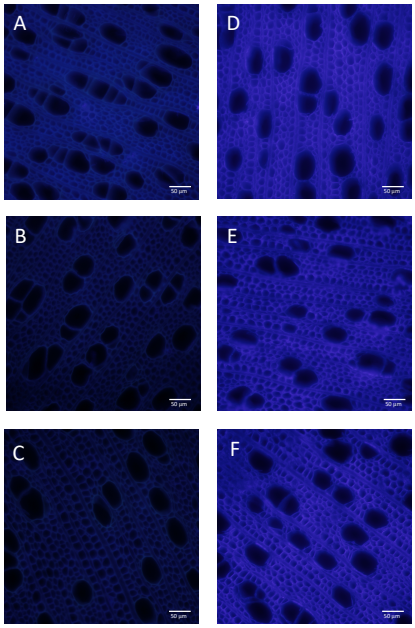

Figure 3.7: Autofluorescence and calcofluor white staining of stem tissue.

Autofluorescence (A-C) and calcofluor white (D-F) staining of wild-type (A,D), *MdCHS3*-poplar line 2 (B,E) and *MdCHS3*-poplar line 7 (C,F). Transgenic lines exhibit no differences in vessel size and number and no increase in cellulose staining with calcofluor white (Magnification 20x, Scale bars= 50 μm).

3.2.3 Naringenin is incorporated into *MdCHS3*-poplar lignins

Flavonoids, such as tricin, naturally incorporate into the lignins of monocot species such as grasses (Del Río et al., 2012; Lan et al., 2016). Moreover, $^{1}H–^{13}C$ correlation (HSQC) NMR has identified naringenin in the lignin-enriched cell wall residue fraction of rice *fnsII* mutants with disrupted tricin biosynthesis (Lam et al., 2017). To determine whether naringenin is incorporated into the lignins of *MdCHS3*-poplar, we compared the lignin fraction (enzyme lignin) of WT and transgenic xylem tissue using 2D $^{1}H–^{13}C$ HSQC NMR. Analysis of the aromatic subregions revealed no significant differences in canonical lignin components between WT and transgenic trees (Figure 3.8). However, trace signals at δ_C/δ_H 94.8/5.98 (C_8), 95.7/6.00 (C_6), and 128.1/7.36 ($C_{2'/6'}$) consistent with naringenin (or its phenolic ether) were observed in the lignin fraction of *MdCHS3*-poplar, but not in WT (Figure 3.8). The $C_{3'/5'}$ peak at δ_C/δ_H 115.0/6.88 of naringenin cannot be visible in the lignin data because it is superimposed on one of normal G-

unit peaks. We confirmed the presence of naringenin in transgenic lignins by comparing the spectra from the transgenic to that of a synthetic lignin polymer containing naringenin, which was prepared via an *in vitro* peroxidase-catalysed polymerization (dehydrogenation polymer, DHP) of naringenin (N) and coniferyl alcohol (CA) (Figure 3.8 & 3.9). In addition, trace signals at δ_C/δ_H 78.3/5.45 and δ_C/δ_H 41.8/3.27 & 2.70 corresponding to C_2 and C_3 of naringenin respectively were observed in the aliphatic subregions of both transgenic lignin fraction and synthetic N+CA lignin polymer HSQC spectra (Figure 3.9). No differences were observed in the polysaccharide anomeric subregions of WT and *MdCHS3*-poplar whole cell wall samples (Figure 3.10). Finally, 2D HSQC NMR of 80% ethanol extracts clearly showed the presence of naringenin in *MdCHS3*-poplar xylem extracts but not in WT extracts (Figure 3.8 & 3.9).

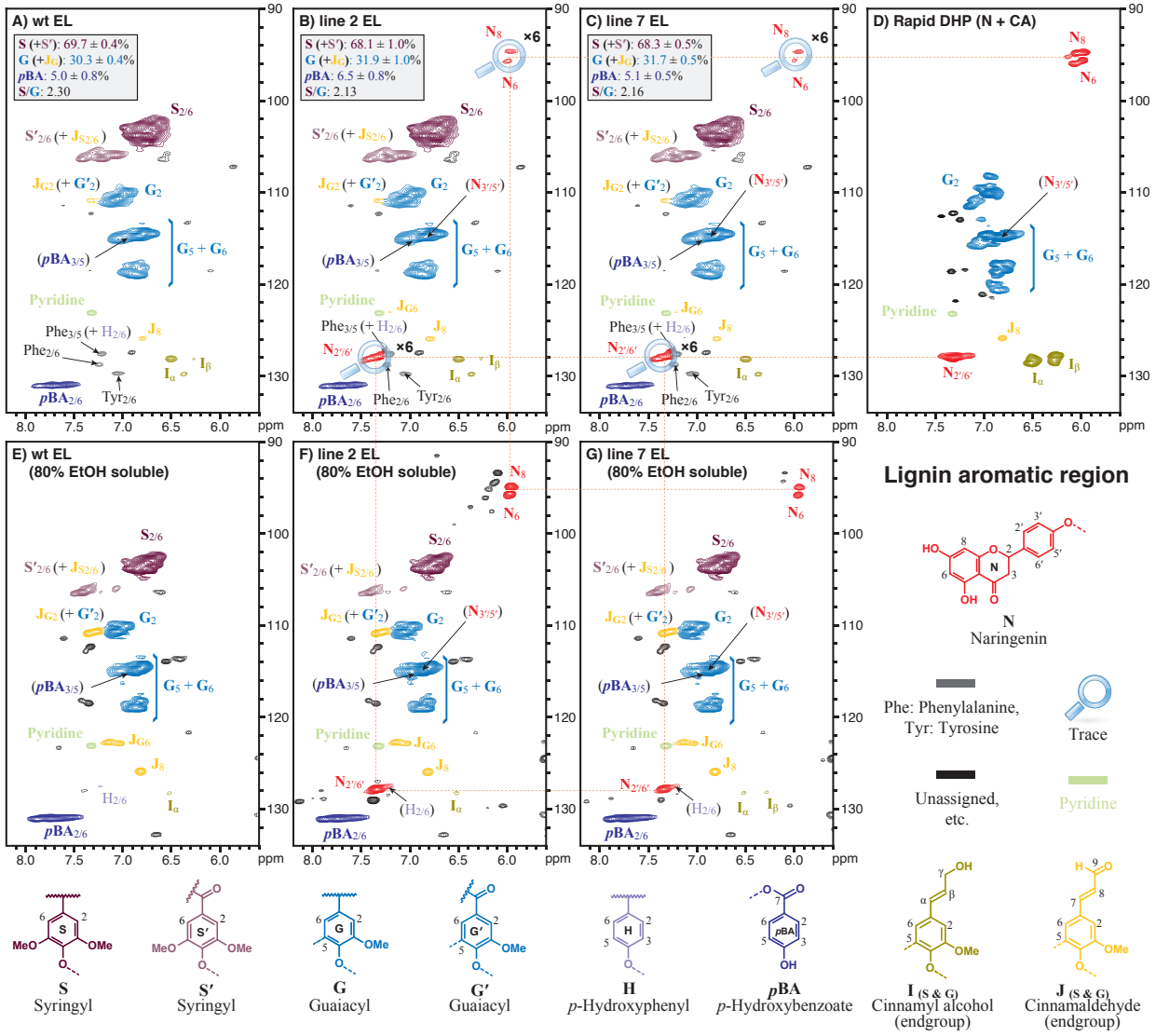

Figure 3.8: Analysis of aromatic region in 2D HSQC-NMR spectra of *MdCHS3*-poplar lignin.

NMR analysis reveals the presence of naringenin in both the soluble extract and polymeric lignin fraction of MdCHS3-poplar xylem tissue. (A-C) Cellulase digested xylem enzyme lignin (EL) fraction of WT and *MdCHS3*-poplar line 2 and line 7 xylem tissue. D, DHP prepared from naringenin and coniferyl alcohol. (E-F) Soluble fraction extracted with 80% ethanol from xylem tissue of WT and *MdCHS3*-poplar line 2 and line 7. Percentages represent the average across three biological replicates per line.

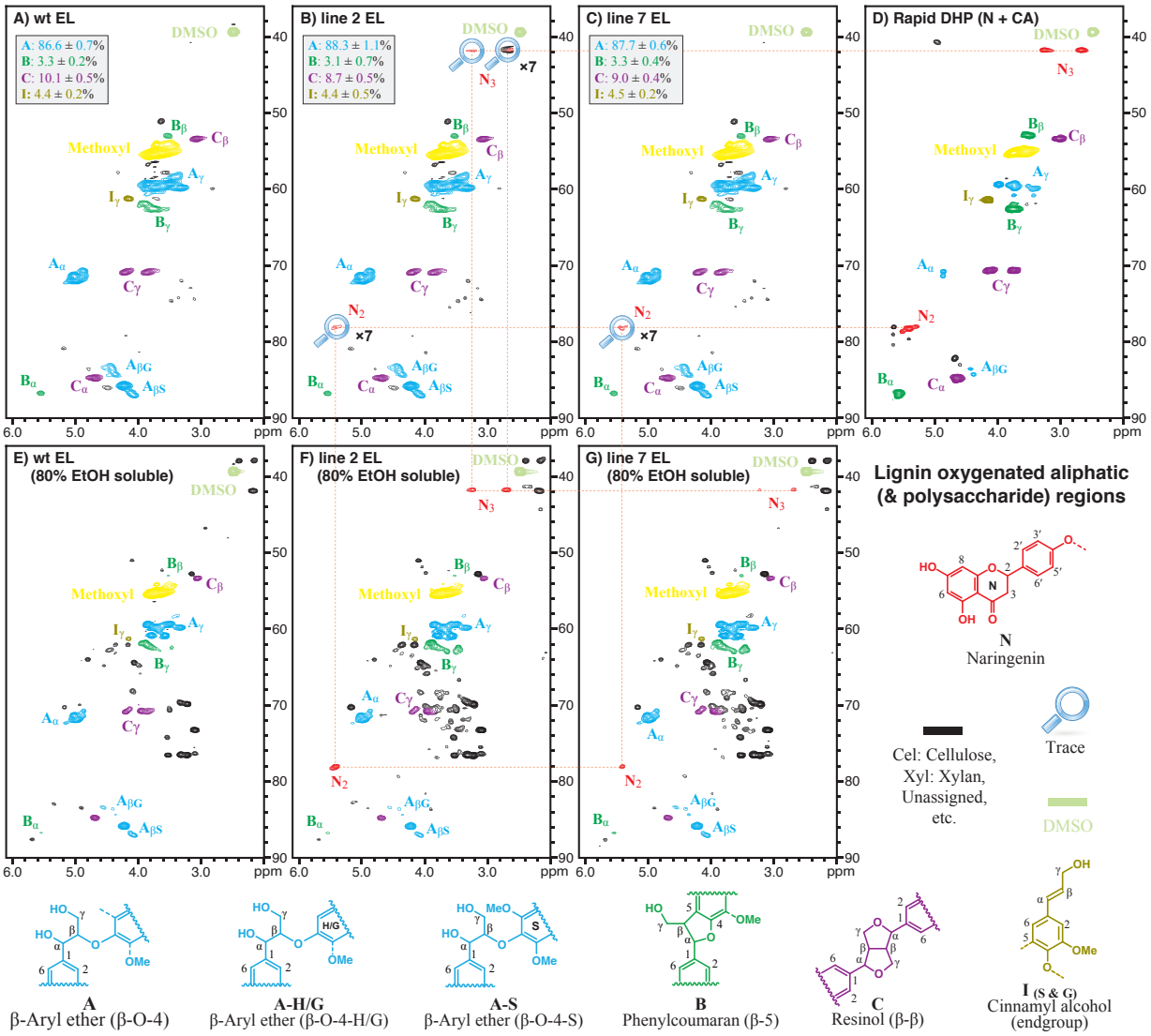

Figure 3.9: Analysis of aliphatic region in 2D-HSQC-NMR of *MdCHS3*-poplar lignin.

Analysis indicates the presence of naringenin in both the soluble extract and lignin fraction of MdCHS3-poplar xylem tissue. (A-C) Cellulase digested enzyme lignin (EL) fraction of WT and *MdCHS3*-poplar line 2 and line 7 xylem tissue. D, DHP prepared from naringenin and coniferyl alcohol. (E-F) Soluble fraction extracted with 80% ethanol from xylem tissue of WT and *MdCHS3*-poplar line 2 and line 7. Percentages represent an average across three biological replicates per line.

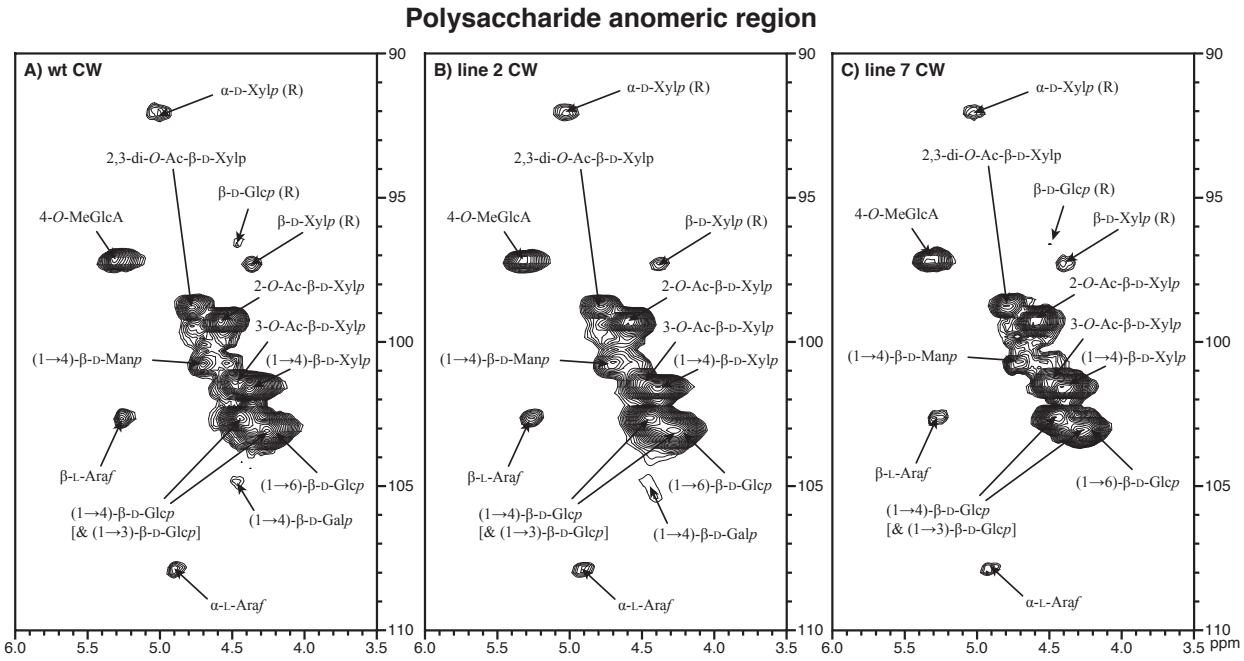

Figure 3.10: 2D HSQC NMR spectra of whole cell walls displaying polysaccharide anomerics.

Little difference observed between WT and *MdCHS3*-poplar lines. Common polysaccharide nomenclature is used for peak identification.

3.2.4 MdCHS3-poplars exhibit improved rates of limited saccharification

Reductions in total lignin have often resulted in improved rates of glucose and xylose release during enzymatic digestion of lignocellulosic biomass, due to relative increase in cell wall polysaccharides and improved accessibility to celluloses and hemicelluloses by cellulytic enzymes (Mooney et al., 1998; Berlin et al., 2005; Mansfield et al., 2012a; Chanoca et al., 2019). To better understand the impact of reduced total lignin observed in *MdCHS3*-poplar combined with increased cell wall polysaccharides and incorporation of naringenin into lignins, we conducted a limited saccharification experiment on poplar wood both untreated and pretreated with dilute acid. Following 72-hours of saccharification, glucose and xylose release reached a plateau (Figure 3.11). All pretreated *MdCHS3* lines and four of the untreated *MdCHS3* lines released significantly more glucose after 72 hours of saccharification (Figure 3.11a). Compared to WT, line 2 released 48% more glucose when not pretreated and 39% more glucose when pretreated with a mild acid (Figure 3.11a). We also observed a significant

increase in xylose released from the two highest expressing lines compared to WT following no pretreatment, line 7 releasing 21% more xylose than WT (Figure 3.12b). No increase in the released xylose was observed for any of the lines pretreated with a mild acid (Figure 3.12b), which is likely a function of the acid pretreatment employed prior to enzymatic hydrolysis that alone could facilitate the hydrolysis of the available xylan into its monomeric constituents.

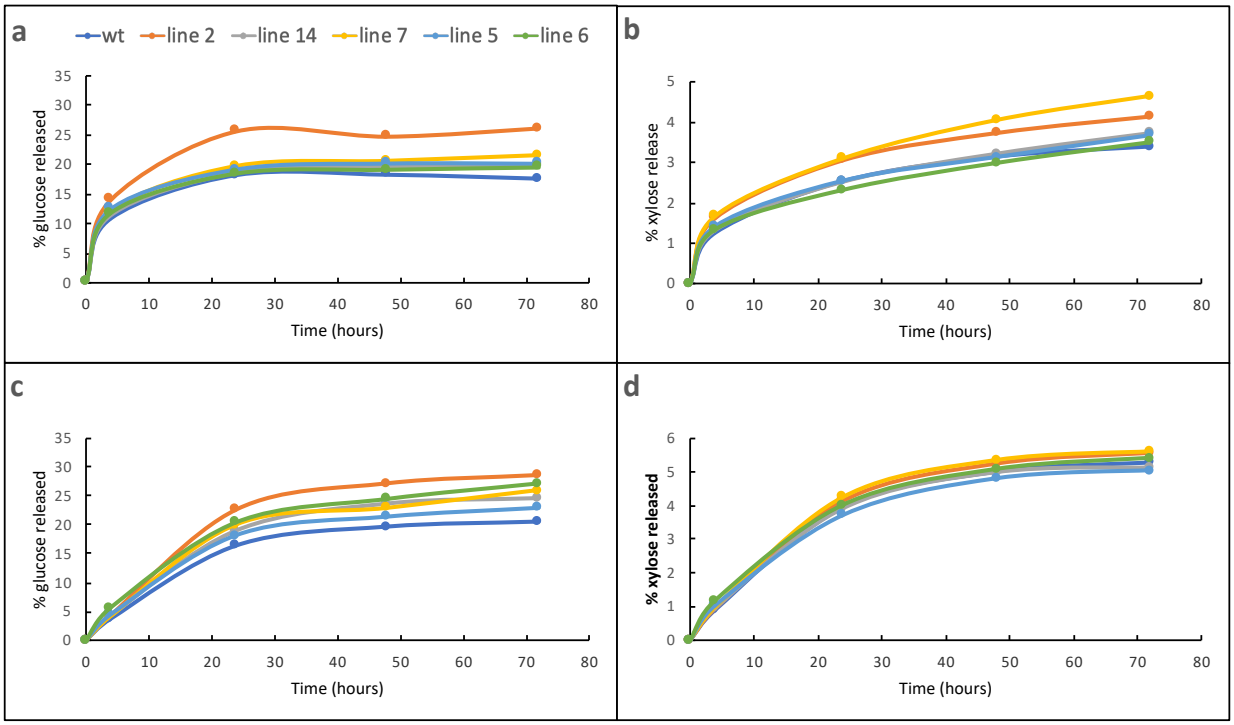

Figure 3.11: Glucose and xylose released from xylem tissue during saccharification.

Release of both glucose and xylose plateaus over time during saccharification. **a,** Percentage of glucose released from xylem tissue after no pretreatment. **b,** Percentage of xylose release after no pretreatment. **c,** Percentage of glucose released after mild acid pretreatment. **d,** Percentage of xylose released after mild acid pretreatment.

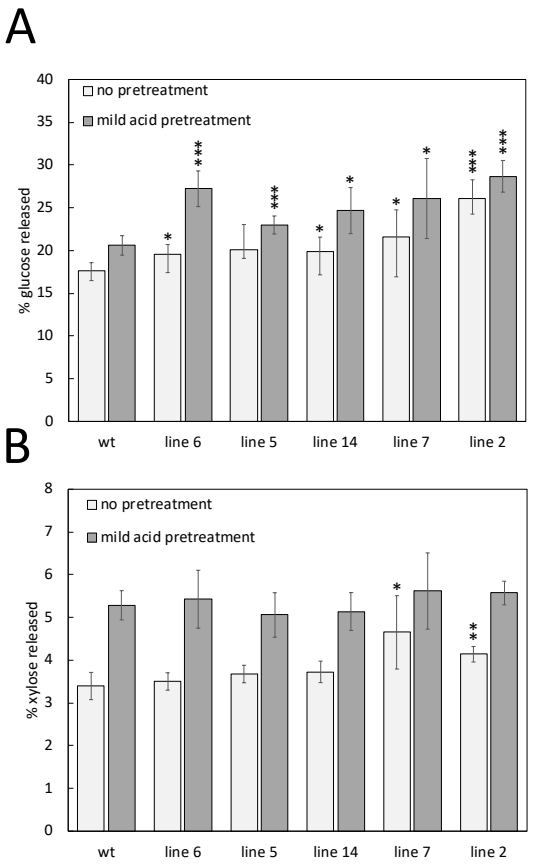

Figure 3.12:MdCHS3-poplar lines display significantly improved saccharification rates.

(A) Percentage of glucose released from non -pretreated and mild-acid pretreated xylem tissue of WT and *MdCHS3*-poplar lines after 72 h saccharification. (B) Percentage of xylose released during saccharification after no pretreatment and after mild acid pretreatment. Values represent the mean taken across five biological replicates, two technical replicates each. Error bars represent standard deviation between biological replicates. Significant differences (*p<0.1, **p<0.05, ***p<0.01) compared to WT are starred and were determined using Student's t-test.

3.3 Discussion

Lignin is an important component of plant secondary cell walls, serving to facilitate water transport throughout the plant, support vertical growth, and protect against pests and pathogens (Weng and Chapple, 2010). Disruption of monolignol biosynthesis has led to significant reductions in lignin content and greatly improved biomass processability, yet these modifications often result in growth penalties (Coleman et al., 2008a; Coleman et al., 2008b; Chanoca et al., 2019). This has motivated interest in genetic modifications of woody feedstock that specifically alter the composition of lignin, such as the incorporation of novel valuable monomers, as a method of improving lignocellulosic biomass (Mottiar et al., 2016; Mahon and Mansfield, 2019).

3.3.1 MdCHS3 expression produces naringenin and lowers lignin

Expression of *MdCHS3* in hybrid poplar xylem resulted in an appreciable accumulation of naringenin in soluble extracts, in the form of glycosides, as well as accumulation of naringenin in the cell wall ostensibly incorporated into lignin. Poplar have been reported to produce naringenin endogenously in apical tissues, consisting of leaves and three youngest internodia (Morreel et al., 2006) as well as bud exudates (W. Greenaway, 1991). Low amounts of naringenin have even been reported in wood of mature poplar species both in its aglycone and glycosylated form (Pietarinen et al., 2006). However, in this study, naringenin was not observed in WT xylem extracts or EL of WT trees, nor does it appear to accumulate in stem tissue of younger trees (Voelker et al., 2010). In addition, we determined that expression levels of endogenous poplar *CHS* genes in WT xylem were significantly lower compared to *MdCHS3* in the lowest expressing transgenic line (line 6) which produced only trace amounts of naringenin in xylem (Figure 3.2). Our data demonstrates that expression of an exogenous *CHS* gene is sufficient to substantially increase production of naringenin in poplar xylem without introduction of an exogenous chalcone isomerase (*CHI*), the enzyme responsible for stereospecific ring closure of naringenin (Figure 3.1; Austin and Noel, 2003). The reduction in lignin observed in the highest-expressing lines could indicate that MdCHS3 is drawing significant carbon away from the biosynthesis of monolignols towards production of naringenin chalcone.

However, naringenin itself may play a role in suppression of lignin biosynthesis and contribute to the reduction in lignin observed in *MdCHS3*-poplar. Work in *Eucalyptus urograndis* demonstrated that root supplementation with naringenin altered lignin composition and resulted in downregulation of several lignin-related genes (Lepikson-Neto et al., 2013), and naringenin has been reported to directly inhibit the activity of 4-coumarate CoA ligase (4CL), an important monolignol biosynthetic gene, *in vitro* (Voo et al., 1995).

3.3.2 Naringenin is incorporated into poplar lignins as a novel lignin monomer

Flavonoids have been found incorporated into the lignins of many grasses and other monocot species (Del Río et al., 2012; Lan et al., 2016). 2D HSQC NMR analysis herein revealed the presence of naringenin in the lignin fraction of *MdCHS3*-poplar. To the best of our knowledge, this is the first report of a flavonoid compound being incorporated into poplar wood lignins as the result of genetic engineering. Naringenin was found to incorporate instead of tricin into the lignins of rice with disrupted *FNSII* expression via reactions occurring at the B ring resulting in 4'-O-β type coupling, which in turn results in β-aryl ether units, and 3'-β type coupling to produce phenylcoumaran units (Lam et al., 2017). Our data are consistent with previous NMR analyses of synthetic lignin polymers generated from radical coupling of naringenin with coniferyl alcohol, which shows that the phloroglucinol ring remains intact, suggesting that coupling occurs mainly at the *p*-hydroxyphenyl B-ring over the phloroglucinol A-ring (Lam et al., 2017). This bears significance as the introduction of lignin monomers capable of single coupling reactions, such as naringenin, into lignifying tissue has been proposed as a strategy to reduce the length of lignin polymers and improve lignin solubilization during pretreatment processing (Eudes et al., 2012; Mottiar et al., 2016; Mahon and Mansfield, 2019). Due to the presence of both 4'-O-β and 3'-β type linkages, quantitative methods such as thioacidolysis, which are targeted at releasing naringenin from lignin, would only cleave 4'-O-β linkages. Considering that thioacidolysis only releases monolignols which account for ~ 10% of total lignin and considering that only trace amounts or naringenin were observed by NMR in the lignin fraction of *MdCHS3*-poplar xylem, thioacidolysis would not serve as an effective method of quantifying the incorporation of naringenin into lignin polymers.

The occurrence of naringenin in the cell wall space raises questions concerning its export across the cell membrane. A comprehensive model describing the mechanisms of monolignol export from the site of synthesis to the cell wall space has yet to emerge (Perkins et al., 2019), although molecular simulations estimating membrane permeability of tricin indicated that passive diffusion alone is sufficient to facilitate transmembrane efflux (Vermaas et al., 2019). It is, therefore, possible that naringenin is similarly capable of passive diffusion across the membrane in its aglycone form; however, active transport by an unknown endogenous poplar transporter cannot be excluded. We also observed high levels of putative *O*-linked naringenin glycosides in methanolic extracts and, considering that flavonoids are often stored in the vacuole in their glycosylated forms, naringenin may also be entering the cell wall space after releasing from the vacuole during programmed cell death (Zhao and Dixon, 2010; Perkins et al., 2019).

3.3.3 Expression of *MdCHS3* improved saccharification efficiency

Some of the *MdCHS3*-poplar lines exhibited a significant increase in alpha cellulose cell wall content (Table 3.2). Analysis of cell wall carbohydrates released after hydrolysis indicated significant increases in glucose, galactose, and rhamnose in *MdCHS3* line 2 compared to WT trees (Table 3.3). The significant improvement in glucose released during saccharification of *MdCHS3*-poplar lines is likely due to the combined relative increases in cell wall carbohydrates, including glucose, and the reduction in total lignin (Table 3.2: Table 3.3). Lignin is thought to contribute to recalcitrance of lignocellulosic biomass by competitively binding cellulolytic enzymes and limiting access to cellulose (Mooney et al., 1998; Mansfield et al., 1999; Berlin et al., 2005), such that genetically modified trees with reduced lignin content often display drastically improved rates of saccharification (Leple et al., 2007; Mansfield et al., 2012a; Sykes et al., 2015). Saccharification rates may also be influenced by the reduction in lignin polymer length, as naringenin is only capable of single coupling and therefore prevents any further polymerization once incorporated (Lam et al., 2017). Reductions in polymer length have been previously associated with improvements in saccharification, ostensibly by reducing cross-linking between lignins and cell wall polysaccharides thereby improving accessibility of hydrolytic enzymes to cellulose and hemicelluloses (Eudes et al., 2012) . In addition, reductions

in cell wall acetyl content, as observed in *MdCHS3*-poplar lines, have also been shown to improve saccharification in hybrid aspen as acetylation is thought to restrict accessibility of glycanases to cell wall polysaccharides (Pawar et al., 2017).

3.4 Conclusion

By expressing *MdCHS3* in lignifying xylem tissue of hybrid poplar, we have produced transgenic trees with reduced total lignin content and increased cell wall carbohydrate content. These trees display significantly improved saccharification rates after both no pretreatment and dilute acid pretreatment. In addition, *MdCHS3*-poplar exhibits no differences in growth or biomass yield compared to WT and produced naringenin, a valuable flavonoid compound in xylem tissue. Moreover, we have identified novel incorporation of naringenin into the poplar wood lignins, demonstrating that if lignin-compatible flavonoid compounds can be produced in lignifying tissue of poplar, these compounds could be incorporated into lignin thereby potentially making them available on a high scale. Moving forward, *MdCHS3*-poplars represent a useful genetic background into which many new flavonoid biosynthetic enzymes may be introduced in order to produce other valuable lignin compatible flavonoid compounds.

Chapter 4: Engineering of tricin biosynthesis in developing xylem of poplar

4.1 Introduction

Lignin is a polyphenolic polymer found abundantly in the secondary cell walls of plant xylem tissue providing the compressive strength and hydrophobicity required to transport water over long distances and support vertical growth (Weng and Chapple, 2010). Lignin is typically composed of three hydroxycinnamoyl alcohols, or monolignols: coniferyl alcohol, sinapyl alcohol, and *p*-coumaryl alcohol, which make up the G-units, S-units, and H-units of lignin, respectively (Vanholme et al., 2010). The polymer is formed in the cell wall space when monolignols, radicalized by peroxidase or laccase enzymes, undergo a series of radical coupling reactions (Ralph et al., 2004; Vanholme et al., 2010). Lignification is a highly plastic process, and a wide diversity of non-canonical monomers have been identified in naturally occurring lignins across the plant kingdom (del Río et al., 2020). Moreover, genetic perturbations to the monolignol biosynthetic pathway have led to significant changes in the composition of lignin and to the incorporation of novel monomers into lignins (Ralph et al., 2004; Leple et al., 2007; Coleman et al., 2008a; Sykes et al., 2015; Chanoca et al., 2019). All of which suggests that if a phenolic compound is chemically compatible with polymerization and is made spatially and temporally available during lignification it could be incorporated into lignins.

Tricin is a high-value flavonoid compound widely incorporated into the ends of lignins in grasses and other monocots where it is proposed to function as a chain initiator/terminator (del Rio et al., 2012; Lan et al., 2016). A comparison of tricin levels across seed plant species demonstrated that an increase in lignin-integrated tricin is correlated with a reduced degree of polymerization (DP), and lower DP, in turn, has been shown to reduce cell wall recalcitrance to enzymatic hydrolysis (Eudes et al., 2012; Lan et al., 2016). Woody feedstocks such as poplar are fast-growing sources of lignocellulosic biomass; however, narrow profit margins continue to

limit the economic feasibility of processing lignocellulosic biomass on an industrial scale. It has been proposed that if valuable novel monomer such as tricin could be introduced into the lignins of lignocellulosic biomass, it could limit the degree of polymerization and improve processing efficiency while simultaneously adding value to lignin, where value is currently limited largely to the calorific value released in heat energy, thereby permitting more complete biomass utilization (Mottiar et al., 2016; Mahon and Mansfield, 2019).

The tricin biosynthetic pathway has recently been fully elucidated in rice (Figure 4.1; Lam et al., 2015). Researchers have identified a cytochrome P450 (CYP450) gene unique to grasses, apigenin 3'/chrysoeriol 5' hydroxylase (A3'H/C5'H) OsCYP75B4, as the key enzyme responsible for the biosynthesis of tricin (Lam et al., 2015). In addition, they have identified OsCYP93G1*,* a flavone synthase II (FNSII), which converts naringenin into apigenin and is responsible for channeling flavones towards the production of tricin *O*-linked glycosides, flavonolignans and lignin-integrated tricin (Lam et al., 2014). Finally, OsROMT9*,* a flavonoid-specific *O*-methyl transferase (OMT), has been found to perform the methylation of luteolin and selgin (Kim et al., 2006; Lam et al., 2014; Lam et al., 2015). Interestingly, *Arabidopsis tt6/tt7* double mutants, deficient in both flavanone 3-hydroxylase and flavonoid 3'-hydroxylase activity, co-expressing rice derived *OsCYP75b4* and *OsCYP93G1* genes accumulated tricin, suggesting that the endogenous OMTs in *Arabidopsis* were sufficient to support biosynthesis of tricin (Lam et al., 2015).

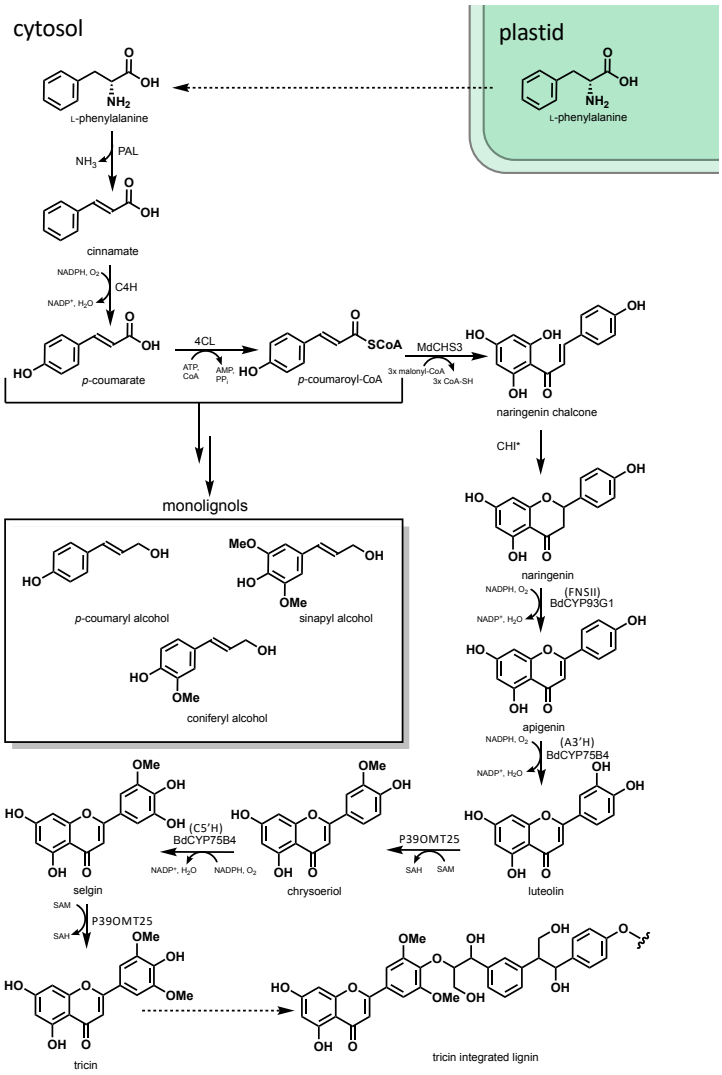

Figure 4.1: Proposed pathway for engineering the biosynthesis of tricin in poplar xylem.

MdCHS3 combines three molecules of malonyl-CoA with *p*-coumaroyl-CoA, producing naringenin chalcone, which is either isomerized by chalcone isomerase (CHI) to become (2S)-naringenin or may undergo non-stereospecific ring closure. Naringenin is converted to apigenin by BdCYP93G1, a flavone synthase. Apigenin is then hydroxylated at the 3' position by BdCYP75B4 to produce luteolin. PaxgOMT25, an endogenous poplar enzyme, methylates luteolin at the 3'-hydroxyl producing chrysoeriol, which is then hydroxylated at the 5' position by BdCYP75B4 to become selgin. Next, PaxgOMT25 methylates selgin at the 5'-hydroxyl to produce tricin. Some tricin may diffuse into the cell wall space (depending on its concentration and rates of lignification), where it will be radicalized by laccase and peroxidase enzymes and undergo oxidative coupling to be incorporated at the ends of lignin polymers.

Previously, using a lignin-specific promoter, we genetically engineered hybrid poplar (*Populus alba* x *grandidentata*) to express a characterized chalcone synthase gene (*MdCHS3*) derived from apple (*Malus* x *domestica*: Mahon et al., 2021). This resulted in the accumulation of naringenin in xylem tissue, as well as the incorporation of naringenin into lignins (Mahon et al., 2021). Here we describe our efforts to build on these promising results and express tricin biosynthetic enzymes in *MdCHS3*-poplar. To that end, we have isolated *BdCYP93G1*, an *FNSII* from *Brachypodium distachyon,* a grass species shown to accumulate high levels of lignin-integrated tricin (Lan *et al.* 2016). We have confirmed through substrate feeding assays that BdCYP93G1 is indeed capable of producing apigenin from naringenin. We have also biochemically characterized *BdCYP75B4*, an A3'H/C5'H isolated from *Brachypodium,* and confirmed through *in vitro* characterization that BdCYP75B4 is capable of hydroxylating both apigenin and chrysoeriol. Moreover, BdCYP75B4 can function as part of a bicistronic vector with BdCYP93G1 to produce luteolin from naringenin when expressed in yeast. Finally, we have isolated and biochemically characterized an endogenous OMT from hybrid poplar (*PaxgOMT25*), which is highly expressed in xylem tissue and participates in monolignol biosynthesis. Through *in vitro* analyses, we have determined that PaxgOMT25 can accept flavonoid substrates, and we have determined through kinetic analysis that PaxgOMT25 is capable of participating in tricin biosynthesis.

Consequently, the combined presence of both naringenin and a highly expressed endogenous *PaxgOMT25* in the xylem tissue of *MdCHS3*-poplar has rendered the production of tricin in lignifying xylem tissue imminently feasible. When a bicistronic construct containing *BdCYP75B4* and *BdCYP93G1* was expressed using a secondary cell wall cellulose synthase promoter (*AtCesA7p*) (*AtCesA7p:: BdCYP75B4-2A-BdCYP93G1*) in *MdCHS3*-poplar, tricin was observed to accumulate in soluble xylem extracts.

However, expression of *BdCYP75B4* and *BdCYP93G1* in *MdCHS3*-poplar severely stunted plant growth and most positive transformants were unable to grow past early shooting stages in tissue culture. In order to further investigate, we transformed wild-type and *MdCHS3* poplar with *AtCesA7p:: BdCYP75B4* and *AtCesA7p::BdCYP93G1* independently as well as with *AtC4Hp::*

BdCYP75B4/BdCYP93G1 using an alternative lignin-specific promoter (*AtC4Hp*). We found that most plants (in both wild-type and *MdCHS3* backgrounds) transformed with *BdCYP93G1* independently and as part of the bicistronic construct with *BdCYP75B4* were unable to establish adventitious roots in tissue culture and growth past the initial shooting phase. On the other hand, several of the plants transformed with *BdCYP75B4* alone were able to establish in tissue culture and grow, albeit at a slower rate than their respective background controls.

4.2 Results

4.2.1 Isolation and *in vitro* characterization of *BdCYP93G1*

OsCYP93G1 is the *FNSII* gene in rice which converts naringenin to apigenin (Figure 4.1) and was previously determined to be responsible for channelling flavones towards the production of *O*-linked tricin glycosides, flavonolignans and lignin-integrated tricin (Lam et al., 2014; Lam et al., 2017). *B. distachyon* is a grass species previously reported to accumulate large quantities of tricin (Lan et al., 2016). A comprehensive phylogenetic analysis of the *CYP93* gene family in land plants identified one putative *CYP93G1* gene in *Brachypodium, BdCYP93G1* (*Bradi5g02460.1*), which clusters closely with *OsCYP93G1* (Du et al., 2016). *BdCYP93G1* displayed 70.1% amino acid sequence identity and 78.3% sequence similarity with *OsCYP93G1* (Figure 4.2). We isolated this gene from the first internode tissue of *Brachypodium* (Bd21-3), hereafter referred to as *BdCYP93G1,* and then cloned it into the *BY4741:PcCPR1* yeast strain engineered to contain lodgepole pine cytochrome P450 reductase (PcCPR) (Geisler et al., 2016) using a galactose inducible yeast expression vector. Substrate feeding assays of *BdCYP93G1*-expressing cultures with naringenin resulted in the production of apigenin, not observed in the *GUS* expressing controls (Figure 4.3).

Figure 4.2: Multiple sequence alignment of CYP93G1 amino acid sequences.

Bradi5g02460 displays highest sequence homology to previously characterized flavone synthase from rice (*OsCYP93G1*). MAFFT amino acid alignment of CYP93 sequence from *Oryza sativa,* putative CYP93G1 sequence from *Brachypodium distachyon* (*Bradi5g02460*) and resulting protein sequence of Bradi5g02460 isolated from *Brachypodium* Bd21-3 internode tissue (*BdCYP93G1*).

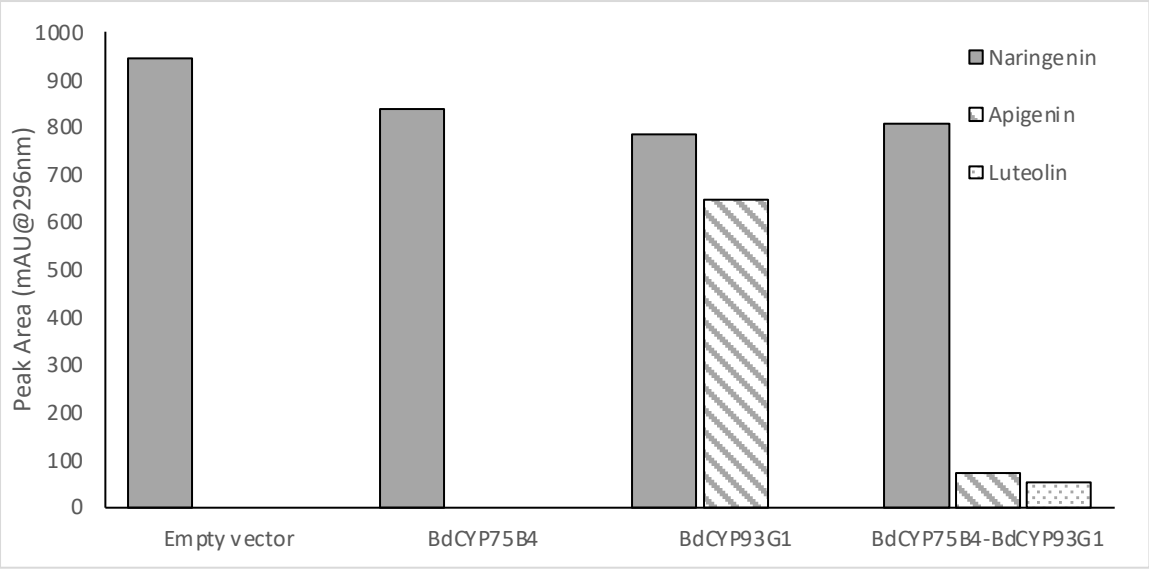

Figure 4.3: Products formed during substrate feeding assays of yeast expressing *BdCYP75B4, BdCYP93G1,* and *BdCYP75B4-2A-BdCYP93G1* fed with naringenin.

BdCYP75B4 expressing cultures produce no detectable flavonoids products, shown as peak area (mAU). *BdCYP93G1* expressing cultures produced apigenin. *BdCYP75B4-2A-BdCYP93G1* expressing cultures produce apigenin and luteolin. Negative control, *GUS* expressing cultures produce no detectable flavonoid products. Error bars represent standard error across two technical replicates. Compounds identified by comparison to elution time and isoabsobance plot of purified standards. Peak area measured at absorbance of 296nm.

4.2.2 Phylogenetic analysis of the CYP75 family in *Brachypodium* and poplar

OsCYP75B4 is the flavonoid hydroxylase which hydroxylates apigenin and chrysoeriol during tricin biosynthesis (Figure 4.1; Lam et al., 2015). In order to facilitate the biosynthesis of tricin in poplar, we isolated a homologue of *OsCYP75B4* from *Brachypodium* (Lam et al., 2015; Lan et al., 2016). Phylogenetic analysis of the flavonoid B ring hydroxylase gene family (CYP75) using amino acid sequences from *Brachypodium,* poplar, and previously characterized *A3'H/C5'H* from various plant species demonstrated that *Brachypodium* genes *Bradi1g24840* and *Bradi4g16560* clustered most closely with other monocot *CYP75B4* genes involved in tricin biosynthesis (Figure 4.4; Lam et al., 2015; Lui et al., 2020). We included the three known poplar *CYP75* genes to better understand their role in endogenous poplar flavonoid production (Nelson et al., 2008; Tanaka and Brugliera, 2013). *PtCYP75B12 (Potri.013G073300)* from poplar

clustered most closely with other dicot *CYP75Bs* known to have general flavonoid 3' hydroxylase (F3'H) activity (Figure 4.4). *PtCYP75A12 (Potri.009G069100)* and *PtCYP75A13 (Potri.001G274600)* clustered with dicot *CYP75As* reported to have F3'5'H activity (Figure 4.3). All three putative poplar *CYP75* genes displayed relatively low expression in the xylem tissue of poplar (Table 4.1).

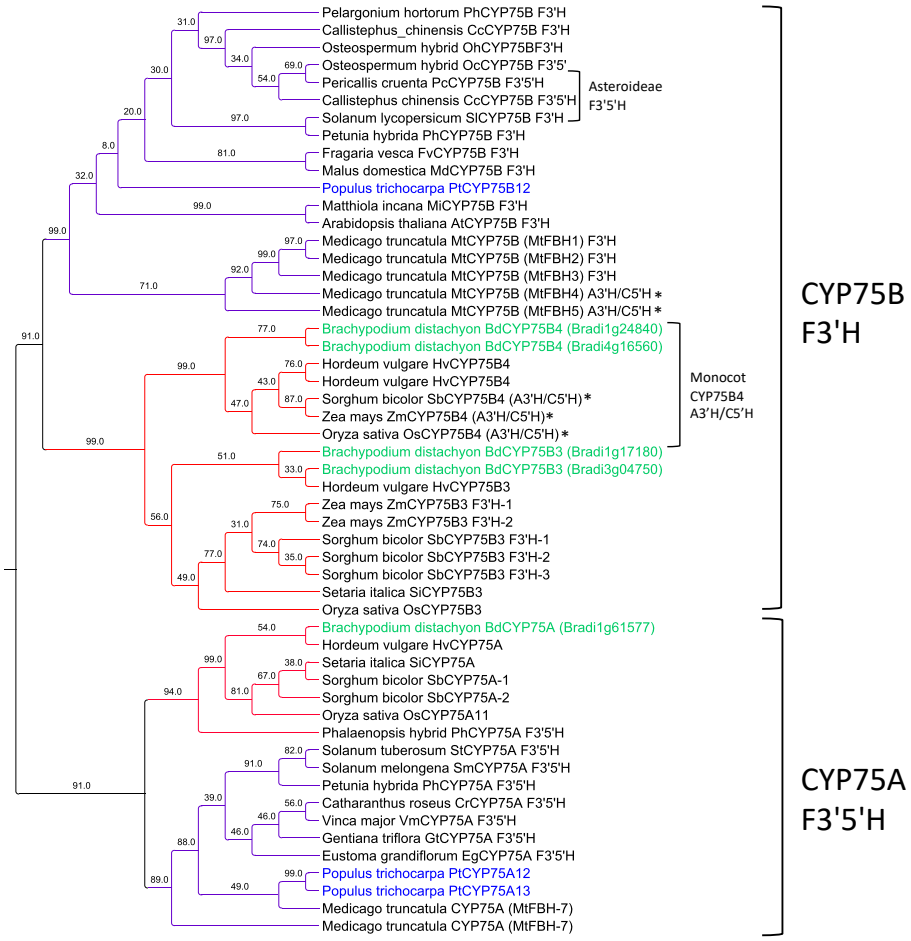

Figure 4.4: Phylogenetic analysis of the flavonoid B hydroxylase (CYP75) gene family.

Neighbour-joining tree of putative CYP75 amino acid sequences from poplar, *Populus trichocarpha* (blue) and *Brachypodium distachyon* (green) as well as previously retrieved CYP75 sequences from *Hordeum vulgare, Oryza sativa, Setaria italica, Sorghum bicolor, Zea mays, Matthiola incana, Arabidopsis thaliana, Pelargonium hortorum, Fragaria vesca, Malus domestica, Solanum lycopersicum, Petunia x hybrida, Callistephus chinensis, Osteospermum hybrid cultivar, Pericallis cruentam, Callistephus chinensis, Osteospermum hybrid, Phalaenopsis hybrid, Solanum tuberosum, Solanum melongena, Catharanthus roseus, Vinca major, Eustoma grandiflorum,* and *Gentiana trifloral* (Lui et al., 2020). Amino acid sequences aligned using MAFFT, and NJ tree constructed with 1000 bootstraps. Confidence values represented above branch points. Members of CYP75B typically catalyse flavonoid 3' hydroxylase (F3'H) reactions whereas members of CYP75A typically catalyse F3'5'H reactions. However, sequences characterized as being involved in tricin biosynthesis (*) are found to cluster in the grass-specific *CYP75B4* subgroup, and two *CYP75B* are found to be derived from the dicot *Medicago truncalata* (Lam et al., 2015; Lui et al., 2020). Genes belonging to the Asteriodeae subfamily have been found to hydroxylate flavonoids at the 3'5' positions.

Table 4.1: Mean expression (FPKM) of putative *flavonoid 3' 5' hydroxylase*, *flavonoid 3' hydroxylase* and *flavone synthase II* genes across 389 *Populus trichocarpa* genotypes in leaf and developing xylem tissue.

Putative function	Gene name	Loci	Mean expression leaf tissue (FPKM)	Mean expression xylem tissue (FPKM)
Flavonoid 3'5' hydroxylase	PtCYP75A12	Potri.001G274600	0.01±0.00	0.00±0.00
	PtCYP75A13	Potri.009G061900	11.82±0.26	9.12±0.12
Flavonoid 3' hydroxylase	PtCYP75B12	Potri.013G073300	82.34±1.51	0.11±0.01
Flavone synthase II	PtCYP93B7	Potri.005G037100	0.00±0.00	0.00±0.00
	PtCYP93B8	Potri.005G037200	0.00±0.00	0.00±0.00
	PtCYP93B33	Potri.013G027000	52.93±1.20	2.10±0.11

Pairwise sequence alignment of both *Bradi4g16560.1* and *Bradi1g24840.1* with *OsCYP75B4* showed that *Bradi4g16560* shares closer amino acid sequence similarity (85.5%) than *Bradi1g24840.1* (79.1%) to the rice derived enzyme (Figure 4.5). Both genes contain a leucine residue at position 8 of substrate recognition sequence 6 (SRS6), determined to be critical in conferring C5'H activity to *CYP75B4* gene members (Lam *et al.* 2015; Lui *et al.* 2020). *Bradi4g16560.1* displays higher levels of expression in lignifying internode tissue, compared to *Bradi1g24840.1*, based on eFP expression browser data (Winter et al., 2007). Therefore, *Bradi4g16560.1* was selected for isolation from *Brachypodium* (Bd21-3) and is hereafter referred to as *BdCYP75B4*.

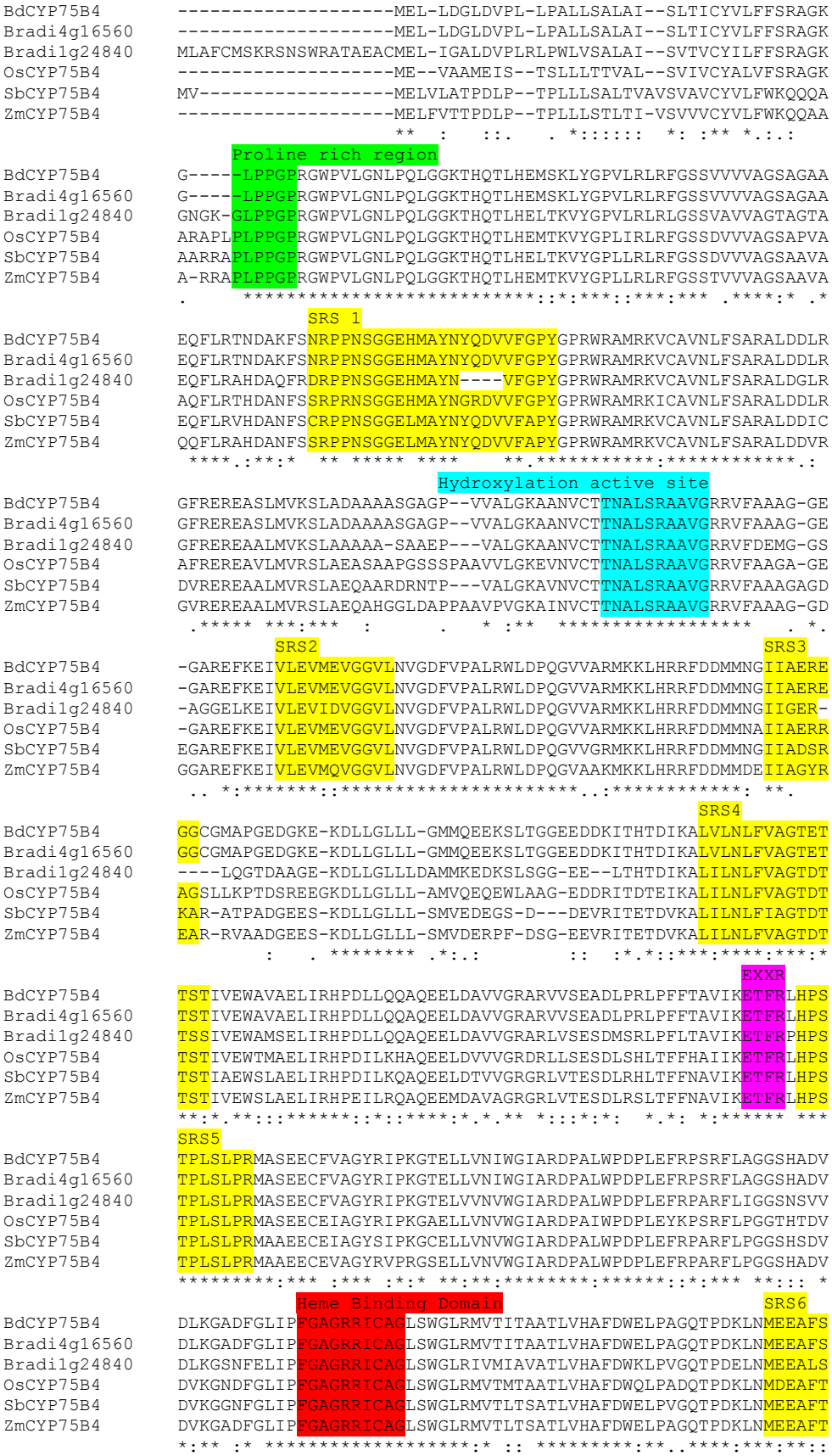
Proline rich region
SRS 1
Hydroxylation active site
SRS2
SRS3
SRS4
EXXR
SRS5
Heme Binding Domain
SRS6

```
BdCYP75B4        LLLQRAMPLMVHPVRRLLPSAYEIV
Bradi4g16560     LLLQRAMPLMVHPVRRLLPSAYEIV
Bradi1g24840     LLLLRAVPLMVHPAPRLLPSAYEIA
OsCYP75B4        LLLQRAEPLVVHPVPRLLPSAYNIA
SbCYP75B4        LLLQRAVPLMAHPIPRLLPSAYEIA
ZmCYP75B4        LLLQRAVPLVARPVPRLLPSAYEIA
```

Figure 4.5: Multiple sequence alignment of CYP75B4 amino acid sequences.

Bradi4g16560 displays the highest sequence homology to previously characterized A3'H/C5'H from rice, corn and sorghum. MAFFT amino acid alignment of *CYP75B4* subgroup, containing sequences from *Oryza sativa, Zea mays,* and *Sorghum bicolor* along with putative *CYP75B4* homologues from *Brachypodium*. *BdCYP75B4* represents Bradi4g16560 isolated from *Brachypodium* internode tissue and used in subsequent *in vitro* characterizations. Substrate recognition sites (yellow) SRS6 is a key site in conferring 5' hydroxylation activity to CYP75B enzymes. Heme binding domain (red), EXXR motif (pink), hydroxylation active site (blue), proline-rich region (green).

4.2.3 Isolation and *in vitro* characterization of *BdCYP75B4* together with *BdCYP93G1*

BdCYP75B4 displayed 100% aa sequence identity to *Bradi4g16560.1* and was initially cloned into the INVSc1 yeast strain using a galactose inducible yeast expression vector. However, *BdCYP75B4*-expressing yeast microsomes were unable to catalyse the hydroxylation of apigenin or chrysoeriol. Next, *BdCYP75B4* was cloned into the *BY4741:PcCPR1* strain of *S. cerevisiae*. *BdCYP75B4*-expressing yeast microsomes isolated from *BY4741:PcCPR1* strain were capable of catalyzing the hydroxylation of apigenin to produce luteolin and the hydroxylation of chrysoeriol to produce a peak that emerges at 49.89 min (Figure 4.6). Since this peak has the same elution time and UV profile as the smaller peak produced in reactions of tricetin incubated recombinant purified PaxgOMT25, and because selgin is not commercially available for direct comparison, we assume that the peak emerging at 49.89 min is selgin. Although we observed a very small peak at 44.68 min in the blank reaction, the corresponding UV profile of this peak was not consistent with selgin (Figure 4.7).

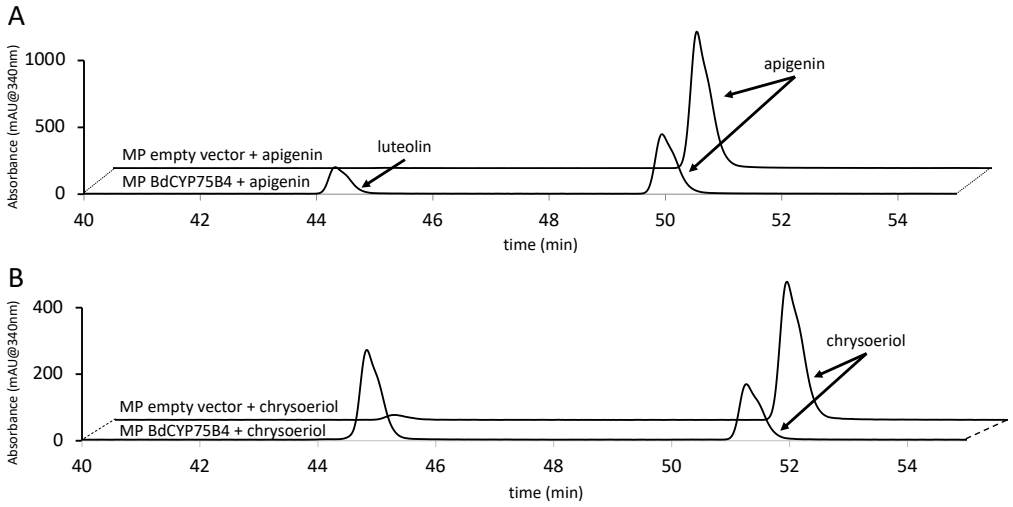

Figure 4.6: HPLC-UV analysis of *in vitro BdCYP75B4* enzyme assays.

A, Luteolin was detected in reactions of microsomal preparations (MP) of yeast expressing *BdCYP95B4* provided with apigenin as a substrate. No luteolin was detected in MP empty vector control reactions. B, Chrysoeriol was consumed when incubated with MPs of yeast expressing *BdCYP95B4*, and a novel flavonoid compound (likely selgin) was detected (see Supplemental Figure 4.1).

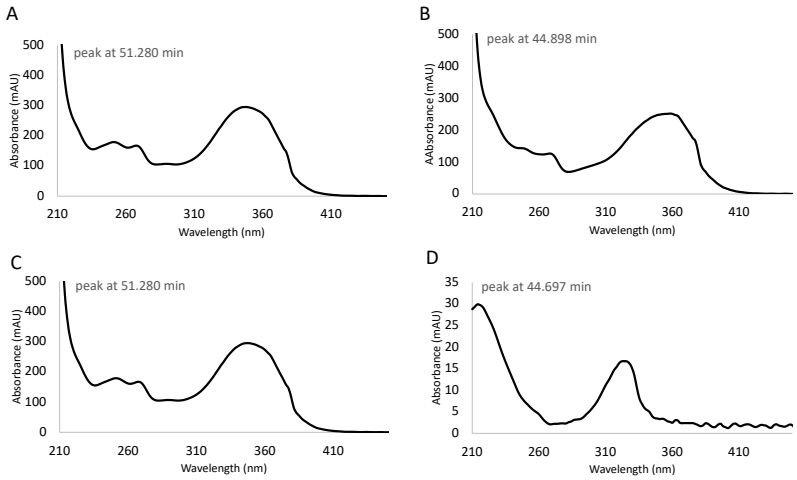

Figure 4.7: UV spectra of reaction products from in vitro enzyme assays with BdCYP75B4 and chrysoeriol.

A, chrysoeriol peak at 51.280 min in reactions containing BdCYP75B4. B, selgin peak at 44.898 in reactions containing BdCYP75B4. C, chrysoeriol peak at 51.280 min in blank reaction. D, peak at 44.697 min in blank reaction is not selgin.

Next, in order to confirm that *BdCYP75B4* and *BdCYP93G1* are able to function together, the two genes were cloned into a bicistronic vector separated by two viral 2A cleavage peptides: porcine teschovirus-1 2A peptide (P2A; Kim et al., 2011) and the FMDV pecorino virus 2A peptide (F2A; Ryan et al., 1991) producing a *BdCYP75B4-2A-BdCYP93G1* construct. *BdCYP75B4-2A-BdCYP93G1* was then cloned into *BY4741:PcCPR1 S. cerevisiae* using a galactose inducible yeast expression vector. *BdCYP75B4-2A-BdCYP93G1* expressing yeast fed with naringenin were determined to produce both apigenin and luteolin, indicating the two proteins were able to function together as part of a bicistronic construct (Figure 4.3).

4.2.4 Phylogenetic analysis of poplar lineage B OMTs

In order to identify an endogenous poplar OMT capable of participating in tricin biosynthesis, we constructed a neighbour-joining tree using 23 amino acid sequences from lineage B of the poplar *OMT* gene family (Barakat et al., 2011) along with 8 *OMT*s previously characterized *in vitro* as being active on tricin precursors (Zhou et al., 2006; Zhou et al., 2010; Eudes et al., 2017; Lam et al., 2019b) and 13 previously characterized *OMTs* belonging to lineage B (Lam et al., 2007; Figure 4.8). The tree was rooted with sequences from two carboxylic acid *OMTs* belonging to lineage A (Lam et al., 2007). Poplar *OMTs* clustered into two distinct clades: Ib and IIb, consistent with groupings observed in previous phylogenetic analysis of the gene family (Figure 4.8; Lam et al., 2007; Barakat et al., 2011). *OMTs* found to participate in tricin biosynthesis also grouped within clade IIb and cluster most closely with two poplar *OMTs*: *PtOMT25* and *PtOMT21* (*Potri.012G006400, Potri.015G003100*; Figure 4.5). In addition, we examined expression levels of poplar *OMTs* in both leaf and xylem tissue using an in-house RNA Seq database of 389 poplar genotypes and found that *PtOMT25* is most highly expressed in xylem tissue (4195.62 ± 1387 FPKM; Figure 4.7). This finding supports PtOMT25's previously described role as a key COMT/CAldOMT in the biosynthesis of monolignols (Shi et al., 2010; Wang et al., 2014).

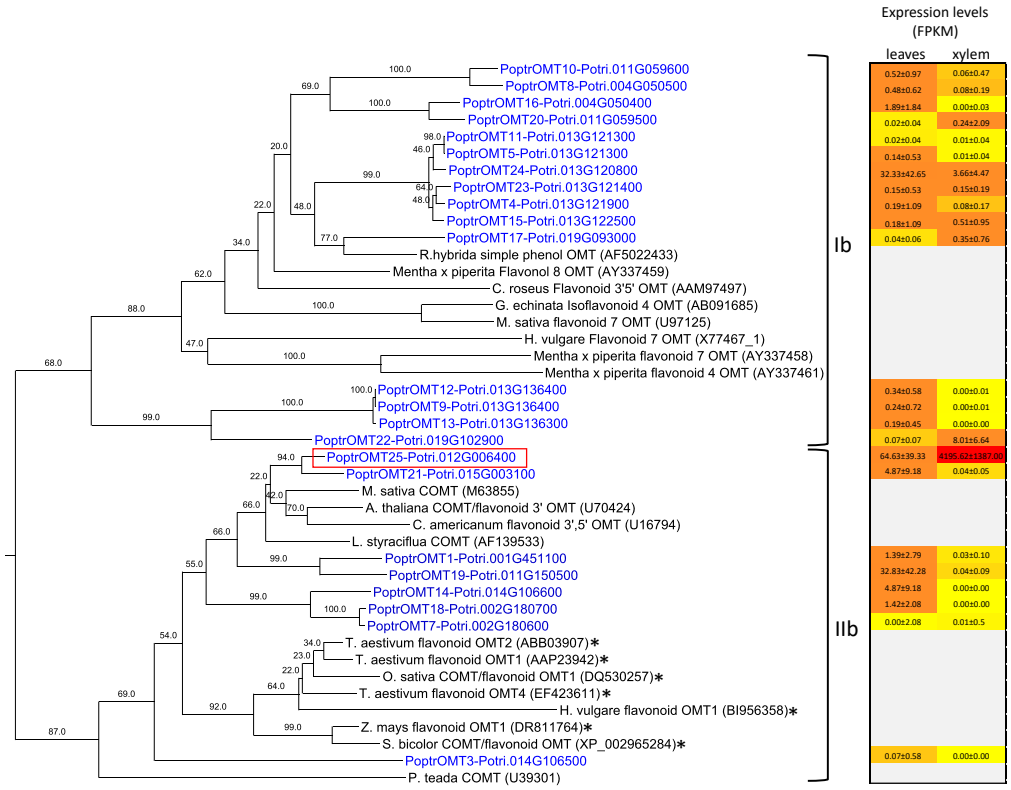

Figure 4.8: Phylogenetic analysis of plant *O*-methyl transferase (OMT) lineage B gene family.

Neighbour-joining tree of putative poplar OMT, lineage B, amino acid sequences and previously characterized OMT genes from *Rosa hybrida, Mentha x perpirata, Cartharanthus roseus*, *Glycine echinta, Medicago sativa, Hordeum vulgare, Arabidopsis thaliana, Chrysosplenium americanum, Liquidambar stryaciflua,* and *Pinus taeda* (Zhou et al., 2006; Zhou et al., 2010; Barakat et al., 2011; Eudes et al., 2017; Lam et al., 2019b). Sequence derived from *Populus trichocarpa* poplar (blue). Sequences previously characterized as participating in the biosynthesis of tricin (*). Poplar *OMT* chosen for isolation and characterization, *PtOMT25* (boxed in red). Amino acid sequences aligned using MAFFT, and NJ tree constructed with 1000 bootstraps. Confidence values represented above branch points, relative distances shown with branch length. Corresponding expression levels of poplar OMTs depicted as a heatmap of FPKM values averaged across 389 separate *Populus trichocarpa* genotypes ± standard error, retrieved from an in-house RNASeq database.

Further examination of the amino acid alignment of sequences found in clade IIb shows conservation of several key residues (Figure 4.9). Residues that closely neighbour the substrate-binding pocket (259, 263, 290, 305, 322) are highly conserved across enzymes previously shown to be involved in tricin biosynthesis and are similarly conserved in *PtOMT25* and *PtOMT21*.

Residue 309, for example, is a critical site for determination of substrate preference (Zhou et al., 2010). Notably, *PtOMT25* contains I309, whereas *PtOMT21* contains V309 (Figure 4.9). Previous work in wheat has shown that a single aa change (I309V) resulted in increased substrate preference for tricetin over 5-hydroxy ferulic acid as replacement of the smaller aa valine allows for larger substrates to enter the binding pocket (Li et al., 2003). Despite containing I309, we choose to isolate and characterize *PtOMT25* due to its high levels of expression in xylem tissue from P39 poplar.

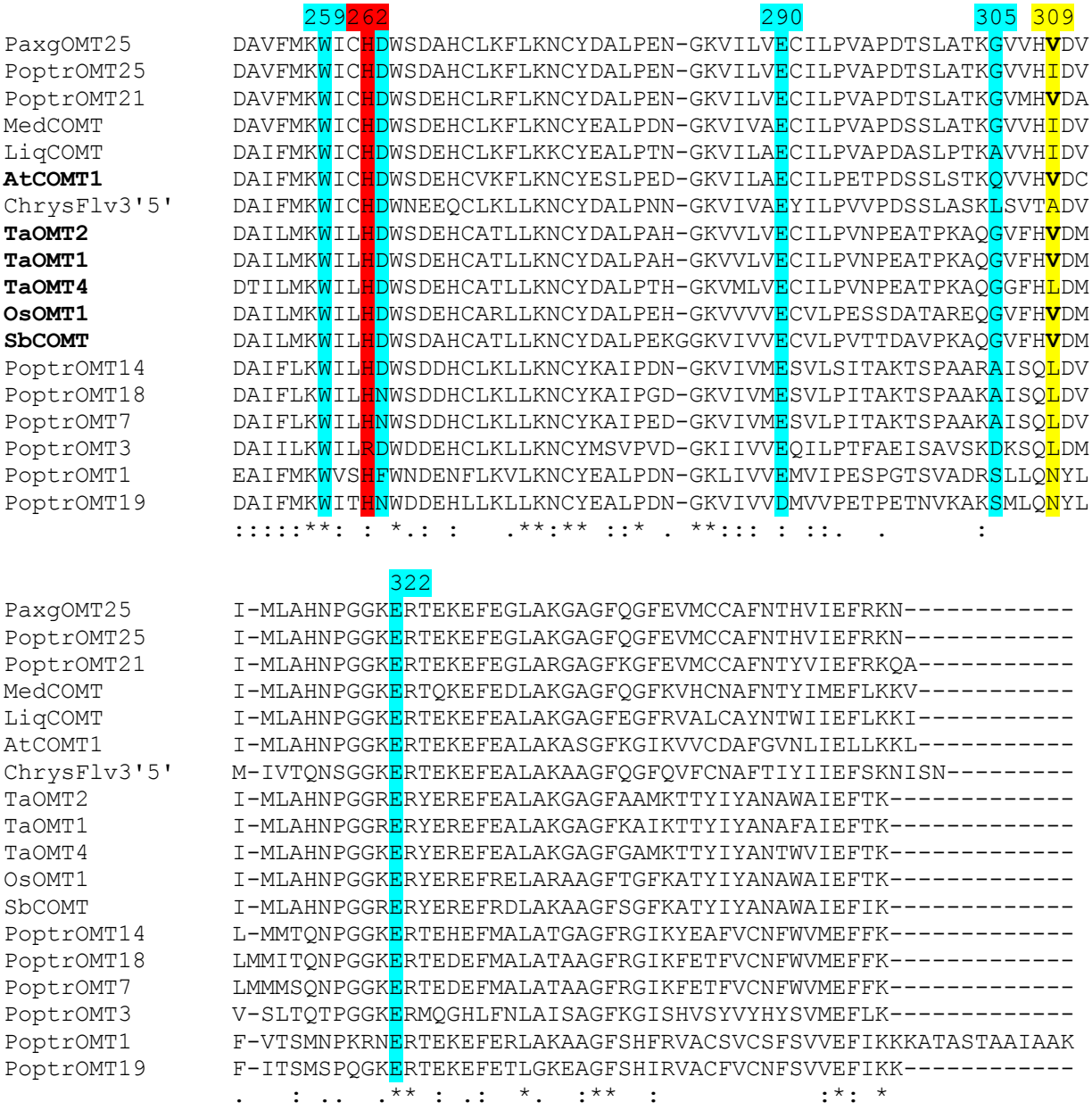

Figure 4.9: Multiple sequence alignment of group IIb plant O-methyltransferase partial amino acid sequences.

Mafft alignment of poplar sequences found in group IIb of the plant OMT family aligned with previously characterized *OMT* sequences derived from *Medicago sativa, Arabidopsis thaliana, Chrysosplenium americanum, Liquidambar stryaciflua, Triticum aestivum, Oryza sativa* and *Sorghum bicolor.* Catalytic residue (red), substrate binding adjacent residues (blue), site determining substrate specificity (yellow). *COMTs* with I309 display preference for hydroxycinnamic acids over flavonoid substrates and *COMTs* with V309 (bolded) typically display substrate preference for flavonoids over hydroxycinnamic acids.

4.2.5 Isolation and *in vitro* characterization of an endogenous poplar *O*-methyltransferase

We isolated and sequenced *PtOMT25* from P39 hybrid poplar tissue, referred to as *PaxgOMT25*. *PaxgPOMT25* displays 98.9% amino acid sequence identity and 100% sequence similarity to *PtOMT25*, with *PaxgOMT25* containing a notable I309V substitution. *PaxgOMT25* was expressed in *E. coli* B21 DE3 with an N-terminal his-tag, and the 42kDa protein was successfully purified using Ni-NTA affinity chromatography, as verified by SDS-PAGE analysis (Figure 4.10). *In vitro* enzyme assays, using the affinity-purified recombinant protein, determined that PaxgOMT25 was able to accept both luteolin and tricetin as substrates (Figure 4.11). Two peaks emerged after incubation with tricetin: tricin, at 50.84 min, along with a peak at 44.98 min. After examining the UV profile of the second peak, we determined that it is likely the tricin intermediate selgin, for which a standard is not commercially available (Figure 4.11). This result is consistent with other flavonoid OMTs from subclass IIb which display stepwise methylation of tricetin to tricin, releasing only small amounts of the intermediate product, selgin, from the binding pocket (Zhou et al., 2006).

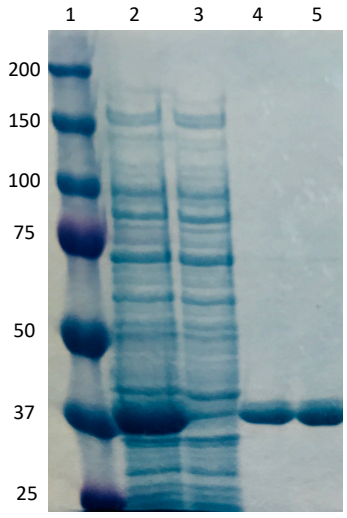

Figure 4.10: SDS-PAGE profile of purified recombinant PaxgOMT25 during affinity purification.

Standard protein markers (1); soluble protein fraction of *E.coli* after induction (2); soluble protein wash (3); elution of PaxgOMT25 (4); concentrated PaxgOMT25 protein (5).

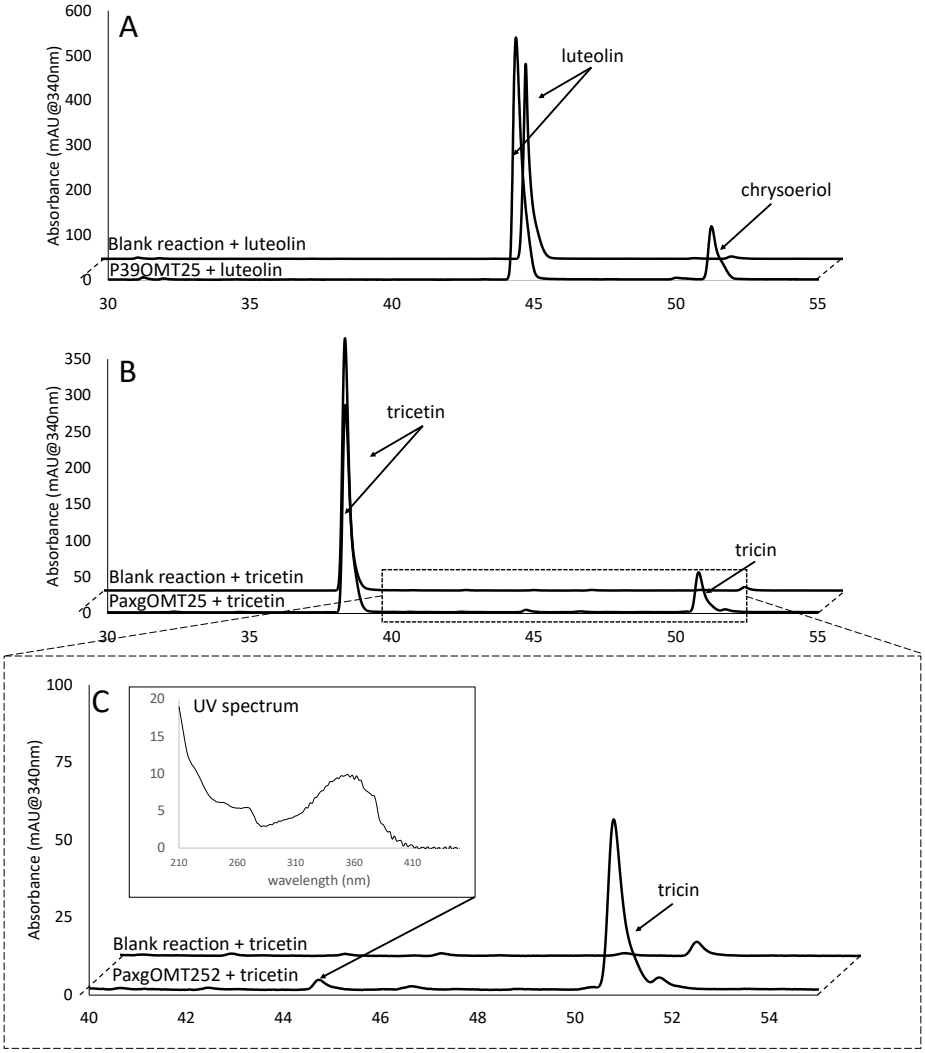

Figure 4.11: HPLC-UV analysis of *in vitro* PaxgOMT25 enzyme assays.

Purified PaxgOMT incubated with luteolin (A) and tricetin (B).Two new peaks detected in PaxgOMT25+tricetin reactions at 50. 84 min (tricin), and at 44.89 min (selgin). Neither peak is detected in the blank reactions. Enlarged chromatogram boxed in panel A showing selgin with corresponding UV profile. Retention time and UV profile match with selgin produced *in vitro* enzyme assays with BdCYP75B4 and chrysoeriol.

Kinetic analysis revealed that recombinant PaxgOMT25 displays substrate preference for caffeic acid over luteolin, exhibiting a lower Km (96 μM) towards caffeic acid compared to luteolin (385.2 μM; Table 4.2; Figure 4.12). However, catalytic efficiency, or turnover rate, is

relatively similar between the two substrates (Table 4.2). This data suggests that if supplied with appropriate flavonoid precursors, PaxgOMT25 can participate in tricin biosynthesis during lignification in xylem tissue.

Table 4.2: Kinetic parameters of PaxgOMT25 purified using his-tagged affinity purification. Km and Vmax were determined using a time stop assay (5 min) using a 25 – 350 μM range of substrate concentration, with three technical replicates per reaction.

Substrate	Km (μM)	Vmax (μM/min)	K_{cat} (min^{-1})	Kcat/Km ($\mu M^{-1}min^{-1}$)
caffeic acid	96.62	7.08	3.07	0.318
luteolin	385.2	37.09	161.26	0.419

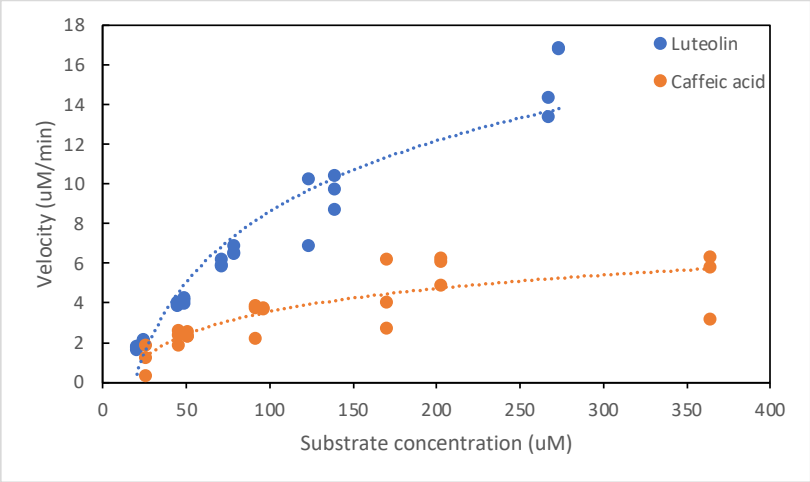

Figure 4.12: Saturation curve of PaxgOMT25 supplied with luteolin and caffeic acid.

Velocity of PaxgOMT25 supplied with a range of luteolin (blue) and caffeic acid (orange) substrate concentrations. Velocity calculated using time stop assays (5 min) across a range of substrate concentrations with three replicate reactions per set concentration. Substrates analyzed using HLPC-UV and final concentrations determined by comparison to standard curves.

4.2.6 Transformation of MdCHS3-poplar with *BdCYP75B*, *BdCYP93G1* and *BdCYP75B4-P2AF2A-BdCYP93G1*

The *BdCYP75B4-2A-BdCYP93G1* construct was inserted into a plant expression vector (pK7WG2) containing *the AtCesA7p* promoter (hereafter referred to as ACP::75/93). ACP::75/93

was transformed into wild-type P39 hybrid poplar (*Populus alba x grandidentata*) as well as a previously generated *MdCHS3*-poplar highest expressing line 2 (CHS2; Mahon et al., 2021) using *Agrobacterium*-mediated transformation. Successful transformants were confirmed by genomic screening. However, only one positive transformants arising from wt and one transformant arising from CHS2 background were able to establish roots and grow successfully in tissue culture (Figure 4.13).

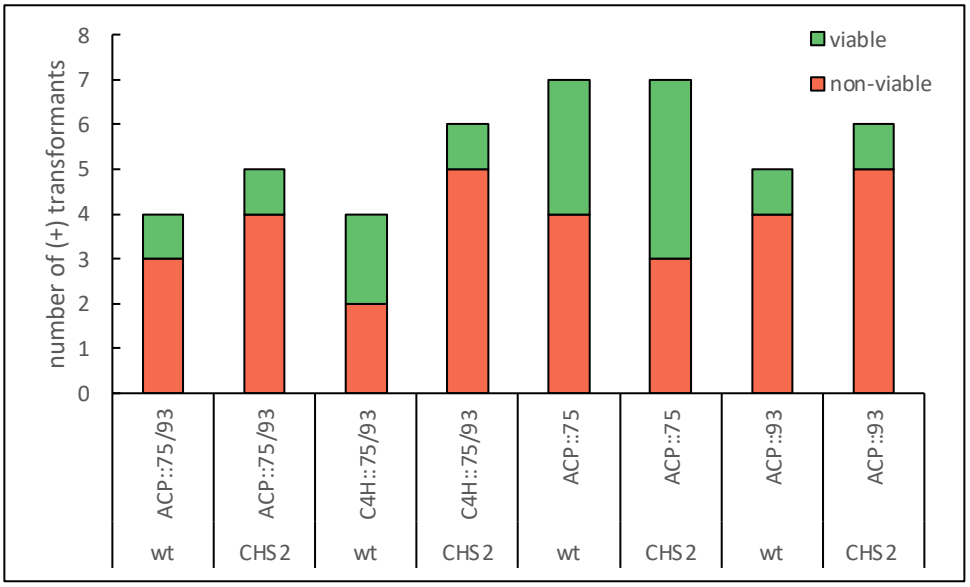

Figure 4.13: Growth condition of poplar expressing *BdCYP75B4* and/or *BdCYP93G1* in wild-type and *MdCHS3* backgrounds.

AtCesA7p::BdCYP75B4-2A-BdCYP93G1 (ACP::75/93), *AtCesA7p::BdCYP75B4* (ACP::75), *AtCesA7p::BdCYP93G1* (ACP::93*), AtC4H:: BdCYP75B4-2A-BdCYP93G1* (C4H::75/93) in wild-type or *MdCHS3*-poplar (CHS2) backgrounds. Plants were examined in tissue culture antibiotic free rooting media eight weeks after being transferred from selective shooting media. Y-axis represents the number of positive transformants arising from incubation of 500 unique leaf discs with *Agrobacterium.*

When grown in soil for six weeks the line of plants expressing *ACP::75/93* in the CHS2 background-exhibited clear reductions in height, stem diameter, and both above and below ground biomass (Table 4.3;Figure 4.14 & 4.15). Expression of the *75/93* transcript was detected in xylem tissue of both CHS2 and wild-type backgrounds (Figure 4.16). Analysis of vessel and

fibre area in stem cross-section revealed a significant reduction in vessel size in (CHS2*)* *ACP::75/93* plants, and no evidence of collapsed or irregular xylem phenotype (Figure 4.17).

Table 4.3: Mean growth measurements of *ACP::75/93* expressing poplar in both wild-type and CHS2 backgrounds.

Values represent the mean growth across three biological replicates per line after six weeks. Standard error is represented in brackets. Significant differences ($p<0.05$) compared to respective background control type are bolded and were determined using Student's t-test.

Line	Height(cm)	Stem diameter (cm)	Above ground biomass (g)	Root length (cm)	Root biomass (g)
WT	16.80	2.69 (0.17)	4.26 (0.71)	30.30 (4.59)	0.14 (0.01)
CHS2	22.07	3.31 (0.34)	7.69 (1.68)	28.00 (7.09)	0.28 (0.06)
ACP::93/75	18.77	3.45 (0.43)	7.19 (1.18)	48.73 (6.68)	0.35 (0.10)
(CHS2) ACP::75/93	**7.57 (1.80)**	**1.78 (0.16)**	**1.16 (0.43)**	19.47 (5.22)	0.023 (0.01)

Figure 4.14: Photos *ACP::75/93* expressing poplar trees.

Photos taken of ACP::75/93 expressing poplar in both wild-type and CHS2 backgrounds compared to their respective controls after six weeks growth.

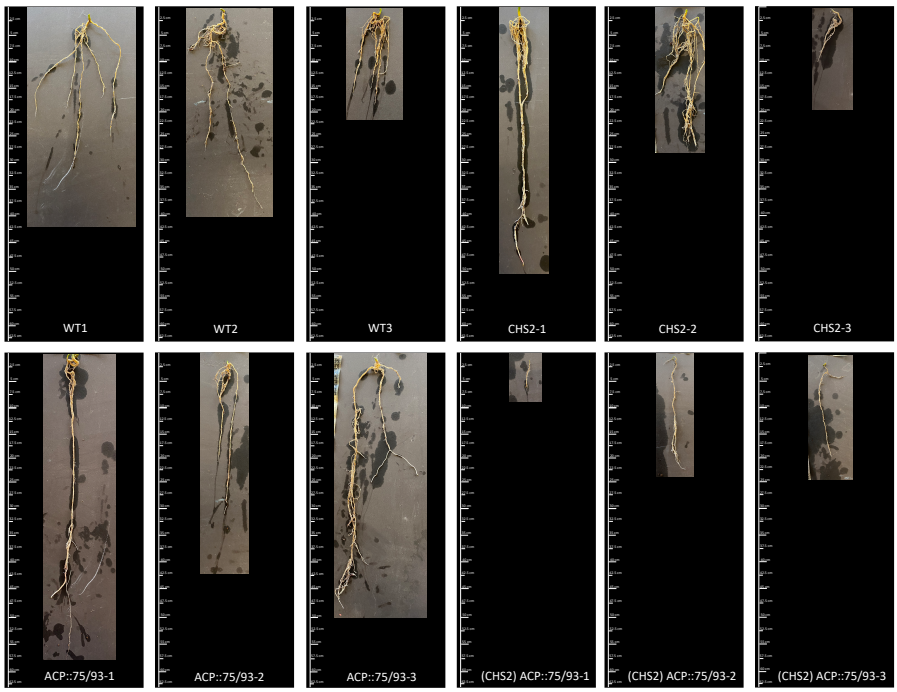

Figure 4.15: Roots of *ACP::75/93* expressing poplar.

Photos of roots of plants expressing *ACP::75/93* in both wild-type and CHS2 backgrounds after six weeks growth.

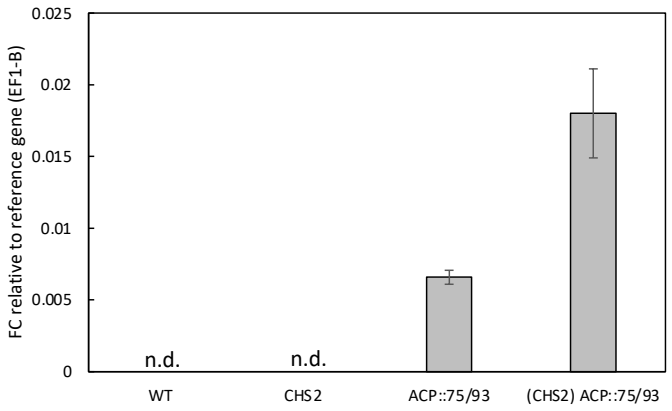

Figure 4.16: Expression levels of the ACP::75/93 bicistronic construct in two successful transformants.

Expression in xylem tissue of six-week-old trees shown for one wild-type and one MdCHS3 poplar backgrounds. Expression levels determined using qRT-PCR, normalized to a reference gene and shown as fold change (FC) relative to the expression of *MdCHS3* in the *MdCHS3*-poplar background. Averaged across three technical replicates, error bars showing standard error.

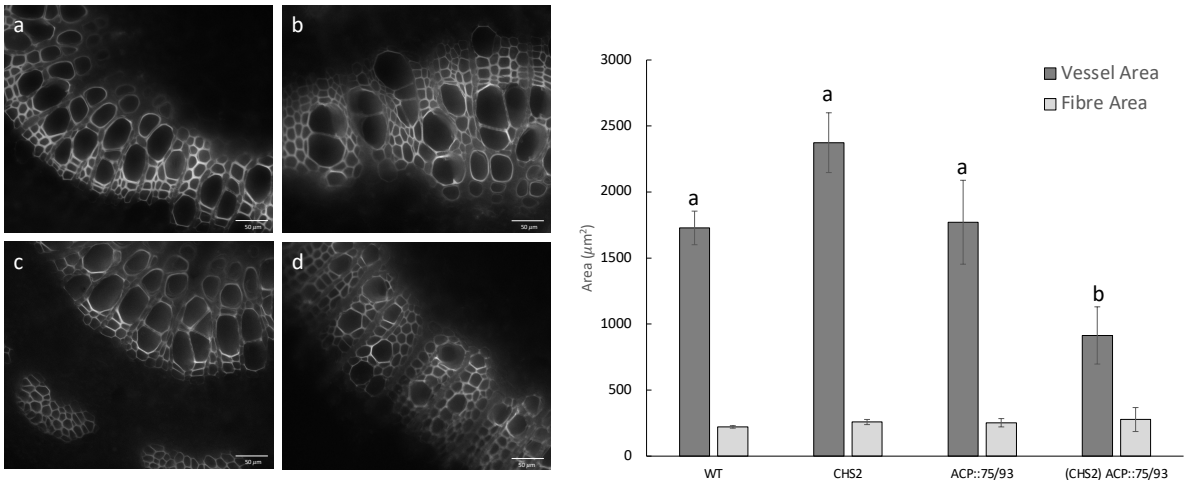

Figure 4.17: Fluorescent imaging of stem cross sections to determine vessel and fibre area on six week old plants transformed with ACP::75/93.

Wild-type (A), CHS2 (B), ACP::75/93 (C), and (CHS2)ACP::75/93 poplar grown in tissue culture sectioned 5 cm from the apical meristem (left). Corresponding area of vessels and fibres measured in six sections per line (below). Expression of ACP::75/93 was found to have a significant impact on vessel and fibre area. Significant differences between lines determined using post hoc pairwise comparisons (with Bonferroni correction) denoted with lower case letters.

Finally, analysis of hydrolyzed soluble methanolic extracts revealed several distinct changes in soluble phenolic profile of *(CHS2) ACP::75/93*-poplar replicates compared to the both wild-type and CHS2 background controls, including peaks with UV profiles consistent with flavones as well as one peak consistent with tricin (Figure 4.18). The novel peaks are not consistent with flavanols quercetin and kaempferol produced endogenously in poplar (Figure 4.18).

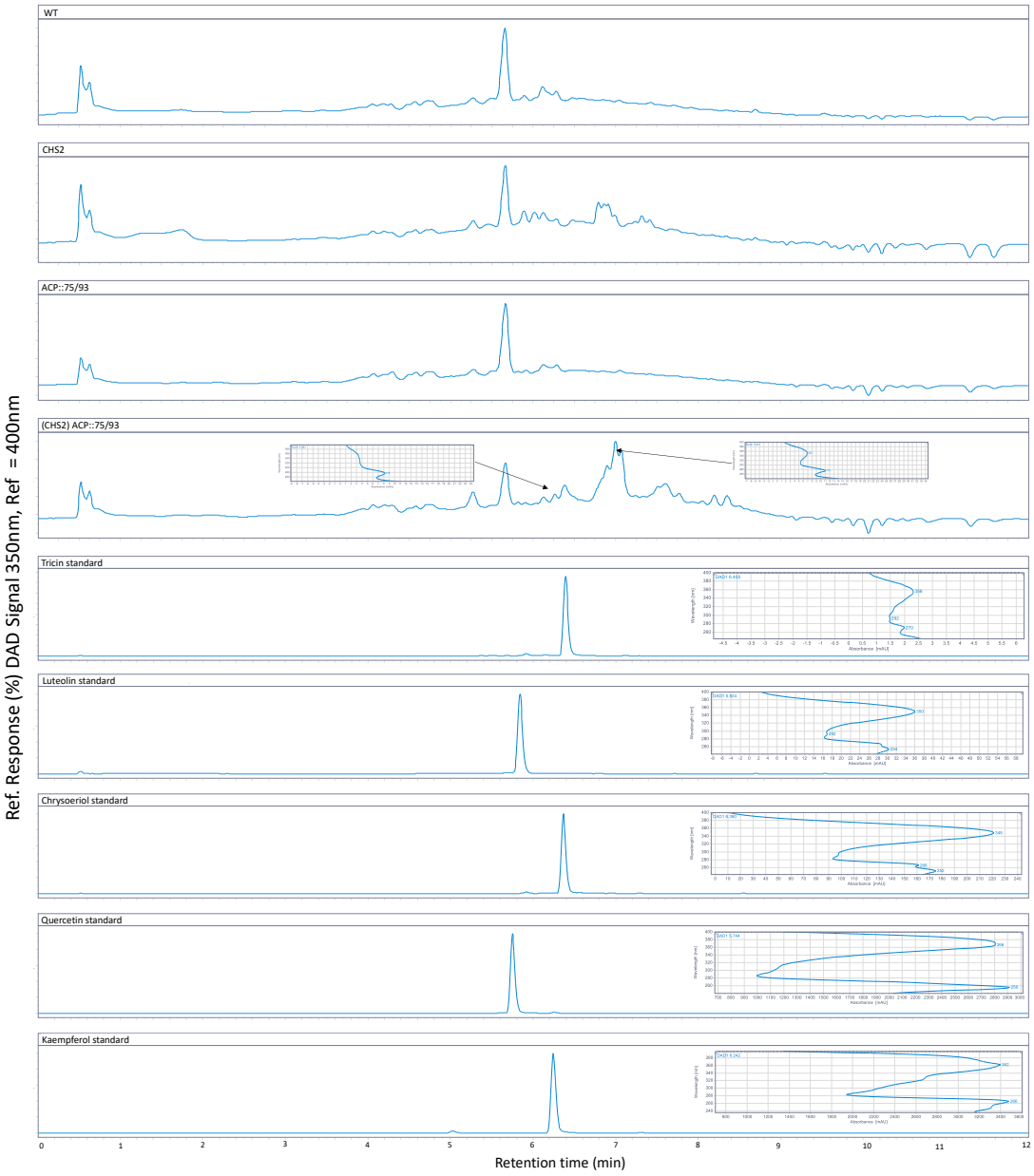

Figure 4.18: Hydrolyzed methanolic extracts from xylem of six-week-old poplar expressing *ACP::75/93.*

UPLC analysis of soluble phenolics from wild-type (WT), *MdCHS3*-poplar line 2 (CHS2), and (MdCHS3-line2), AtCesA7p::BdCYP75B4-2A-BdCYP93G1, and (MdCHS3 line2) AtCesA7p::BdCYP75B4-2A-BdCYP93G1 ((CHS2)ACP::75/93) trees. Profiles are consistent across three biological replicates per line. Purified flavone standards tricin, luteolin and chrysoeriol display UV absorbance at 350-360 nm consistent with observed exclusively in extracts (CHS2)ACP::75/93 trees. Quercetin and kaempferol standards display absorbance at 360-370nm.

In order to determine whether expression of one or both genes in the *ACP::75/93* construct prevent growth, we transformed *ACP::75* and *ACP::93* separately into both wild-type and CHS2 backgrounds. We also transformed both wild-type and *MdCHS3*-poplar with *C4H::75/93* to investigate the possibility that the timing of *BdCYP75B4-P2AF2A-BdCYP93G1* expression may be impacting plant viability, as the *ACP* promoter induces expression during cellulose deposition in the secondary cell wall, whereas the *C4H* promoter induces expression later during lignin deposition. Three of the four positively transformed with *C4H::75/93* in the wild-type background were determined to be viable, whereas only one of six positively transformed plants were able to grow in the CHS2 background (Figure 4.13). Several wild-type and CHS2 plants transformed with the ACP::75 construct were viable, however a portion of each failed to produce roots in tissue culture (Figure 4.13). Finally, almost all of the plants transformed with the *ACP::93* were unable to establish roots in and grow in tissue culture with the exception of two very slow-growing positive transformants in either background (Figure 4.13).

4.3 Discussion

4.3.1 BdCYP93G1 converts naringenin to apigenin

The first committed step in the production of the flavone tricin in lignifying poplar xylem tissue is the conversion of naringenin into the flavone apigenin (Figure 4.1). There are two distinct types of FNS enzymes found in dicots (Martens and Mithofer, 2005); FNSI, soluble dioxygenases which require Fe^{2+} as a cofactor and are found to function primarily in members of the Apiaceae family (Gebhardt et al., 2007), and FNSII, CYP450s belonging to the family CYP93B (Du et al., 2010). Three putative *CYP93B* genes have been identified in the genome of poplar, with expression levels appearing to be relatively low in xylem tissue (Table 4.1). Therefore, in order to produce sufficient apigenin in *MdCHS3*-poplar xylem tissue, we identified and isolated *BdCYP93G1,* a homologue of *OsCYP93G1*, an FNSII which channels the flavone pathway towards the production of tricin *O*-linked conjugates (Du et al., 2010; Lam et al., 2014). We confirmed through substrate feeding assays that BdCYP93G1 is capable of producing apigenin when provided with naringenin (Figure 4.3).

In monocots, *FNSII* genes are found within the *CYP93G* subfamily, which is further divided into *CYP93G1* and *CYP93G2* (Du et al., 2010). CYP93G1s convert flavanones directly to flavones, channelling production towards *O*-glycosylated flavonoids, whereas CYP93G2s act as flavanone-2-hydroxylases (F2H), leading to the production of *C*-glycosylated flavones through the combined action of *C*-glycosyl transferases (CGT) and dehydratases (Du et al., 2010). In rice, disruption of *OsCYP93G1* results in the depletion of soluble *O*-linked tricin glycosides and tricin-linked lignins, whereas disruption of *OsCYP93G2* resulted in depletion of soluble apigenin and luteolin *C*-linked glycosides, indicating that lignin-integrated tricin is produced via the action of OsCYP93G1 (Du et al., 2010; Lam et al., 2017).

4.3.2 BdCYP75B4 functions in hydroxylation of apigenin and chrysoeriol

Members of the *CYP75* gene family play an important role in the biosynthesis of flavonoids by catalyzing hydroxylation of the B-ring at the 3' and 5' positions and cluster into two subfamilies: *CYP75A (F3'5'H)* and *CYP75B (F3'H)*, thought to have diverged prior to the

divergence of angiosperms and gymnosperms (Zhang et al., 2019; Xiao et al., 2021). Consistent with previous phylogenetic analyses, our analysis displays a clear separation of *CYP75A* and *CYP75B* with sequences from monocots and dicots grouping into distinct clades within the subfamilies (Figure 4.4; Lam et al., 2019a). Additionally, we observed clustering of monocot *CYP75B*s into two groups: *CYP75B4* and *CYP75B3* (Seitz et al., 2006; Jia et al., 2019). In rice, OsCYP75B3 displays 3' hydroxylation activity on a broad range of flavonoid substrates and has been shown to play a role in the production of *C*-linked luteolin glycosides (Lam et al., 2019a). OsCYP75B4 has been previously characterized as the key enzyme responsible for the biosynthesis of tricin in rice belonging to a clade of grass-specific *A3'H/C5'Hs (CYP75B4s*) that have acquired the capacity to hydroxylate chrysoeriol at the 5' position (Lam et al., 2015). The occurrence of this unique clade of flavonoid hydroxylases corresponds to tricin's wide-ranging occurrence in a number of grass species (Lan et al., 2016). We identified two *Brachypodium* sequences clustering within the *CYP75B4* group, one of which shared the closest homology to *OsCYP75B4* and displayed expression patterns consistent with the high levels of tricin, and lignin-integrated tricin, found in *Brachypodium* internode tissue (Lan et al., 2016). Moreover, both *Brachypodium* sequences contain a leucine at position eight of SRS6 consistent with other A3'H/C5'Hs found in grasses (Figure 4.5). Within SRS6 of the *CYP75B* subfamily, amino acid differences at position eight have been linked to the acquisition of 5' chrysoeriol hydroxylation activity (Lui et al., 2020). All members of the grass-specific CYP75B4 (A3'H/C5'H) clade contain a leucine at SRS6-8, whereas both monocot and dicot members of the CYP75B subfamily with only F3'H activity contain a strictly conserved threonine (Lam et al., 2015; Lui et al., 2020). Some species found in the Asteroidea subfamily contain independently evolved CYP75Bs also capable of F3'5'H hydroxylation and carry a serine or alanine at SRS6-8 (Seitz et al., 2006). Moreover, *MtFBH-5*, an independently evolved dicot *CYP75B*, contains a glycine at SRS6-8 and is capable of acting as an A3'H/C5'H in the biosynthesis of tricin, further underscoring the importance of this residue (Lui et al., 2020). It appears that members of the *CYP75B* subfamily require very few amino acid changes to gain F3'5'H activity explaining the independent acquisition F5'H of multiple branches of the *CYP75B* subfamily (Seitz et al., 2006).

We determined through *in vitro* assays that BdCYP75B4 is capable of hydroxylating apigenin at the 3' position and chrysoeriol at the 5' position, indicating its likely role in tricin biosynthesis in *Brachypodium* (Figure 4.6). Contrary to earlier work, in which tricin was believed to arise from simultaneous hydroxylation at 3' and 5' positions of apigenin through the action of a CYP75A (F3'5'H) followed by methylation (Cummins et al., 2006), tricin is produced by two sequential hydroxylation/methylation steps mediated by a CYP75B and an OMT respectively (Lam et al., 2015). A similar mechanism was shown to have evolved independently in the dicot, alfalfa (Lan et al., 2016; Lui et al., 2020). Our work shows that BdCYP75B4 is likewise incapable of hydroxylating apigenin at both 3' and 5' positions to produce tricetin, requiring a flavonoid substrate to be *O*-methylated at the 3' position in order to facilitate 5' hydroxylation.

When *BdCYP75B4* was co-expressed in a bicistronic vector with *BdCYP93G1,* the two CYP450s were capable of converting naringenin to apigenin to luteolin (Figure 4.3). *BdCYP93G1* is closely related to *OsCYP93G1*, and it is likely that BdCYP93G1 and BdCYP75B4 function closely together in the production of tricin-*O*-linked conjugates and lignin-integrated tricin, similar to their homologous counterparts in rice (Lam et al., 2015; Lam et al., 2017). Our *in vitro* analyses indicate that tricin should be produced when *BdCYP93G1* and *BdCYP75B4* are co-expressed in xylem tissue of *MdCHS3*-poplar, as long as there is an endogenous poplar COMT capable of methylating flavonoid substrates present.

4.3.3 PaxgOMT25 can function in both monolignol and tricin biosynthetic pathways

Our phylogenetic analysis of *OMT* lineage B genes in poplar is consistent with previous analyses (Barakat et al., 2011; Liu et al., 2021) and indicates that of all putative poplar *OMTs*, *PtOMT25* and *PtOMT21* cluster most closely with other previously characterized *OMTs* derived from grasses shown to play a role in tricin biosynthesis (Figure 4.8; Lam et al., 2015; Eudes et al., 2017; Lam et al., 2019b). In addition, *PtOMT25* is more highly expressed in poplar xylem tissue compared to *PtOMT21*, making it a likely candidate for participation in tricin biosynthesis (Figure 4.8). Plant *O*-methyltransferases have been traditionally categorized into two major

groups based on molecular weight and catalytic mechanism; caffeoyl-CoA OMTs (CCoAOMTs), which participate in the biosynthesis of monolignols and caffeic acid OMTs (COMTs), which can accept both phenylpropanoid and flavonoid substrates and function by catalyzing the transfer of a methyl group from *S*-adenosylmethionine (SAM) to a hydroxylated phenylpropanoid or flavonoid acceptor (Joshi and Chiang, 1998). More recent phylogenetic analysis of the *OMT* gene family in plants revealed two distinct lineages. Lineage A *OMT*s cluster into two sister clades; Ia, which contains *CCoACOMTs*, and IIa, which includes COMTs active on aliphatic carboxyl groups (Joshi and Chiang, 1998; Lam et al., 2007). Lineage B *OMTs* similarly cluster into two distinct clades; clade Ib, which contains COMTs active on alkaloids, and the A ring of flavonoids, and clade IIb which contains COMTs active on monolignol precursors and the B ring of flavonoid substrates (Lam et al., 2007). It's been suggested that *CCoAOMT* genes found in clade Ia evolved earlier than other *OMT* genes (Lam et al., 2007; Weng and Chapple, 2010). The remaining *COMT* genes found in lineage A and B likely evolved later and accept a diversity of substrates, with members of lineage IIa evolving to methylate signalling molecules such as salicylic acid, jasmonic acid, and indoleacetic acid, and members of Ib and IIb methylating a highly diverse array of flavonoids and phenylpropanoids, lending COMTs a higher degree of metabolic plasticity than CCoAOMTs (Lam et al., 2007).

It had been well established that *PtOMT25* plays a key role in the phenylpropanoid pathway, with disruption of this gene leading to an accumulation of monolignol precursors, as well as reductions to lignin and significant alterations in lignin composition (Jouanin et al., 2000; Marita et al., 2001). However, in grasses, such as rice and sorghum, IIb COMTs appear to play a bifunctional role by acting on both phenylpropanoid and tricin biosynthetic pathways (Eudes et al., 2017; Lam et al., 2019b). Group IIb COMTs derived from wheat appear to accept both phenylpropanoids and flavonoids, with only a single amino acid change, I309V, mediating preference for flavonoids over hydroxycinnamic acids (Zhou et al., 2010). Moreover, tricin was reported to accumulate in transgenic *Arabidopsis* co-expressing rice derived *OsCYP75b4* and *OsFNSII* (*OsCYP93G*) genes, suggesting that endogenous OMTs in *Arabidopsis* are sufficient to support biosynthesis of tricin by participating in both the 3' methylation of luteolin to produce chrysoeriol and the 5' methylation of selgin to produce tricin (Lam et al., 2015). Considering the

broad substrate preference of type IIb COMTs in both dicots and monocots, it is likely that those derived from dicots are similarly capable of dual functionality if provided with both flavonoid and phenylpropanoid precursors.

To investigate this, we isolated a homologue of *PtOMT25* from P39 hybrid poplar, *PaxgOMT25,* and determined, *in vitro,* that PaxgOMT25 is capable of methylating luteolin and tricetin (Figure 4.10 & 4.11). The production of tricin from tricetin clearly demonstrates the capability of PaxgOMT25 to methylate not only the 3' OH position on tricetin but also the 5'OH position of the intermediate selgin. These results show that PaxgOMT25 is capable of participating in the methylation of luteolin and selgin, both key steps in the biosynthesis of tricin. Moreover, these results confirm that members of the dicot IIb COMT clade display the same bifunctionality as their monocot counterparts.

Our kinetic analysis indicates that PaxgOMT25 exhibits greater substrate specificity for caffeic acid compared to luteolin, suggesting that PaxgOMT25 likely exhibits even greater substrate affinity for other monolignol intermediates, such as 5-hydroxyconferaldehyde towards which poplar derived PtrOMT25 (AldOMT2) was previously shown to have the greatest substrate affinity (Table 4.2; Wang et al., 2014). This result is somewhat surprising as kinetic analysis of a COMT from wheat demonstrated that a single amino change at position 309 (V309I) was sufficient to alter substrate preference from tricetin to 5-hydroxyferulic acid ostensibly by reducing the volume of the binding pocket (Zhou et al., 2010). Our amino acid alignment of group IIb *COMT* genes revealed that *PaxgOMT25* P39 contains V309, suggesting that PaxgOMT25 should display substrate preference for flavonoids (Figure 4.9). This disparity may in part be due to other unaccounted for differences in dicot sequences, as *AtOMT1* is also shown to contain V309 yet displays a catalytic preference for phenylpropanoid substrates (Muzac et al., 2000). Regardless of substrate preference, large reductions in *COMT* expression are typically required to impact total lignin content (Jouanin et al., 2000; Marita et al., 2001), indicating that COMT is produced in excess compared to available substrates (Wang et al., 2014). Our kinetic analysis suggests that, as long as an excess amount of PtOMT25 is available, both monolignol and flavonoid precursors can be methylated.

4.3.4 Expression of *AtCesA7p::BdCYP75B4-2A-BdCYP93G1* in *MdCHS3*-poplar alters the soluble phenolic profile of xylem extracts.

Analysis of hydrolyzed methanolic extracts in (CHS2) ACP::75/93 poplar revealed the presence of several unique peaks (not observed in wild-type, CHS2, or ACP::75/93 controls) displaying UV absorbance profiles consistent with flavones, one of which displays similar elution time and UV absorbance pattern as tricin (Figure 4.18). Flavones, such as tricin, chrysoeriol and luteolin exhibit two peaks at 240-280nm and 300-350nm termed band II and band I, respectively (Figure 4.18). Flavonols, on the other hand typically display absorbance around 350-385 nm, and the UV profiles of the flavanols produced at high levels in poplar, quercetin and keamferol, are not consistent with the profiles of the novel peaks identified in the xylem extracts of (CHS2) ACP::75/93. This would indicate that expression of ACP::75/93 results in the ectopic production of flavones, some of which is likely tricin, in xylem tissue. The occurrence of novel peaks with UV absorbances similar to tricin (band II=272nm, band I=354nm) eluting at a later time could even indicate the presence of modified tricin conjugates, not released by the hydrolysis (Figure 4.18). However (CHS2) ACP::75/93 poplar exhibit severely reduced growth and significantly smaller vessel size compared to background controls indicating that expression of *ACP::75/93* is impacting plant growth and cell differentiation during xylogenesis. It is important to note that analysis of biological replicates arising from only one transformation event limits conclusions we can make from these results, however, the results looks very promising.

4.3.5 Impact of *MdCHS3, BdCYP75B4,* and *BdCYP93G1* expression on growth and viability

Many of the wild-type and CHS2 plants transformed with ACP::75/93 and (CHS2) C4H::75/93 were unable to establish roots in tissue culture and grow past the initial shooting phase (Figure 4.13). This would indicate that expression of the *BdCYP75B4-2A-BdCYP93G1* construct during lignin rather than cellulose deposition does not alleviate the negative impact on plant growth. Several of the plants transformed with *ACP::75* were able to grow in tissue

culture, although at slower rates than their respective background controls. Most of the wild-type and CHS2 poplar transformed with *ACP::93*, on the other hand, were unable to establish roots and grow past the shooting phase in tissue culture. This would suggest that while both *BdCYP75B4* and *BdCYP93G1* appear to impact plant viability, it is likely that expression of *BdCYP93G1* negatively impacts growth to a greater degree.

While the precise mechanism responsible for impacting the growth and viability of plants expressing *BdCYP75B4-2A-BdCYP93G1* is unclear, the occurrence of reduced vessel area, dwarf phenotype, and failure to produce adventitious roots is consistent with potential disruption in auxin transport and signalling. Overexpression of *PtoIAA9*, an auxin signalling repressor in poplar, led to a reduction in vessel and fibre area as well as fewer layers of early developing xylem indicating inhibition in the number of periclinal divisions at the cambial meristem (Xu et al., 2019). In addition, transgenic poplar overexpressing *PtoIAA9* were significantly shorter than their wild-type counterparts. Although cross-talk between several different phytohormones occurs in the initiation of adventitious roots, auxin is considered the master regulator (Bannoud and Bellini, 2021). Poplar shoots treated in tissue culture with inhibitors of polar auxin transport, anti-auxin agents, or indole-3-acetic acid (IAA) competitors, induction of adventitious rooting was prevented (Bellamine et al., 1998). Moreover, several key components of the auxin signalling pathway have been shown to be involved in adventitious rooting (Bannoud and Bellini, 2021). For instance, overexpression of auxin receptor *TIR1* (PagFBL1) in the poplar hybrid *P. alba x glandulosa* induced formation of adventitious rooting by interacting with the AUX/IAA protein, PagIAA28, allowing for expression of auxin response factors (ARFs; Shu et al., 2019). Poplar genes *ARF8* and *ARF17* have also both been shown to regulate adventitious rooting by inducing root formation when overexpressed (Cai et al., 2019; Liu et al., 2020).

Flavonoids have long been reported to influence auxin signalling by either inhibiting polar auxin transport (Buer et al., 2010; Buer et al., 2013), limiting IAA oxidation during auxin biosynthesis (Gayomba et al., 2016) and/or modulating ROS-dependent signalling mechanisms (Brunetti et al., 2018; Gayomba and Muday, 2020). Flavonoids have even more recently been

proposed to act as signalling molecules functioning at very low concentrations through inhibitory interactions with protein kinases (Brunetti et al., 2018), for example, through the inhibition of PID kinases that aid in locating PIN proteins for polar auxin transport (Brown et al., 2001; Peer and Murphy, 2007). Therefore, it is possible that expression of *BdCYP93G1* and/or *BdCYP75B4* results in the production of unique flavonoids at the vascular cambium during early xylem development that may act as signalling molecules causing disruption of auxin signalling. However, further investigations into the auxin signalling pathway of plants expressing *BdCYP75B4-2A-BdCYP93G1, BdCYP93G1,* and *BdCYP75B4* are required to confirm this possibility. It is also possible that expression of *BdCYP93G1* and *BdCYP75B4* impact plant viability through production of toxic products by activity on non-target substrates, although to date, no substrates beyond flavonoids have been reported for members of the CYP75B4 and CYP93G subfamilies (Du et al., 2016).

A final possibility is that production of exogenous CYP450s themselves in developing xylem tissue inhibits growth and development. This may occur through disruption of metabolons complexes facilitating phenylpropanoid biosynthesis during active lignification. Metabolons are weakly bound assemblies of enzymes involved in specific sequential metabolic pathways, which allows for rapid and more efficient production of metabolites through "metabolic channelling". In both phenylpropanoid and flavonoid biosynthesis, metabolons are localized to the ER through weak associations of soluble enzymes with the ER anchored CYP450s. For example, in rice soluble CHS was associated with OsCYP75B3, an F3'H (Shih et al., 2008), the soluble lignin biosynthetic enzymes; 4CL1 and CCR were both shown to associate with ER-localized C4H (Gou et al., 2018). CYP450s may also associate with one another as the isoflavone synthase, CYP93B1, derived from both soybean and alfalfa, directly interacts with C4H derived from *Arabidopsis* (Dastmalchi et al., 2016; Waki et al., 2016; Gou et al., 2018). Therefore, it is possible that BdCYP93G1 and BdCYP75B4 disrupt monolignol biosynthesis through interactions with C4H, or other lignin biosynthetic enzymes, thereby disrupting the ordered assembly of the metabolon at the cytoplasmic face of the ER. In *Arabidopsis*, the indirect association of the CYP450s, C4H, C3H, and F5H was found to be mediated by MSBP proteins which act as a scaffold for the assembly of the phenylpropanoid metabolon (Gou et al.,

2018). Downregulation of *MSBPs* resulted in plants with stunted growth, fewer seeds, and slightly lower lignin, indicating that disruption of the lignin biosynthetic metabolon resulted in less efficient production of monolignols (Gou et al., 2018).

4.4 Conclusion

By isolating and characterizing PaxgOMT25, BdCYP75B4, and BdCYP93G1, we were able to infer that when provided naringenin, these enzymes in combination could produce tricin in developing xylem of poplar. However, most plants expressing *ACP::75/93* were unable to establish adventitious roots and grow in tissue culture, preventing further analysis of their secondary xylem characteristics. Analysis of stem methanolic extracts taken from six-week-old (CHS2) ACP::75/93-poplar revealed presence of a unique peak with elution time and UV profile consistent with tricin, not observable in background controls. This would indicate that xylem specific co-expression of *MdCHS3, BdCYP75B4* and *BdCYP93G1* is sufficient to drive production of tricin in developing xylem of poplar.

However, these trees also exhibited stunted growth, and most positive transformants were unable to grow past the initial shooting phase in tissue culture. Moreover, examination of stem sections revealed that (CHS2) ACP::75/93-poplar contained smaller vessels compared to all three controls. Similar reductions in viability observed in plants transformed with *C4H::75/93, ACP::93,* and, to a lesser extent, *ACP::75*, indicating that expression of *BdCYP93G1,* in particular, may be limiting to plant growth and viability. The exact mechanism by which expression of *BdCYP93G1* and/or *BdCYP75B4* impacts growth and development remains unclear. However, disruption of auxin signalling or interference with the assembly of the phenylpropanoid metabolon are both possible causes and could merit further investigation. Finally, while the incorporation of flavonoids into poplar lignins is an appealing target for production of value-added, less recalcitrant, lignocellulosic biomass, the work presented here clearly shows that exogenous expression of flavonoid modifying enzyme may impact plant growth as well as cell differentiation and development at the vascular cambium in unexpected

ways. Therefore, a better understanding of the mechanism by which flavonoids impact these processes is required in order to further optimize flavonolignan aimed engineering strategies.

Chapter 5: Conclusion and future directions

The remarkable metabolic plasticity of lignin biosynthesis has been well established. The non-enzymatic nature of the radical coupling reaction in lignin polymerization allows for the production of completely unique lignins, all with distinct sequences of monomers and linkages (Ralph et al., 2004). This allows lignins to not only lend plant vasculature the necessary strength for solute transport, but also act as a barrier to pests and pathogens (Vanholme et al., 2010; Coleman et al., 2008b). In the last two decades, extensive work manipulating the monolignol biosynthetic pathway has led to substantial alterations in total lignin content, monomer (S:G) composition, and to the introduction of novel lignin monomers (Chanoca et al., 2019; Ralph et al., 2019). Moreover, in the last ten years, advances in NMR technology have allowed for better investigations into the structure of naturally occurring lignins and has led to the discovery of many new non-canonical lignin monomers (Ralph and Landucci, 2010; Mansfield et al., 2012b; Ralph et al., 2019). It now appears that opportunities for incorporation of novel lignin monomers are abundant. The objective of this dissertation was to further investigate the limits of lignin engineering through the ectopic production of flavonoids in developing xylem of poplar in order to determine if flavonoids could be engineered into poplar lignins.

5.1 Major Findings in Chapters 3

My work in chapter 3 shows that not only can flavonoids be engineered into the lignins of poplar, but that carbon flux may be diverted away from monolignol biosynthesis resulting in lower total lignin trees with no growth penalties. Lignification of xylem tissue is considered a defining feature of all tracheophytes, believed to be essential in providing the structural support required to grow vertically on land (Weng and Chapple, 2010). Early work into the disruption of the monolignol biosynthetic pathway resulted in plants with lower total lignin, but often at the expense of growth (Li et al., 2003; Leple et al., 2007; Coleman et al., 2008a; Voelker et al., 2011; Sykes et al., 2015; Saleme et al., 2017). While it was initially assumed that dwarfing was the result of compromised structural integrity in the vasculature of low lignin poplar, later work has suggested that pleiotropic effects of blocking monolignol biosynthesis such as the build up of toxic phenolic byproducts and disruption of the source to sink relationship in poplar

trees also play a significant role in dwarfing phenotypes (Coleman et al., 2008a; El Houari et al., 2021). Because actively lignifying xylem tissue acts as a powerful carbon sink in growing poplar, disruption of monolignol biosynthesis results in a disruption of source to sink balance leading to a reduction in the overall photosynthetic rate of the plant (Coleman et al., 2008b). Expression of *MdCHS3* in poplar xylem resulted in lower total lignin due to alterations in carbon flux, presumably without compromising sink strength of lignifying tissues. However, it is worth noting, that the *MdCHS3*-poplar did not exhibit any reductions in lignin severe enough to match levels observed in low lignin dwarfed poplar lines. Therefore, the role that compromised sink strength plays in effecting growth penalty of low lignin trees remains to be seen. Moreover, the precise contribution that phenolic glycoside build up, disrupted source to sink balance, and compromised structural integrity plays in the dwarfing phenotype of low lignin poplar trees is yet to be determined. However, strategies of lignin engineering that work to divert carbon away from monolignol biosynthesis and towards the production of specialty chemicals such as naringenin offer the possibility of working around this obstacle by producing plants with slightly lower lignin, while concomitantly producing value-added phenolics where compromised source to sink balance and build up of toxic byproducts from the monolignol pathway do not limit growth.

The accumulation of flavonoids is known to inhibit auxin transport (Buer et al., 2013). It was even proposed that flavonoids accumulating in *Arabidopsis* with perturbed monolignol biosynthesis were responsible for stunted growth in the low lignin mutants (Besseau et al., 2007). However, this was disproved when *Arabidopsis tt4,* mutant lines unable to produce flavonoids, were shown to have the same dwarfing phenotype when monolignol biosynthesis was similarly disrupted (Li et al., 2010). The work presented in chapter 3 demonstrates that ectopic production of naringenin in developing xylem of poplar did not impair growth, adding further support to the findings in *Arabidopsis* that accumulation of flavonoids in xylem tissue are not responsible for low lignin dwarf phenotypes. However, *MdCHS3*-poplar did display a significantly lower rate of sylleptic branching when compared to wild-type grown in the same conditions (Figure 5.1), a trait known to be controlled by auxin and cytokinin cross talk (Cline and Dong, 2002). This result would indicate that production of naringenin does have an impact

on tree growth and architecture potentially through inhibition of auxin transport along the developing cambial meristem, suggesting that possible interactions between ectopic naringenin and auxin signalling in developing xylem of MdCHS3-poplar poplar cannot be discounted.

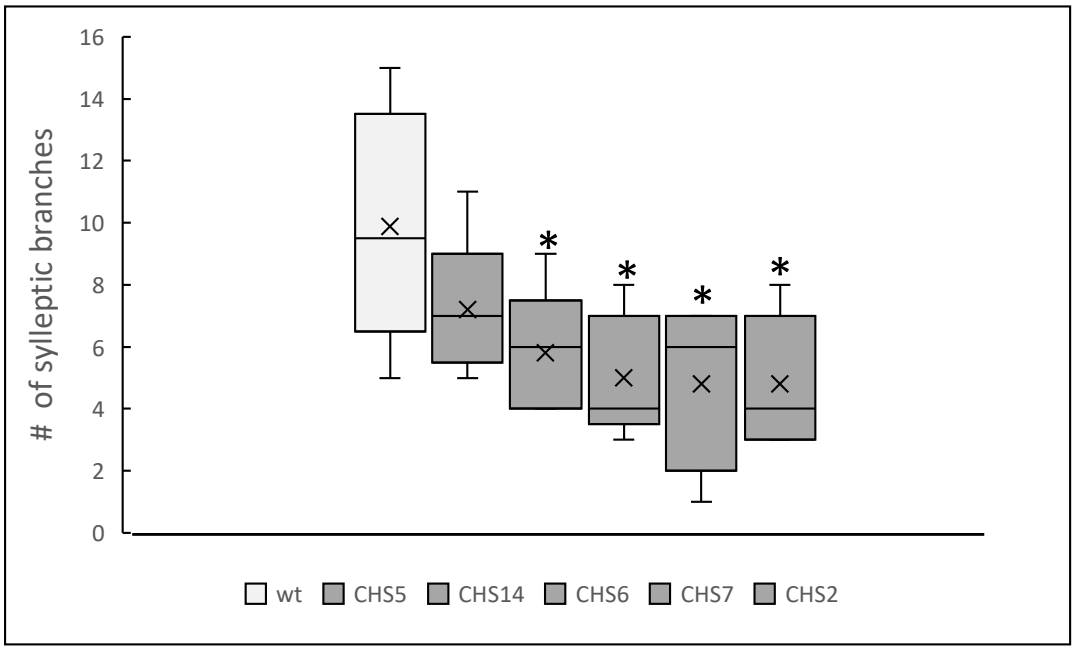

Figure 5.1: Number of sylleptic branches observed across *MdCHS3*-poplar lines.

Sylleptic branches counted on sixteen-week-old wild-type and *MdCHS3*-poplar lines. Five individuals counted per line. Counts displayed as boxplots with mean marked as an X. Significant differences compared to wild-type determined using student's t-test and indicated with an astericks (*).

The incorporation of naringenin into *MdCHS3*-poplar lignins marks the first time a flavonoid has been engineered into lignins of poplar or any other plant species that does not otherwise produce flavonolignans naturally. Naringenin is also among the first phenolic compounds found outside the phenylpropanoid pathway to be incorporated into lignins as a result of genetic engineering (Oyarce et al., 2019; del Río et al., 2020). This finding not only further expands our understanding of the plasticity of lignification but provides important groundwork for the introduction of other flavonoids, beyond naringenin, into poplar lignins. The widespread occurrence of tricin-integrated lignin in members of the grass family has demonstrated that flavonoids are chemically compatible with lignification (Lan et al., 2016). The

work presented in chapter 3, describing the successful incorporation of naringenin into poplar lignins, demonstrates that the production of flavonolignins is an entirely feasible lignin-first strategy adding further value to lignocellulosic feedstock. Moreover, considering the broad diversity of the flavonoids found across the plant kingdom, the possibilities of novel flavonoid targets for engineering into lignins are seemingly limitless.

5.2 Major Findings in Chapter 4

Together, OsCYP75B4 and OsCYP93G1 play a key role in the production of *O*-linked tricin glycosides and tricin-integrated lignins in rice (Lam *et al.* 2015; Lam *et al.* 2014). In Chapter 4, I show that homologous genes in *Brachypodium, BdCYP75B4* and *BdCYP93G1*, are similarly capable of working in tandem to produce tricin precursors. Poplar contains three putative *CYP75 g*enes, none of which appear to display high levels of expression in poplar xylem tissue (Nelson et al., 2008), and three putative *CYP93B* (*FNSII*) genes (Du et al., 2016), only one of which is expressed at very low levels in poplar xylem compared to leaf tissue. Expression of both *BdCYP75B4* and *BdCYP93G1* in the xylem tissue of *MdCHS3*-poplar trees is likely necessary for the production of tricin.

In Chapter 4, I conducted *in vitro* analysis of an endogenous poplar OMT (PaxgOMT25) and demonstrated that this key enzyme in monolignol biosynthesis is capable of methylating flavonoids such as luteolin and tricetin. Disruption of tricin biosynthesis in grasses leads to reductions in total lignin, despite tricin-integrated lignin only accounting for 3% of total lignin, indicating a synergistic relationship between flavonoid and monolignol biosynthetic pathways leading to the production of lignin (Lam et al., 2017). Therefore, the presence of an OMT enzyme capable of participating in methylation of both phenylpropanoid and flavonoid substrates in grasses is unsurprising (Eudes et al., 2017). Efforts to engineer the production of tricin in *Arabidopsis,* a species in which monolignol and flavonoid pathways are thought to compete, have demonstrated the presence of a similarly bifunctional OMT (Lam et al., 2015). Taken together with the analysis of PaxgOMT25 presented in chapter four, it seems likely that lineage B subfamily of *OMTs* did not co-evolve with tricin's occurrence in the grass family to

participate in both monolignol and flavonoid biosynthesis, but rather the capability of this subfamily to participate in both processes can be found across all angiosperms.

Finally, in chapter 4 I demonstrate that co-expression of *MdCHS3, BdCYP75B4,* and *BdCYP93G1* in developing poplar xylem, is sufficient to produce tricin. Analysis of soluble phenolics extracted from xylem tissue of six-week-old (CHS2) ACP::75/93-poplar revealed several distinct differences compared to background controls, including the appearance of a peak consistent with tricin, as well as several other peaks consistent with flavones. While this indicates the successful production of tricin, the analysis is limited by small amounts of tissue available for extraction as well the use of biological replicates arising from only one successful transformation.

In this chapter, I further explore the negative impact of SCW-specific expression of *BdCYP75B4* and *BdCYP93G1* on plant growth and viability. While it is difficult to pinpoint the exact mechanism underlying the reductions in growth, I propose three possible explanations. Firstly, I propose that interactions between BdCYP93G1 and BdCYP75B4 disrupt the assembly of endogenous poplar metabolon responsible for efficient production of phenylpropanoids. However, none of the positive transformants exhibit a collapsed xylem phenotype typically characteristic of lower lignin plants with compromised monolignol biosynthesis. Secondly, I proposed that the action of BdCYP93G1 and BdCYP75B4 results in the accumulation of toxic phenolic byproducts which impact growth and development. Clear differences were observed in the soluble phenolic extracts of a low expressing (CHS2) *ACP::75/93*-poplar line compared to background controls, suggesting that toxic products may accumulate to toxic levels in higher expressing lines thereby preventing growth. Soluble phenylpropanoid induced dwarfism (SPID) is one of the models offered to explain the dwarfing observed in *Arabidopsis* mutants with disrupted phenylpropanoid biosynthesis (El Houari et al., 2021). There is evidence that accumulation of certain phenolics may be responsible for the dwarfing of some low lignin mutants, although in many cases the evidence remains indirect. For example, salicylic acid (SA) build up is responsible for stunting in *hct* mutant *Arabidopsis* (Gallego-Giraldo et al., 2011), however, confoundingly, SA does not seem to be responsible for the same phenotype in *c3'h*

mutants (Bonawitz et al., 2014). Accumulation of ferulic acid has been proposed to cause reduction in leaf size through ROS scavenging during cell proliferation in *ccr1-4* mutant *Arabidopsis* (Xue et al., 2015); yet growth was rescued in *ccr1-6* mutants when lignification was fully restored, despite the continued accumulation of ferulic acid (De Meester et al., 2018). In poplar, the accumulation of ester-linked *p*-coumarate glycoside conjugates has been proposed to be partly responsible for the dwarfing phenotype of low lignin poplar with severely suppressed expression of *C3'H* (Coleman et al., 2008a; Coleman et al., 2008b). However, no direct link between accumulation of toxic soluble products and growth penalties observed in mutant poplar with disrupted monolignol biosynthesis has been established indicating that a similar link in *BdCYP75B4-2A-BdCYP93G1* expressing plants is unlikely.

Finally, the phenotypic changes (stunted growth, inhibition of adventitious root formation, and alteration to vessel/fibre area) observed in (CHS2) ACP::75/93 expressing poplar, as well as poplar transformed with C4H::75/93, ACP::93 and ACP::75 are consistent with changes observed in poplar in which auxin signalling has been disrupted (Bellamine et al., 1998; Nilsson et al., 2008; Xu et al., 2019). Flavonoids have long been reported to regulate processes such as cell growth and differentiation at the vascular cambium as well as adventitious root initiation from cuttings through interactions with several phytohormones, namely auxin (Brunetti et al., 2018; Bannoud and Bellini, 2021). While flavonoids have been proposed to regulate auxin signalling by modulating intercellular and intracellular auxin transport, limiting IAA oxidation and/or attenuating stress-induced ROS activation of MAPK signalling cascades, flavonoids have been more recently proposed to act as signalling molecules at very low levels by inhibiting MAPK signalling cascades (Brunetti et al., 2018). This is supported by the unexplained localization of some flavonoids to the nucleus, where many MAPK are localized (Agati et al., 2012; Komis et al., 2018) and by the remarkable capacity of flavonoids to act at very low levels as inhibitors of cancerous cell proliferation in human medical studies through their action as protein kinase inhibitors (Hou and Kumamoto, 2010). It has even been proposed that regulation of phytohormones was the primary role of flavonoids in the emergence of land plants rather than protection against UV-B radiation (Brunetti et al., 2018). All of which is to say that flavonoids may act as powerful inhibitory signalling molecules at very low levels when they

are ectopically produced at the vascular cambium, a meristematic tissue that relies on auxin to initiate radial expansion and xylogenesis. In chapter 4, I propose that the flavonoids produced through the action of BdCYP93G1 and/or BdCYP75B4 may be acting at low levels to impact xylem cell differentiation and development in low expressing lines and concurrently prevent growth in higher expressing lines. It is important to note that while endogenous flavonoid enzymes in poplar are not expressed highly in secondary xylem tissue, they are expressed in phloem tissue (Figure 5.2; Sundell et al., 2017). This is consistent with a metabolomic study of developing poplar wood which found that flavonoids, namely the dihydroflavonol catechin, accumulate almost exclusively in the phloem tissue (Figure 5.2; Abreu et al., 2020). Coincidentally, both C4H and secondary cell wall CesA promoters drive expression in phloem, albeit to a lesser extent than xylem tissue (Figure 5.2; Sundell et al., 2017). Since wild-type and *MdCHS3* poplar expressing *BdCYP93G1* and/or *BdCYP75B4* displayed stunted growth, the enzymes may be acting on endogenous flavonoid substrates in phloem tissue to produce flavonoids that impact auxin signalling in the vascular cambium.

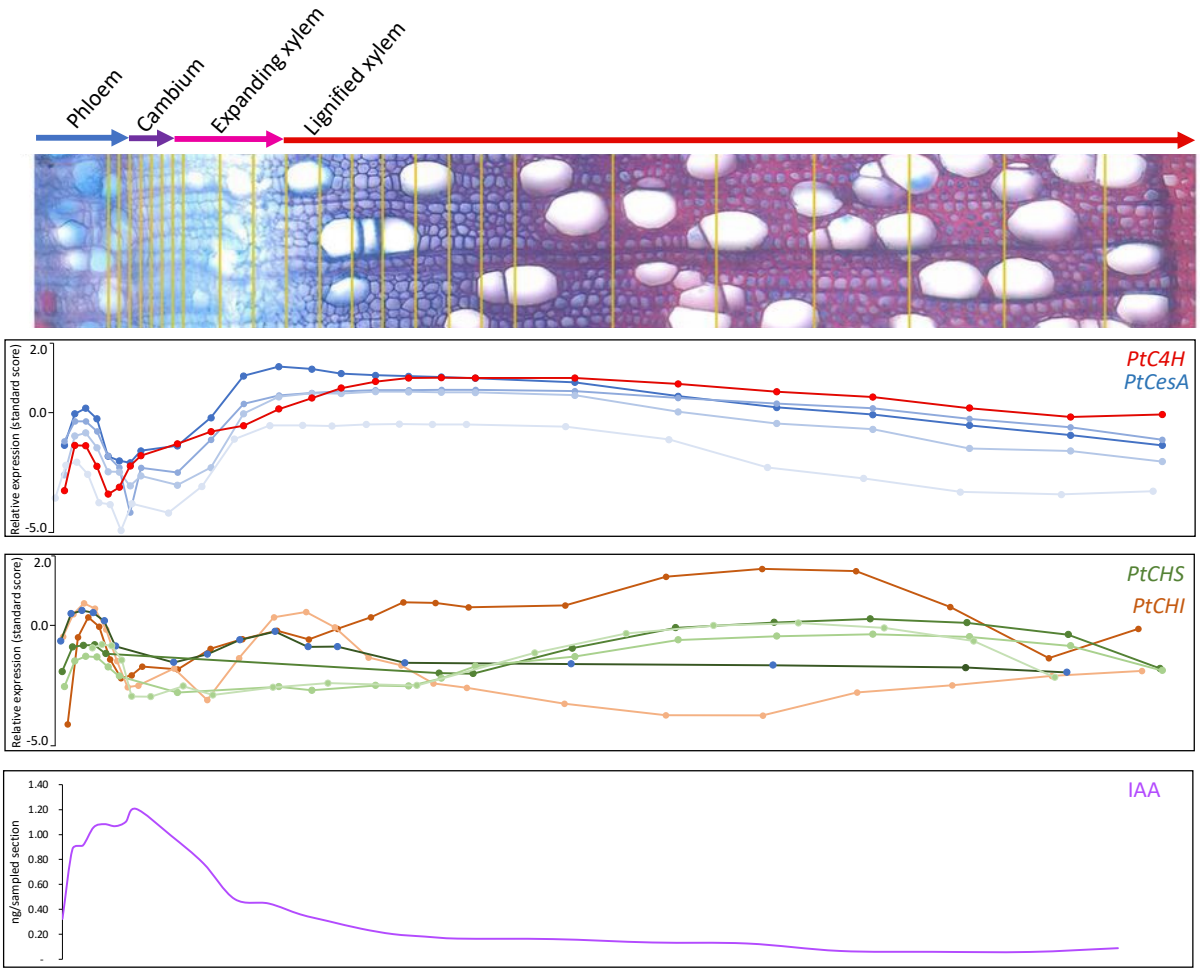

Figure 5.2: Relative expression of secondary cell wall and flavonoid biosynthetic genes compared to concentration of auxin across developing poplar wood.

Expression of cinnamate-4-hydroxylase (C4H), secondary cell wall cellulose synthases (SCW CesAs), chalcone synthases (CHSs) and chalcone isomerase (CHI) genes compared to the concentration of indole-3-acetic acid (IAA). Gene expression of PtCHS4 (Potri.013G157900), CesA8 (Potri.011G069600), CesA8 (Potri.004G059600), CesA7-A (Potri.006G181900), CesA7-B (Potri.018G103900), CesA4 (Potri.002G257900) and CHS (Potri.001G051500, Potri.001G051600, Potri.014G145100, Potri.003G176700) retrieved from (Sundell et al., 2017). Relative expression shown as standard score across the full data set of 10 genes. Concentration of IAA retrieved from (Abreu et al., 2020). Data represents averages of ng/section of wood taken from five individuals.

5.3 Outstanding Questions and Future Directions

5.3.1 Increasing production of naringenin in *MdCHS3*-poplar xylem

Expression of *MdCHS3* in poplar xylem resulted in the production of naringenin and its subsequent incorporation into lignins; however, naringenin was only incorporated at trace levels. In order to further optimize poplar with naringenin-integrated lignin, more work needs to be done exploring the factors limiting the production of naringenin. For example, cytosolic acetyl-CoA carboxylase (ACCase) is responsible for providing malonyl-CoA to CHS in the production of flavonoids and stilbenoid compounds. Expression of cytosolic *ACCase* is relatively low in developing xylem tissue, suggesting that the availability of malonyl-CoA in the cytosol may be limiting production of naringenin (Winter et al., 2007; Sundell et al., 2017). Transforming *MdCHS3* poplar with the previously characterized *AtACCase1* using a lignin-specific promoter may increase the availability of the malonyl-CoA substrate used by CHS.

This would allow us to understand the extent to which carbon may be diverted from monolignol biosynthesis toward flavonoid biosynthesis without reducing total lignin to the point of compromising vascular integrity. It would also provide us with a better understanding of the extent to which naringenin may be incorporated into poplar lignins. Moreover, an increase in naringenin-integrated lignin will allow us to examine the DP of lignins to determine if polymer length is in fact reduced as a result of flavonoid incorporation. Finally, increasing the amount of naringenin produced in developing xylem tissue may help us to further elucidate the impact on xylem differentiation and development when naringenin accumulates near the vascular cambium.

5.3.2 Investigating mechanism by which *BdCYP75B4* and *BdCYP93G1* expression impacts plant growth

The results presented in chapter 4 clearly show that engineering flavonoid production in developing xylem tissue can have a negative impact on plant growth and viability. It is critical to understand the mechanism by which expression of flavonoid-modifying enzymes using secondary cell wall promoters impacts growth and development in poplar. I suggested three

possible mechanisms by which the impact of *BdCYP75B4* and *BdCYP93G1* on plant growth, all of which are testable following the generation of more independent lower expressing lines.

Firstly, soluble extracts taken from lower expressing plants could be further analysed using more sensitive analytical techniques, such as LC-MS, in order to determine the identity of any toxic products that are accumulating and impacting cell growth and differentiation. Secondly, transcriptomic analysis of the low expressing lines may point to changes in expression of key developmental signalling pathways and help to elucidate the mechanism by which plant growth is impacted. Additionally, we can test these mutants for differences in auxin transport using radiolabelled IAA (Rashotte et al., 2000) and determine if auxin transport is inhibited by expression of *BdCYP75B4* and *BdCYP93G1*. Of course, the major limitation to working with only low expressing lines is that the phenotypic changes observed in higher expressing lines may not be detectable. Both the spatial and temporal nature of *BdCYP75B4* and *BdCYP93G1* expression may be impacting the growth and differentiation of xylem cells at the cambium. Therefore, using different promoters/promoter combinations may work to alleviate their negative effects on growth. For example, use of the fibre-specific synthetic poplar promoter (*PdDUF579*; Song et al., 2014) or vessel-specific synthetic promoter (*PdXCP1*; Funk et al., 2002) rather than the secondary cell wall promoters used in chapter 4 could alleviate growth impairment observed poplar expressing *BdCYP75B4* and *BdCYP93G1* by preventing expression in phloem tissue.

Finally, it may be interesting to confirm that *BdCYP75B4* and *BdCYP93G1* do, in fact, localize at the cytosolic face of the ER through the use of fluorescent tags in an inducible *VND7* system, which induces ectopic formation of secondary cell walls in mesophyll cells (Watanabe et al., 2015). Additionally, it would be helpful to use this system to determine if these CYP450s co-localize with other monolignol biosynthetic enzymes and do not disrupt normal assembly of the monolignol biosynthetic metabolon.

5.3.3 Potential flavonoid targets for production in developing xylem of poplar

While the work presented in this thesis has revealed serious obstacles to the production of flavonoid-integrated lignins in poplar, the possibility of producing value-added lignin using flavonoids is still an exciting one. By using the *MdCHS3*-poplar generated in chapter 3, many

new flavonoids may be produced by modifying naringenin, the precursor molecule to most other flavonoids.

A broad array of flavonoids and flavonoid-rich extracts derived from various plant species are reported to have anti-cancer, antioxidant, anti-inflammatory, and antiviral properties (Ullah et al., 2020), and while the majority of these positive health benefits can be gained through a plant-rich diet, many purified flavonoids show promise in pharmaceutical applications. Aurones, for example, are a class of flavonoids which rarely occur in nature yet have garnered substantial interest for their ability to act as highly potent anticancer agents through the direct inhibition of a number of targets, including cyclin dependent kinases, adenosine receptors, telomerases, histone deacetylases, and microtubule formation during cell proliferation (Alsayari et al., 2019). These compounds are often produced semi-synthetically by relying on the extraction of aurones from members of the *Coreopsis* genus in the sunflower family to use as a base molecule for further synthetic modifications (Alsayari et al., 2019). *In planta* aurones are produced from naringenin chalcone through the action of *aurone synthase (ANS)*, which is a polyphenol oxidase expressed at high levels in the petals of *Coreopsis grandiflora* (Molitor et al., 2015). Expression of an *ANS* in *MdCHS3*-poplar could facilitate the production of aurones in developing xylem and, considering that the phenolic B-ring remains intact, could result in the incorporation of aurones into poplar lignins. This could increase the value of poplar lignins as well as the availability of aurone base molecules for use in the production of chemo-preventative pharmaceuticals.

Alternative flavonoid targets include quercetin, a potent therapeutic agent in the treatment of colorectal cancer. Quercetin can be synthesized from naringenin through the combined action of flavanone-3-hydroxylase (F3H), flavanol synthase (FLS), and an F3′H. It would likely be incorporated into lignins, although the exact manner would need to be determined *in vitro* through production of dehydrogenation polymers. The production of flavanols in xylem tissue, however, may impact plant growth as flavanols are reported to have the strongest inhibitory effect on auxin transport in *Arabidopsis* (Brown et al., 2001; Brunetti et al., 2018). Finally, the isoflavone geneticin purified from soy is reported to induce growth arrest

and apoptosis in prostate cancer cells and proposed to partly account for the lower rates of prostate cancer in individuals with soy-rich diets (Mahmoud et al., 2014). Genistein is produced from naringenin through the action of isoflavone synthase (IFS; Jung et al., 2000). *MdCHS3* poplar would require transformation with only one gene to produce the isoflavone. Additionally, since poplar trees do not naturally produce isoflavones, it's less likely that accumulation of geneticin in developing xylem will have inhibitory effects on cell growth and differentiation.

References

Abreu IN, Johansson AI, Sokołowska K, Niittylä T, Sundberg B, Hvidsten TR, Street NR, Moritz T (2020) A metabolite roadmap of the wood-forming tissue in *Populus tremula*. New Phytologist **228:** 1559-1572

Agati G, Azzarello E, Pollastri S, Tattini M (2012) Flavonoids as antioxidants in plants: location and functional significance. Plant Science **196:** 67-76

Albersheim P, Darvill A, Roberts K, Sederoff R, Staehelin A (2010) Plant cell walls. Garland Science

Alcalde-Eon C, Ignacio García-Estévez, Rivas-Gonzalo JC, David Rodríguez de la Cruz, Escribano-Bailón. MT (2016) Anthocyanins of the anthers as chemotaxonomic markers in the genus *Populus L*.. Differentiation between *Populus nigra*, *Populus alba* and *Populus tremula*. Phytochemistry **128:** 35-49

Alsayari A, Muhsinah AB, Hassan MZ, Ahsan MJ, Alshehri JA, Begum N (2019) Aurone: A biologically attractive scaffold as anticancer agent. European Journal of Medical Chemistry **166:** 417-431

Aoki D, Hanaya Y, Akita T, Matsushita Y, Yoshida M, Kuroda K, Yagami S, Takama R, Fukushima. K (2016) Distribution of coniferin in freeze-fixed stem of *Ginkgo biloba L.* by cryo-TOF-SIMS/SEM. Scientific reports **6:** 1-9

Austin MB, Noel JP (2003) The chalcone synthase superfamily of type III polyketide synthases. Natural Products Reports **20:** 79-110

Baas P, Ewers FW, Davis SD, Wheeler EA (2004) Evolution of xylem physiology, Vol 21. Elsevier Academic Press, London, UK

Bannoud F, Bellini C (2021) Adventitious Rooting in. Frontiers in Plant Science **12:** 668837

Barakat A, Choi A, Yassin NB, Park JS, Sun Z, Carlson JE (2011) Comparative genomics and evolutionary analyses of the O-methyltransferase gene family in *Populus*. Gene **479:** 37-46

Barbehenn RV, Constabel PC (2011) Tannins in plant–herbivore interactions. Phytochemistry **72:** 1551-1565

Bellamine J, Penel C, Greppin H, Gaspar T (1998) Confirmation of the role of auxin and calcium in the late phases of adventitious root formation. *In*, Vol 26, Plant growth regulation, pp 191-194

Berim A, Gang DR (2015) Methoxylated flavones: occurrence, importance, biosynthesis. Phytochemistry Reviews **15:** 363-390

Berlin A, Gilkes N, Kurabi A, Bura R, Tu M, Kilburn D, Saddler J (2005) Weak lignin-binding enzymes: a novel approach to improve activity of cellulases for hydrolysis of lignocellulosics. Applied Biochemistry and Biotechnology **121-124:** 163-170

Besseau S, Hoffmann L, Geoffroy P, Lapierre C, Pollet B, Legrand M (2007) Flavonoid accumulation in *Arabidopsis* repressed in lignin synthesis affects auxin transport and plant growth. Plant Cell **19:** 148-162

Bhalla A, Bansal N, Pattathil S, Li M, Shen W, Particka CA, Karlen SD, Phongpreecha T, Semaan RR, Gonzales-Vigil E, Ralph J, Mansfield SD, Ding S-Y, Hodge DB, Hegg EL (2018) Engineered Lignin in Poplar Biomass Facilitates Cu-Catalyzed Alkaline-Oxidative Pretreatment. ACS Sustainable Chemistry & Engineering **6:** 2932-2941

Björklund S, Antti H, Uddestrand I, Moritz T, Sundberg B (2007) Cross-talk between gibberellin and auxin in development of *Populus* wood: gibberellin stimulates polar auxin transport and has a common transcriptome with auxin. The Plant Journal **52:** 499-511

Boerjan W, Ralph J, Baucher M (2003) Lignin biosynthesis. Annual Reviews of Plant Biology **54:** 519-546

Bonawitz ND, Kim JI, Tobimatsu Y, Ciesielski PN, Anderson NA, Ximenes E, Maeda J, Ralph J, Donohoe BS, Ladisch M, Chapple C (2014) Disruption of Mediator rescues the stunted growth of a lignin-deficient *Arabidopsis* mutant. Nature **509:** 376-380

Brackmann K, Qi J, Gebert M, Jouannet V, Schlamp T, Grünwald K, Wallner ES, Novikova DD, Levitsky VG, Agustí J, Sanchez P (2018) Spatial specificity of auxin responses coordinates wood formation. Nature communications **9:** 1-15

Brown DE, Rashotte AM, Murphy AS, Normanly J, Tague BW, Peer WA, Taiz L, Muday GK (2001) Flavonoids act as negative regulators of auxin transport in vivo in *Arabidopsis*. Plant Physiology **126:** 524-535

Brunetti C, Fini A, Sebastiani F, Gori A, Tattini M (2018) Modulation of phytohormone signaling: a primary function of flavonoids in plant–environment interactions. *In*, Vol 9, *Frontiers in Plant science*, p 1042

Brunner AM (2010) Reproductive development in *Populus*. Genetics and genomics of *Populus* 155-170

Buer CS, Imin N, Djordjevic MA (2010) Flavonoids: new roles for old molecules. Journal of Integrated Plant Biology **52:** 98-111

Buer CS, Kordbacheh F, Truong TT, Hocart CH, Djordjevic MA (2013) Alteration of flavonoid accumulation patterns in transparent testa mutants disturbs auxin transport, gravity responses, and imparts long-term effects on root and shoot architecture. Planta **238:** 171-189

Busse-Wicher M, Gomes TC, Tryfona T, Nikolovski N, Stott K, Grantham NJ, Bolam DN, Skaf MS, Dupree P (2014) The pattern of xylan acetylation suggests xylan may interact with cellulose microfibrils as a twofold helical screw in the secondary plant cell wall of *Arabidopsis thaliana*. Plant Journal **79:** 492-506

Cai H, Yang C, Liu S, Qi H, Wu L, Xu LA, Xu M (2019) MiRNA-target pairs regulate adventitious rooting in Populus: a functional role for miR167a and its target Auxin response factor 8. Tree Physiology **39:** 1922-1936

Chang S, Puryear J, Cairney J (1993) A simple and efficient method for isolating RNA from pine trees. Plant Molecular Biology Reporter **11:** 113-116

Chanoca A, de Vries L, Boerjan W (2019) Lignin engineering in forest trees. Frontiers in Plant Science **10:** 912

Chebli Y, Geitmann A (2017) Cellular growth in plants requires regulation of cell wall biochemistry. Current Opinion in Cell Biology **44:** 28-35

Chou EY, Schuetz M, Hoffmann N, Watanabe Y, Sibout R, Samuels AL (2018) Distribution, mobility, and anchoring of lignin-related oxidative enzymes in Arabidopsis secondary cell walls. Journal of Experimental Botany **69:** 1849-1859

Cline MG, Dong IK (2002) A preliminary investigation of the role of auxin and cytokinin in sylleptic branching of three hybrid poplar clones exhibiting contrasting degrees of sylleptic branching. Annals of Botany **90:** 417-421

Coleman HD, Ellis DD, Gilbert M, Mansfield SD (2006) Up-regulation of sucrose synthase and UDP-glucose pyrophosphorylase impacts plant growth and metabolism. Plant Biotechnology Journal **4:** 87-101

Coleman HD, Park J-Y, Nair R, Chapple C, Mansfield SD (2008a) RNAi-mediated suppression of *p*-coumaroyl-CoA 3'-hydroxylase in hybrid poplar impacts lignin deposition and soluble secondary metabolism. Proceedings of the National Academy of Sciences **105:** 4501-4506

Coleman HD, Samuels AL, Guy RD, Mansfield SD (2008b) Perturbed lignification impacts tree growth in hybrid poplar--a function of sink strength, vascular integrity, and photosynthetic assimilation. Plant Physiology **148:** 1229-1237

Cummins I, Brazier-Hicks M, Stobiecki M, Franski R, Edwards R (2006) Selective disruption of wheat secondary metabolism by herbicide safeners. Phytochemistry **67:** 1722-1730

Dai X, Hu Q, Cai Q, Feng K, Ye N, Tuskan GA, Milne R, Chen Y, Wan Z, Wang Z, Luo W (2014) The willow genome and divergent evolution from poplar after the common genome duplication. Cell Research **24:** 1274-1277

Dastmalchi M, Bernards MA, Dhaubhadel S (2016) Twin anchors of the soybean isoflavonoid metabolon: evidence for tethering of the complex to the endoplasmic reticulum by IFS and C4H. Plant Journal **85:** 689-706

De Meester B, de Vries L, Özparpucu M, Gierlinger N, Corneillie S, Pallidis A, Goeminne G, Morreel K, De Bruyne M, De Rycke R, Vanholme R, Boerjan W (2018) Vessel-Specific Reintroduction of CINNAMOYL-COA REDUCTASE1 (CCR1) in dwarfed *ccr1* mutants restores vessel and xylary fiber integrity and increases biomass. Plant Physiology **176:** 611-633

De Paoli HC, Tuskan GA, Yang X (2016) An innovative platform for quick and flexible joining of assorted DNA fragments. Science Reports **6:** 19278

del Río JC, Gutiérrez A, Martínez ÁT (2004) Identifying acetylated lignin units in non-wood fibers using pyrolysis-gas chromatography/mass spectrometry. Rapid communications in Mass Spectrometry **18:** 1181-1185

del Río JC, Marques G, Rencoret J, Martínez ÁT, Gutiérrez A, Marques G, Rencoret J, Martínez ÁT, Gutiérrez A (2007) Occurrence of naturally acetylated lignin units. Journal of Agricultural and Food Chemistry **55:** 5461-5468

del Rio JC, Rencoret J, Marques G, Gutiérrez A, Ibarra D, Santos JI, Jiménez-Barbero J, Zhang L, Martínez AT (2008) Highly acylated (acetylated and/or *p*-coumaroylated) native lignins from diverse herbaceous plants. Journal of Agricultural and food Chemistry **56:** 9525-9534

del Rio JC, Rencoret J, Prinsen P, Martinez AT, Ralph J, Gutierrez A (2012) Structural characterization of wheat straw lignin as revealed by analytical pyrolysis, 2D-NMR, and reductive cleavage methods. Journal of Agricultural Food Chemistry **60:** 5922-5935

del Río JC, Rencoret J, Gutiérrez A, Kim H, Ralph J (2017) Hydroxystilbenes are monomers in palm fruit endocarp lignins. Plant Physiology **174:** 2072-2082

del Río JC, Rencoret J, Gutiérrez A, Kim H, Ralph J (2018) Structural characterization of lignin from maize (*Zea mays L.*) fibers: evidence for diferuloylputrescine incorporated into the lignin polymer in maize kernels. Journal of Agricultural and Food Chemistry **66:** 4402-4413

del Río JC, Rencoret J, Gutiérrez A, Elder T, Kim H, Ralph J (2020) Lignin Monomers from beyond the Canonical Monolignol Biosynthetic Pathway: Another Brick in the Wall. ACS Sustainable Chemistry & Engineering **8:** 4997-5012

de Vries L, MacKay HA, Smith RA, Mottiar Y, Karlen SD, Unda F, Muirragui E, Bingman C, Vander Meulen K, Beebe ET, Fox BG, Ralph J, Mansfield SD (2021) pHBMT1, a BAHD-family monolignol acyltransferase, mediates lignin acylation in poplar. Plant Physiology:

Dickmann DI (2009) An overview of the genus *Populus*. *In* JGI D.I. Dickmann, J.E. Eckenwalder, and J. Richardson., ed, Poplar culture in north America Part A Ed 2. NRC Research Press, National Research Council of Canada, Ottawa, pp 1-42

Dima O, Morreel K, Vanholme B, Kim H, Ralph J, Boerjan W (2015) Small glycosylated lignin oligomers are stored in *Arabidopsis* leaf vacuoles. Plant Cell **27:** 695-710

Du Y, Chu H, Chu IK, Lo C (2010) CYP93G2 is a flavanone 2-hydroxylase required for C-glycosylflavone biosynthesis in rice. Plant Physiology **154:** 324-333

Du H, Ran F, Dong HL, Wen J, Li JN, Liang Z (2016) Genome-Wide Analysis, Classification, Evolution, and Expression Analysis of the Cytochrome P450 93 Family in Land Plants. PLoS One **11:** e0165020

El Houari I, Boerjan W, Vanholme B (2021) Behind the Scenes: The Impact of Bioactive Phenylpropanoids on the Growth Phenotypes of *Arabidopsis* Lignin Mutants. Frontiers in Plant Science **12:** 734070

Eloy NB, Voorend W, Lan W, Saleme MdLS, Cesarino I, Vanholme R, Smith RA, Goeminne G, Pallidis A, Morreel K, Nicomedes J, Ralph J, Boerjan W (2017) Silencing CHALCONE SYNTHASE in maize impedes the incorporation of tricin into lignin and increases lignin content. Plant Physiology **173:** 998-1016

Eudes A, George A, Mukerjee P, Kim JS, Pollet B, Benke PI, Yang F, Mitra P, Sun L, Cetinkol OP, Chabout S, Mouille G, Soubigou-Taconnat L, Balzergue S, Singh S, Holmes BM, Mukhopadhyay A, Keasling JD, Simmons BA, Lapierre C, Ralph J, Loque D (2012) Biosynthesis and incorporation of side-chain-truncated lignin monomers to reduce lignin polymerization and enhance saccharification. Plant Biotechnology Journal **10:** 609-620

Eudes A, Sathitsuksanoh N, Baidoo EE, George A, Liang Y, Yang F, Singh S, Keasling JD, Simmons BA, Loque D (2015) Expression of a bacterial 3-dehydroshikimate dehydratase reduces lignin content and improves biomass saccharification efficiency. Plant Biotechnology Journal **13:** 1241-1250

Eudes A, Dutta T, Deng K, Jacquet N, Sinha A, Benites VT, Baidoo EEK, Richel A, Sattler SE, Northen TR, Singh S, Simmons BA, Loque D (2017) SbCOMT (Bmr12) is involved in the biosynthesis of tricin-lignin in sorghum. PLoS One **12:** e0178160

Fornale S, Shi X, Chai C, Encina A, Irar S, Capellades M, Fuguet E, Torres JL, Rovira P, Puigdomenech P, Rigau J, Grotewold E, Gray J, Caparros-Ruiz D (2010) ZmMYB31 directly represses maize lignin genes and redirects the phenylpropanoid metabolic flux. Plant Journal **64:** 633-644

Frangne N, Eggmann T, Koblischke C, Weissenböck G, Martinoia E, Klein M (2002) Flavone glucoside uptake into barley mesophyll and Arabidopsis cell culture vacuoles. Energization occurs by H+-antiport and ATP-binding cassette-type mechanisms. Plant Physiology **128:** 726-733

Franke R, Hemm MR, Denault JW, Ruegger MO, Humphreys JM, Chapple C (2002) Changes in secondary metabolism and deposition of an unusual lignin in the ref8 mutant of Arabidopsis. Plant Journal **30:** 47-59

Franke R, McMichael CM, Meyer K, Shirley AM, Cusumano JC, Chapple C (2000) Modified lignin in tobacco and poplar plants over-expressing the Arabidopsis gene encoding ferulate 5-hydroxylase. Plant Journal **22:** 223-234

Funada R (2008) Microtubules and the control of wood formation. Springer, Berlin, Heidelberg

Funk V, Kositsup B, Zhao C, Beers EP (2002) The *Arabidopsis* xylem peptidase XCP1 is a tracheary element vacuolar protein that may be a papain ortholog. Plant Physiology **128:** 84-94

Gallego-Giraldo L, Escamilla-Trevino L, Jackson LA, Dixon RA (2011) Salicylic acid mediates the reduced growth of lignin down-regulated plants. Proceedings National Academy of Science **108:** 20814-20819

Gayomba SR, Watkins JM, Muday GK (2016) Flavonols regulate plant growth and development through regulation of auxin transport and cellular redox status. *In,* Recent Advances in Polyphenol Research pp. 143-170

Gayomba SR, Muday GK (2020) Flavonols regulate root hair development by modulating accumulation of reactive oxygen species in the root epidermis. Development **147:** dev185819

Gebhardt YH, Witte S, Steuber H, Matern U, Martens S (2007) Evolution of flavone synthase I from parsley flavanone 3beta-hydroxylase by site-directed mutagenesis. Plant Physiology **144:** 1442-1454

Geisler K, Jensen NB, Yuen MM, Madilao L, Bohlmann J (2016) Modularity of Conifer Diterpene Resin Acid Biosynthesis: P450 Enzymes of Different CYP720B Clades Use Alternative Substrates and Converge on the Same Products. Plant Physiology **171:** 152-164

Gerttula S, Zinkgraf M, Muday GK, Lewis DR, Ibatullin FM, Brumer H, Hart F, Mansfield SD, Filkov V, Groover A (2015) Transcriptional and hormonal regulation of gravitropism of woody stems in Populus. The Plant Cell **27:** 2800-2813

Gill US, Uppalapati SR, Gallego-Giraldo L, Ishiga Y, Dixon RA, Mysore KS (2018) Metabolic flux towards the (iso) flavonoid pathway in lignin modified alfalfa lines induces resistance against *Fusarium oxysporum* f.sp*. medicaginis*. Plant, Cell & Environment **41:** 1997-2007

Giummarella N, Lawoko M (2016) Structural Basis for the Formation and Regulation of Lignin–Xylan Bonds in Birch. ACS Sustainable Chemistry & Engineering **4:** 5319-5326

Goiris K, Muylaert K, Voorspoels S, Noten B, De Paepe DE, Baart GJ, De Cooman L (2014) Detection of flavonoids in microalgae from different evolutionary lineages. Journal of Phycology **50:** 483-492

Gou M, Ran X, Martin DW, Liu CJ (2018) The scaffold proteins of lignin biosynthetic cytochrome P450 enzymes. Nature Plants **4:** 299-310

Greenaway SE, May J, Whatley FH (1991) Chemotaxonomy of section Leuce poplars by GC-MS of bud exudates. Biochemical Systematics and Ecology **19:** 507-518

Gu Z, Men S, Zhu J, Hao Q, Tong N, Liu ZA, Zhang H, Shu Q, Wang L (2019) Chalcone synthase is ubiquitinated and degraded via interactions with a RING-H2 protein in petals of Paeonia 'He Xie'. Journal of Experimental Botany **70:** 4749-4762

Hoch WA, Singsaas EL, McCown BH (2003) Resorption protection: anthocyanins facilitate nutrient recovery in autumn by shielding leaves from potentially damaging light levels. Plant Physiology **133:** 1296-1305

Hoffmann L, Besseau S, Geoffroy P, Ritzenthaler C, Meyer D, Lapierre C, Pollet B, Legrand M (2004) Silencing of hydroxycinnamoyl-coenzyme A shikimate/quinate hydroxycinnamoyltransferase affects phenylpropanoid biosynthesis. The Plant Cell **16:** 1446-1465

Hou DX, Kumamoto T (2010) Flavonoids as protein kinase inhibitors for cancer chemoprevention: direct binding and molecular modeling. Antioxididant Redox Signalling **13:** 691-719

Huntley SK, Ellis D, Gilbert M, Chapple C, Mansfield SD (2003) Improved pulping efficiency in C4H-F5H transformed poplar. Journal of Agricultural and Food Chemistry **51:** 6178–6183

Huntley SK, Ellis D, Gilbert M, Chapple C, Mansfield SD (2003) Significant increases in pulping efficiency in C4H-F5H-transformed poplars: improved chemical savings and reduced environmental toxins. Journal of Agricultural and Food Chemistry **51:** 6178-6183

Immanen J, Nieminen K, Smolander OP, Kojima M, Serra JA, Koskinen P, Zhang J, Elo A, Mähönen AP, Street NR, Bhalerao RP (2016) Cytokinin and auxin display distinct but interconnected distribution and signaling profiles to stimulate cambial activity. Current Biology **26:** 1990-1997

Jacobs M, Rubery PH (1988) Naturally occurring auxin transport regulators. Science **241:** 346-349

James AM, Ma D, Mellway R, Gesell A, Yoshida K, Walker V, Tran L, Stewart D, Reichelt M, Suvanto J, Salminen JP (2017) Poplar MYB115 and MYB134 transcription factors regulate proanthocyanidin synthesis and structure. Plant Physiology **174:** 154-171

Jansson S, Douglas CJ (2007) Populus: a model system for plant biology. Annual Reviews of Plant Biology. **58:** 435-458

Jia Y, Li B, Zhang Y, Zhang X, Xu Y, Li C (2019) Evolutionary dynamic analyses on monocot flavonoid 3′-hydroxylase gene family reveal evidence of plant-environment interaction. *In*, Vol 19, BMC Plant Biology, pp 1-16

Jiang N, Doseff AI, Grotewold E (2016) Flavones: From Biosynthesis to Health Benefits. Plants **5:**27

Johnson AM, Kim H, Ralph J, Mansfield SD (2017) Natural acetylation impacts carbohydrate recovery during deconstruction of Populus trichocarpa wood. Biotechnology for Biofuels **10:** 48

Joshi CP, Chiang VL (1998) Conserved sequence motifs in plant S-adenosyl-L-methionine-dependent methyltransferases. Plant Molecular Biology **37:** 663-674

Jouanin L, Goujon T, de Nadaı V, Martin MT, Mila I, Vallet C, Pollet B, Yoshinaga A, Chabbert B, Petit-Conil M, Lapierre C (2000) Lignification in transgenic poplars with extremely reduced caffeic acid O-methyltransferase activity. Plant Physiology **123:** 1363-1374

Jung W, Yu O, Lau SM, O'Keefe DP, Odell J, Fader G, McGonigle B (2000) Identification and expression of isoflavone synthase, the key enzyme for biosynthesis of isoflavones in legumes. Nature Biotechnology **18:** 208-212

Karlen SD, Zhang C, Peck ML, Smith RA, Padmakshan D, Helmich KE, Free HC, Lee S, Smith BG, Lu F, Sedbrook JC (2016) Monolignol ferulate conjugates are naturally incorporated into plant lignins. Science Advances **2:** 1600393

Keegstra K (2010) Plant cell walls. Plant Physiology **154:** 483-486

Kim BG, Lee Y, Hur HG, Lim Y, Ahn JH (2006a) Flavonoid 3'-*O*-methyltransferase from rice: cDNA cloning, characterization and functional expression. Phytochemistry **67:** 387-394

Kim H, Ralph J (2010) Solution-state 2D NMR of ball-milled plant cell wall gels in DMSO-d(6)/pyridine-d(5). Organic Biomolecular Chemistry **8:** 576-591

Kim BG, Kim DH, Sung SH, Kim DE, Chong Y, Ahn JH (2010a) Two *O*-methyltransferases from *Picea abies*: characterization and molecular basis of different reactivity. Planta **232:** 837-844

Kim JH, Lee SR, Li LH, Park HJ, Park JH, Lee KY, Kim MK, Shin BA, Choi SY (2011) High cleavage efficiency of a 2A peptide derived from porcine teschovirus-1 in human cell lines, zebrafish and mice. PLoS One **6:** e18556

Kim KH, Dutta T, Ralph J, Mansfield SD, Simmons BA, Singh S (2017a) Impact of lignin polymer backbone esters on ionic liquid pretreatment of poplar. Biotechnology for Biofuels **10:** 101

Kim H, Padmakshan D, Li Y, Rencoret J, Hatfield RD, Ralph J (2017b) Characterization and elimination of undesirable protein residues in plant cell wall materials for enhancing lignin analysis by solution-state nuclear magnetic resonance spectroscopy. Biomacromolecules **18:** 4184-4195

Komis G, Šamajová O, Ovečka M, Šamaj J (2018) Cell and Developmental Biology of Plant Mitogen-Activated Protein Kinases. Annual Reviews in Plant Biology **69:** 237-265

Kong CH, Zhao H, Xu XH, Wang P, Gu Y (2007) Activity and allelopathy of soil of flavone o-glycosides from rice. Journal of Agricultural Food Chemistry **55:** 6007-6012

Kong CH, Xu XH, Zhang M, Zhang SZ (2010) Allelochemical tricin in rice hull and its aurone isomer against rice seedling rot disease. Pest Management Science **66:** 1018-1024

Laffont C, Blanchet S, Lapierre C, Brocard L, Ratet P, Crespi M, Mathesius U, Frugier F (2010) The compact root architecture1 gene regulates lignification, flavonoid production, and polar auxin transport in *Medicago truncatula*. Plant Physiology **153:** 1597-1607

Lam KC, Ibrahim RK, Behdad B, Dayanandan S (2007) Structure, function, and evolution of plant *O*-methyltransferases. Genome **50:** 1001-1013

Lam PY, Zhu FY, Chan WL, Liu H, Lo C (2014) Cytochrome P450 93G1 is a flavone synthase II that channels flavanones to the biosynthesis of tricin *O*-Linked conjugates in rice. Plant Physiology **165:** 1315-1327

Lam PY, Liu H, Lo C (2015) Completion of tricin biosynthesis pathway in rice: cytochrome P450 75B4 is a unique chrysoeriol 5'-hydroxylase. Plant Physiology **168:** 1527-1536

Lam PY, Tobimatsu Y, Takeda Y, Suzuki S, Yamamura M, Umezawa T, Lo C (2017) Disrupting flavone synthase II alters lignin and improves biomass digestibility. Plant Physiology **174:** 972-985

Lam PY, Lui ACW, Yamamura M, Wang L, Takeda Y, Suzuki S, Liu H, Zhu FY, Chen MX, Zhang J, Umezawa T, Tobimatsu Y, Lo C (2019a) Recruitment of specific flavonoid B-ring hydroxylases for two independent biosynthesis pathways of flavone-derived metabolites in grasses. New Phytologist **223:** 204-219

Lam PY, Tobimatsu Y, Matsumoto N, Suzuki S, Lan W, Takeda Y, Yamamura M, Sakamoto M, Ralph J, Lo C, Umezawa T (2019b) OsCAldOMT1 is a bifunctional O-methyltransferase involved in the biosynthesis of tricin-lignins in rice cell walls. Science Reports **9:** 11597

Lan W, Lu F, Regner M, Zhu Y, Rencoret J, Ralph SA, Zakai UI, Morreel K, Boerjan W, Ralph J (2015) Tricin, a flavonoid monomer in monocot lignification. Plant Physiology **167:** 1284-1295

Lan W, Rencoret J, Lu F, Karlen SD, Smith BG, Harris PJ, Del Rio JC, Ralph J (2016) Tricin-lignins: occurrence and quantitation of tricin in relation to phylogeny. Plant Journal **88:** 1046-1057

Lapierre C, Pilate G, Pollet B, Mila I, Leplé JC, Jouanin L, Kim H, Ralph J (2004) Signatures of cinnamyl alcohol dehydrogenase deficiency in poplar lignins. Phytochemistry **65:** 313-321

Larson PR (2012) The vascular cambium: development and structure. Springer Science & Business Media

Lepikson-Neto J, Alves AMM, Simões RF, Deckmann AC, Camargo ELO, Salazar MM, Rio MCS, do Nascimento LC, Pereira GAG, Rodrigues JC (2013) Flavonoid supplementation reduces the extractive content and increases the syringyl/guaiacyl ratio in Eucalyptus grandis x Eucalyptus urophylla hybrid trees. BioResources **8:** 1747-1757

Leple JC, Dauwe R, Morreel K, Storme V, Lapierre C, Pollet B, Naumann A, Kang KY, Kim H, Ruel K, Lefebvre A, Joseleau JP, Grima-Pettenati J, De Rycke R, Andersson-Gunneras S, Erban A, Fehrle I, Petit-Conil M, Kopka J, Polle A, Messens E, Sundberg B, Mansfield SD, Ralph J, Pilate G, Boerjan W (2007) Downregulation of cinnamoyl-coenzyme A reductase in poplar: multiple-level phenotyping reveals effects on cell wall polymer metabolism and structure. Plant Cell **19:** 3669-3691

Li L, Zhou Y, Cheng X, Sun J, Marita JM, Ralph J, Chiang VL (2003) Combinatorial modification of multiple lignin traits in trees through multigene cotransformation. Proceedings National Academy of Science USA **100:** 4939-4944

Li X, Bonawitz ND, Weng JK, Chapple C (2010) The growth reduction associated with repressed lignin biosynthesis in *Arabidopsis thaliana* is independent of flavonoids. Plant Cell **22:** 1620-1632

Li M, Pu Y, Yoo CG, Ragauskas AJ (2016) The occurrence of tricin and its derivatives in plants. Green Chemistry **18:** 1439-1454

Lin CY, Eudes A (2020) Strategies for the production of biochemicals in bioenergy crops. Biotechnology for Biofuels **13:** 71

Liu S, Yang C, Wu L, Cai H, Li H, Xu M (2020) The peumiR160a PeARF171/PeARF172 module participates in the adventitious root development of poplar. Plant Biotechnology Journal **18:**457-469

Liu Y, Wang Y, Pei J, Li Y, Sun H (2021) Genome-wide identification and characterization of COMT gene family during the development of blueberry fruit. BMC Plant Biology **21:** 5

Lu F, Ralph J (1999) Detection and determination of p-coumaroylated units in lignins. Journal of Agricultural and Food Chemistry **47:** 1988-1992

Lu F, Ralph J (2002) Preliminary evidence for sinapyl acetate as a lignin monomer in kenaf. Chemical Communications **1:** 90-91

Lu F, Marita JM, Lapierre C, Jouanin L, Morreel K, Boerjan W, Ralph J (2010) Sequencing around 5-hydroxyconiferyl alcohol-derived units in caffeic acid O-methyltransferase-deficient poplar lignins. Plant Physiology **153:** 569-579

Lu F, Karlen SD, Regner M, Kim H, Ralph SA, Sun RC, Kuroda KI, Augustin MA, Mawson R, Sabarez H, Singh T (2015) Naturally p-hydroxybenzoylated lignins in palms. BioEnergy Research **8:** 934-952

Lui AC, Lam PY, Chan KH, Wang L, Tobimatsu Y, Lo C (2020) Convergent recruitment of 5'-hydroxylase activities by CYP75B flavonoid B-ring hydroxylases for tricin biosynthesis in Medicago legumes. New Phytologist **228:** 269-284

Lyczakowski JJ, Wicher KB, Terrett OM, Faria-Blanc N, Yu X, Brown D, Krogh K, Dupree P, Busse-Wicher M (2017) Removal of glucuronic acid from xylan is a strategy to improve the conversion of plant biomass to sugars for bioenergy. Biotechnology for Biofuels **10:** 224

Mahmoud AM, Yang W, Bosland MC (2014) Soy isoflavones and prostate cancer: a review of molecular mechanisms. Journal of Steroid Biochemistry and Molecular Biology **140:** 116-132

Mahon EL, Mansfield SD (2019) Tailor-made trees: engineering lignin for ease of processing and tomorrow's bioeconomy. Current Opinions in Biotechnology **56:** 147-155

Mahon EL, de Vries L, Jang SK, Middar S, Kim H, Unda F, Ralph J, Mansfield SD (2021) Exogenous chalcone synthase expression in developing poplar xylem incorporates naringenin into lignins. Plant Physiology https://doi.org/10.1093/plphys/kiab499

Maloney GS, DiNapoli KT, Muday GK (2014) The anthocyanin reduced tomato mutant demonstrates the role of flavonols in tomato lateral root and root hair development. Plant Physiology **166:** 614-631

Mansfield SD, Mooney C, Saddler JN (1999) Substrate and enzyme characteristics that limit cellulose hydrolysis. Biotechnology Progress **15:** 804-816

Mansfield SD, Kang KY, Chapple C (2012a) Designed for deconstruction–poplar trees altered in cell wall lignification improve the efficacy of bioethanol production. New Phytologist **194:** 91-101

Mansfield SD, Kim H, Lu F, Ralph J (2012b) Whole plant cell wall characterization using solution-state 2D NMR. Nature Protocols **7:** 1579-1589

Marita JM, Ralph J, Lapierre C, Jouanin L, Boerjan W (2001) NMR characterization of lignins from transgenic poplars with suppressed caffeic acid O-methyltransferase activity. Journal of the Chemical Society, Perkin Transactions **1:** 2939-2945

Martens S, Mithofer A (2005) Flavones and flavone synthases. Phytochemistry **66:** 2399-2407

McFarlane HE, Döring A, Persson S (2014) The cell biology of cellulose synthesis. Annual Review of Plant Biology **65:** 69-94

McNeil M, Darvill AG, Fry SC, Albersheim P (1984) Structure and function of the primary cell walls of plants. Annual Review of Biochemistry **53:** 625-663

Meents MJ, Watanabe Y, Samuels AL (2018) The cell biology of secondary cell wall biosynthesis. Annals of Botany **121:** 1107-1125

Mellerowicz EJ, Baucher M, Sundberg B, Boerjan W (2001) Unravelling cell wall formation in the woody dicot stem. Plant Cell Walls **239-274**

Mellerowicz EJ, Gorshkova TA (2012) Tensional stress generation in gelatinous fibres: a review and possible mechanism based on cell-wall structure and composition. Journal of Experimental Botany **63:** 551-565

Meyermans H, Morreel K, Lapierre C, Pollet B, De Bruyn A, Busson R, Herdewijn P, Devreese B, Van Beeumen J, Marita JM, Ralph J (2000) Modifications in lignin and accumulation of phenolic glucosides in poplar xylem upon down-regulation of caffeoyl-coenzyme A O-methyltransferase, an enzyme involved in lignin biosynthesis. Journal of Biological Chemistry **275:** 36899-36909

Mohnen D (2008) Pectin structure and biosynthesis. Current Opinion in Plant Biology **11:** 226-277

Molitor C, Mauracher SG, Pargan S, Mayer RL, Halbwirth H, Rompel A (2015) Latent and active aurone synthase from petals of *C. grandiflora*: a polyphenol oxidase with unique characteristics. Planta **242:** 519-537

Mooney CA, Mansfield SD, Touhy MG, Saddler JN (1998) The effect of initial pore volume and lignin content on the enzymatic hydrolysis of softwoods. Bioresource technology **64:** 113-119

Morreel K, Goeminne G, Storme V, Sterck L, Ralph J, Coppieters W, Breyne P, Steenackers M, Georges M, Messens E, Boerjan W (2006) Genetical metabolomics of flavonoid biosynthesis in Populus: a case study. The Plant Journal **47:** 224-237

Morris H, Brodersen C, Schwarze FW, Jansen S (2016) The parenchyma of secondary xylem and its critical role in tree defense against fungal decay in relation to the CODIT model. Frontiers in Plant Science **7:** 1665

Mottiar Y, Vanholme R, Boerjan W, Ralph J, Mansfield SD (2016) Designer lignins: harnessing the plasticity of lignification. Current Opinion in Biotechnology **37:** 190-200

Muzac I, Wang J, Anzellotti D, Zhang H, Ibrahim RK (2000) Functional expression of an Arabidopsis cDNA clone encoding a flavonol 3'-O-methyltransferase and characterization of the gene product. Archives of Biochemistry and Biophysics **375:** 385-388

Negral J, Pollet B, Lapierre C (1996) Ether-linked ferulic acid amides in natural and wound periderms of potato tuber. Phytochemistry **43:** 1195-1199

Nelson DR, Ming R, Alam M, Schuler MA (2008) Comparison of Cytochrome P450 Genes from Six Plant Genomes. Tropical Plant Biology **1:** 216-235

Nicolescu C, Sandré C, Jouanin L, Chriqui D (1996) Modification de l'expression du métabolisme phénolique chez le Peuplier en relation avec la résistance aux agents pathogènes. Acta Botanica Gallica **143:** 539-546

Nilsson J, Karlberg A, Antti H, Lopez-Vernaza M, Mellerowicz E, Perrot-Rechenmann C, Sandberg G, Bhalerao RP (2008) Dissecting the molecular basis of the regulation of wood formation by auxin in hybrid aspen. Plant Cell **20:** 843-855

Oyarce P, De Meester B, Fonseca F, de Vries L, Goeminne G, Pallidis A, De Rycke R, Tsuji Y, Li Y, Van den Bosch S, Sels B, Ralph J, Vanholme R, Boerjan W (2019) Introducing curcumin biosynthesis in Arabidopsis enhances lignocellulosic biomass processing. Nature Plants **5:** 225-237

Paredez AR, Somerville CR, Ehrhardt DW (2006) Visualization of cellulose synthase demonstrates functional association with microtubules. Science **312:** 1491-1495

Pauly M, Keegstra K (2016) Biosynthesis of the plant cell wall matrix polysaccharide xyloglucan. Annual Review of Plant Biology **67:** 235-259

Pawar PMA, Ratke C, Balasubramanian VK, Chong SL, Gandla ML, Adriasola M, Sparrman T, Hedenström M, Szwaj K, Derba-Maceluch M (2017) Downregulation of RWA genes in hybrid aspen affects xylan acetylation and wood saccharification. New Phytologist **214:** 1491-1505

Peer WA, Bandyopadhyay A, Blakeslee JJ, Makam SN, Chen RJ, Masson PH, Murphy AS (2004) Variation in expression and protein localization of the PIN family of auxin efflux facilitator proteins in flavonoid mutants with altered auxin transport in Arabidopsis thaliana. The Plant Cell **16:** 1898-1911

Peer WA, Murphy AS (2007) Flavonoids and auxin transport: modulators or regulators? Trends in Plant Science **12:** 556-563

Perkins M, Smith RA, Samuels L (2019) The transport of monomers during lignification in plants: Anything goes but how? Current Opinion in Biotechnology **56:** 69-74

Perkins ML, Schuetz M, Unda F, Smith RA, Sibout R, Hoffmann NJ, Wong DCJ, Castellarin SD, Mansfield SD, Samuels L (2020) Dwarfism of high-monolignol Arabidopsis plants is rescued by ectopic LACCASE overexpression. Plant Direct **4:** e00265

Petrussa E, Braidot E, Zancani M, Peresson C, Bertolini A, Patui S, Vianello A (2013) Plant flavonoids biosynthesis, transport and involvement in stress responses. International Journal Molecular Sciences **14:** 14950-14973

Pietarinen SP, Willför SM, Vikström FA, Holmbom BR (2006) Aspen knots, a rich source of flavonoids. Journal of Wood Chemistry and Technology **26:** 245-258

Plett JM, Martin F (2012) Poplar root exudates contain compounds that induce the expression of MiSSP7 in Laccaria bicolor. Plant Signaling & Behavior **7:** 12-15

Ralph J, Hatfield RD, Piquemal J, Yahiaoui N, Pean M, Lapierre C, Boudet AM (1998) NMR characterization of altered lignins extracted from tobacco plants down-regulated for lignification enzymes cinnamyl-alcohol dehydrogenase and cinnamoyl-CoA reductase. Proceedings of the National Academy of Sciences **95:** 12803-12808

Ralph J, Lundquist K, Brunow G, Lu F, Kim H, Schatz PF, Marita JM, Hatfield RD, Ralph SA, Christensen JH, Boerjan W (2004) Lignins: natural polymers from oxidative coupling of 4-hydroxyphenyl-propanoids. Phytochemistry Reviews **3:** 29-60

Ralph J, Landucci LL (2010) NMR of lignins. CRC Press (Taylor & Francis Group)

Ralph J, Lapierre C, Boerjan W (2019) Lignin structure and its engineering. Current Opinions in Biotechnology **56:** 240-249

Rashotte AM, Brady SR, Reed RC, Ante SJ, Muday GK (2000) Basipetal auxin transport is required for gravitropism in roots of *Arabidopsis*. Plant Physiology **122:** 481-490

Rausher MD (2006) The evolution of flavonoids and their genes. Springer, New York, NY,

Reiterer A, Burgert I, Sinn G, Tschegg S (2002) The radial reinforcement of the wood structure and its implication on mechanical and fracture mechanical properties—a comparison between two tree species. Journal of Materials Science **37**

Rencoret J, Ralph J, Marques G, Gutierrez A, Martinez A, del Rio JC (2013) Structural characterization of lignin isolated from coconut (*Cocos nucifera*) coir fibers. Journal of Agricultural Food Chemistry **61:** 2434-2445

Rencoret J, Neiva D, Marques G, Gutiérrez A, Kim H, Gominho J, Pereira H, Ralph J, Del Río JC (2019) Hydroxystilbene glucosides are incorporated into Norway spruce bark lignin. Plant Physiology **180:** 1310-1321

Robinson AR, Mansfield SD (2009) Rapid analysis of poplar lignin monomer composition by a streamlined thioacidolysis procedure and near-infrared reflectance-based prediction modeling. The Plant Journal **58:** 706-714

Ruel K, Berrio-Sierra J, Derikvand MM, Pollet B, Thévenin J, Lapierre C, Jouanin L, Joseleau JP (2009) Impact of CCR1 silencing on the assembly of lignified secondary walls in Arabidopsis thaliana. New Phytol **184:** 99-113

Ryan MD, King AM, Thomas GP (1991) Cleavage of foot-and-mouth disease virus polyprotein is mediated by residues located within a 19 amino acid sequence. Journal of General Virology **72 (Pt 11):** 2727-2732

Saleme MLS, Cesarino I, Vargas L, Kim H, Vanholme R, Goeminne G, Van Acker R, Fonseca FCA, Pallidis A, Voorend W, Junior JN, Padmakshan D, Van Doorsselaere J, Ralph J, Boerjan W (2017) Silencing CAFFEOYL SHIKIMATE ESTERASE Affects Lignification and Improves Saccharification in Poplar. Plant Physiology **175:** 1040-1057

Sanchez P, Nehlin L, Greb T (2012) From thin to thick: major transitions during stem development. Trends Plant Science **17:** 113-121

Scheller HV, Ulvskov P (2010) Hemicellulose. Annual Review of Plant Biology 61: **61:** 263-289

Schilmiller AL, Stout J, Weng JK, Humphreys J, Ruegger MO, Chapple C (2009) Mutations in the cinnamate 4-hydroxylase gene impact metabolism, growth and development in Arabidopsis. Plant J **60:** 771-782

Seitz C, Eder C, Deiml B, Kellner S, Martens S, Forkmann G (2006) Cloning, functional identification and sequence analysis of flavonoid 3′-hydroxylase and flavonoid 3′, 5′-hydroxylase cDNAs reveals independent evolution of flavonoid 3′, 5′-hydroxylase in the Asteraceae family. Plant Molecular Biology Reporter **61:** 365-381

Shi R, Sun YH, Li Q, Heber S, Sederoff R, Chiang VL (2010) Towards a systems approach for lignin biosynthesis in Populus trichocarpa: transcript abundance and specificity of the monolignol biosynthetic genes. Plant and Cell Physiology **51:** 144-163

Shih CH, Chu H, Tang LK, Sakamoto W, Maekawa M, Chu IK, Wang M, Lo C (2008) Functional characterization of key structural genes in rice flavonoid biosynthesis. Planta **228:** 1043-1054

Shooshtarian A, Anderson JA, Armstrong GW, Luckert MK (2018) Growing hybrid poplar in western Canada for use as a biofuel feedstock: A financial analysis of coppice and single-stem management. Biomass and Bioenergy **113:** 45-54

Showalter AM (1993) Structure and function of plant cell wall proteins. The Plant Cell **5:** 9

Shu W, Zhou H, Jiang C, Zhao S, Wang L, Li Q, Yang Z, Groover A, Lu MZ (2019) The auxin receptor TIR 1 homolog (Pag FBL 1) regulates adventitious rooting through interactions with Aux/IAA 28 in Populus. Plant Biotechnology Journal **17:** 338-349

Smith DC (1955) p-Hydroxybenzoate groups in the lignin of aspen (*Populus tremula*). Journal of the Chemical Society 2347-2351

Smith RA, Schuetz M, Roach M, Mansfield SD, Ellis B, Samuels L (2013) Neighboring parenchyma cells contribute to Arabidopsis xylem lignification, while lignification of interfascicular fibers is cell autonomous. Plant Cell **25:** 3988-3999

Smith RA, Gonzales-Vigil E, Karlen SD, Park JY, Lu F, Wilkerson CG, Samuels L, Ralph J, Mansfield SD (2015) Engineering Monolignol p-Coumarate Conjugates into Poplar and Arabidopsis Lignins. Plant Physiology **169:** 2992-3001

Song D, Sun J, Li L (2014) Diverse roles of PtrDUF579 proteins in Populus and PtrDUF579-1 function in vascular cambium proliferation during secondary growth. Plant Molecular Biology **85:** 601-612

Stewart JJ, Akiyama T, Chapple C, Ralph J, Mansfield SD (2009) The effects on lignin structure of overexpression of ferulate 5-hydroxylase in hybrid poplar. Plant Physiology **150:** 621-635

Sundell D, Street NR, Kumar M, Mellerowicz EJ, Kucukoglu M, Johnsson C, Kumar V, Mannapperuma C, Delhomme N, Nilsson O, Tuominen H, Pesquet E, Fischer U, Niittylä T, Sundberg B, Hvidsten TR (2017) AspWood: High-Spatial-Resolution Transcriptome Profiles Reveal Uncharacterized Modularity of Wood Formation in. Plant Cell **29:** 1585-1604

Sykes RW, Gjersing EL, Foutz K, Rottmann WH, Kuhn SA, Foster CE, Ziebell A, Turner GB, Decker SR, Hinchee MA, Davis MF (2015) Down-regulation of p-coumaroyl quinate/shikimate 3'-hydroxylase (C3' H) and cinnamate 4-hydroxylase (C4H) genes in the lignin biosynthetic pathway of Eucalyptus urophylla× E. grandis leads to improved sugar release. Biotechnology for Biofuels **8:** 1-10

Taiz L, Zeiger E (2010) Plant Physiology, Ed 5th edition. Sinauer Associates Inc., Sunderland, Massachusetts U.S.A.

Tanaka Y, Brugliera F (2013) Flower colour and cytochromes P450. Philosophical Transactions of the Royal Society B: Biological Sciences **368**

Terashima N, Ko C, Matsushita Y, Westermark U (2016) Monolignol glucosides as intermediate compounds in lignin biosynthesis. Revisiting the cell wall lignification and new 13C-tracer experiments with *Ginkgo biloba* and *Magnolia liliiflora*. Holzforschung **70:** 801-810

Terrett OM, Dupree P (2019) Covalent interactions between lignin and hemicelluloses in plant secondary cell walls. Current Opinion in Biotechnology **56:** 97-104

Tian Y, Li Q, Rao S, Wang A, Zhang H, Wang L, Li Y, Chen J (2021) Metabolic profiling and gene expression analysis provides insights into flavonoid and anthocyanin metabolism in poplar. Tree Physiology **41:** 1046-1064

Timell TE (1967) Recent progress in the chemistry of wood hemicelluloses. Wood Science and Technology **1:** 45-70

Tsuyama T, Takabe K (2014) Distribution of lignin and lignin precursors in differentiating xylem of Japanese cypress and poplar. Journal of Wood Science **60:** 353-361

Tuskan GA, Difazio S, Jansson S, Bohlmann J, Grigoriev I, Hellsten U, Putnam N, Ralph S, Rombauts S, Salamov A, Schein J (2006) The genome of black cottonwood, *Populus trichocarpa* (Torr. & Gray). Science **313:** 1596-1604

Ullah A, Munir S, Badshah SL, Khan N, Ghani L, Poulson BG, Emwas AH, Jaremko M (2020) Important flavonoids and their role as a therapeutic agent. Molecules **25:** 5243

Van Acker R, Vanholme R, Storme V, Mortimer JC, Dupree P, Boerjan W (2013) Lignin biosynthesis perturbations affect secondary cell wall composition and saccharification yield in Arabidopsis thaliana. Biotechnology for Biofuels **6:** 46

Van Acker R, Leple JC, Aerts D, Storme V, Goeminne G, Ivens B, Legee F, Lapierre C, Piens K, Van Montagu MC, Santoro N, Foster CE, Ralph J, Soetaert W, Pilate G, Boerjan W (2014) Improved saccharification and ethanol yield from field-grown transgenic poplar deficient in cinnamoyl-CoA reductase. Proceedings in the National Academy of Science USA **111:** 845-850

Van Doorsselaere J, Baucher M, Chognot E, Chabbert B, Tollier MT, Petit-Conil M, Leplé JC, Pilate G, Cornu D, Monties B, Van Montagu M (1995) A novel lignin in poplar trees with a reduced caffeic acid/5-hydroxyferulic acid *O*-methyltransferase activity. The Plant Journal **8:** 855-864

Vanholme R, Demedts B, Morreel K, Ralph J, Boerjan W (2010) Lignin biosynthesis and structure. Plant Physiology **153:** 895-905

Vanholme R, De Meester B, Ralph J, Boerjan W (2019) Lignin biosynthesis and its integration into metabolism. Current Opinion in Biotechnology **56:** 230-239

Vermaas JV, Dixon RA, Chen F, Mansfield SD, Boerjan W, Ralph J, Crowley MF, Beckham GT (2019) Passive membrane transport of lignin-related compounds. Proceedings of the National Academy of Sciences **116:** 23117-23123

Voelker SL, Lachenbruch B, Meinzer FC, Jourdes M, Ki C, Patten AM, Davin LB, Lewis NG, Tuskan GA, Gunter L, Decker SR, Selig MJ, Sykes R, Himmel ME, Kitin P, Shevchenko O, Strauss SH (2010) Antisense down-regulation of 4CL expression alters lignification, tree growth, and saccharification potential of field-grown poplar. Plant Physiology **154:** 874-886

Voelker SL, Lachenbruch B, Meinzer FC, Strauss SH (2011) Reduced wood stiffness and strength, and altered stem form, in young antisense 4CL transgenic poplars with reduced lignin contents. New Phytologist **189:** 1096-1109

Voo KS, Whetten RW, O'Malley DM, Sederoff RR (1995) 4-Coumarate: coenzyme A ligase from loblolly pine xylem (isolation, characterization, and complementary DNA cloning). Plant Physiology **108:** 85-97

Wadenback J, von Arnold S, Egertsdotter U, Walter MH, Grima-Pettenati J, Goffner D, Gellerstedt G, Gullion T, Clapham D (2008) Lignin biosynthesis in transgenic Norway spruce plants harboring an antisense construct for cinnamoyl CoA reductase (CCR). Transgenic Res **17:** 379-392

Wagner A, Tobimatsu Y, Phillips L, Flint H, Torr K, Donaldson L, Pears L, Ralph J (2011) CCoAOMT suppression modifies lignin composition in *Pinus radiata*. Plant Journal **67:** 119-129

Waki T, Yoo D, Fujino N, Mameda R, Denessiouk K, Yamashita S, Motohashi R, Akashi T, Aoki T, Ayabe S, Takahashi S, Nakayama T (2016) Identification of protein-protein interactions of isoflavonoid biosynthetic enzymes with 2-hydroxyisoflavanone synthase in soybean (*Glycine max (L.) Merr*.). Biochemical and Biophysical Research Communications **469:** 546-551

Wang JP, Matthews ML, Williams CM, Shi R, Yang C, Tunlaya-Anukit S, Chen H-C, Li Q, Liu J, Lin C-Y (2018) Improving wood properties for wood utilization through multi-omics integration in lignin biosynthesis. Nature Communications **9:** 1-16

Wang JP, Naik PP, Chen HC, Shi R, Lin CY, Liu J, Shuford CM, Li Q, Sun YH, Tunlaya-Anukit S, Williams CM, Muddiman DC, Ducoste JJ, Sederoff RR, Chiang VL (2014) Complete

proteomic-based enzyme reaction and inhibition kinetics reveal how monolignol biosynthetic enzyme families affect metabolic flux and lignin in *Populus trichocarpa*. Plant Cell **26:** 894-914

Watanabe Y, Meents MJ, McDonnell LM, Barkwill S, Sampathkumar A, Cartwright HN, Demura T, Ehrhardt DW, Samuels AL, Mansfield SD (2015) Visualization of cellulose synthases in *Arabidopsis* secondary cell walls. Science **350:** 198-203

Weng JK, Chapple C (2010) The origin and evolution of lignin biosynthesis. New Phytologist **187:** 273-285

Wilkerson CG, Mansfield SD, Lu F, Withers S, Park JY, Karlen SD, Gonzales-Vigil E, Padmakshan D, Unda F, Rencoret J, Ralph J (2014) Monolignol ferulate transferase introduces chemically labile linkages into the lignin backbone. Science **344:** 90-93

Willats WG, McCartney L, Mackie W, Knox JP (2001) Pectin: cell biology and prospects for functional analysis. Plant Molecular Biology **47:** 9-27

Williams CA, Grayer RJ (2004) Anthocyanins and other flavonoids. Natural Product Reports **21:** 539-573

Winkel BS (2006) The biosynthesis of flavonoids. Springer, New York, NY,

Winkel-Shirley BS (2001) It Takes a Garden: How Work on Diverse Plant Species Has Contributed to an Understanding of Flavonoid Metabolism. Plant Physiology **127:** 1399-1404

Winter, Vinegar B, Ammar R, Nahal H, Wilson GV, Provart N (2007) An 'Electronic Fluorescent Pictograph' Browser for Exploring and Analyzing Large-Scale Biological Data Sets. Plos One, **8:** 718

Xiao Y, Wen J, Meng R, Meng Y, Zhou Q, Nie ZL (2021) The expansion and diversity of the CYP75 gene family in Vitaceae. PeerJ **9:** e12174

Xu C, Shen Y, He F, Fu X, Yu H, Lu W, Li Y, Li C, Fan D, Wang HC, Luo K (2019) Auxin-mediated Aux/IAA-ARF-HB signaling cascade regulates secondary xylem development in *Populus*. New Phytologist **222**

Xue J, Luo D, Xu D, Zeng M, Cui X, Li L, Huang H (2015) CCR1, an enzyme required for lignin biosynthesis in Arabidopsis, mediates cell proliferation exit for leaf development. Plant Journal **83:** 375-387

Y. W, J. MM, M. ML (2015) Visualization of cellulose synthases in Arabidopsis secondary cell walls. Science **350:** 198–203

Yahyaa M, Ali S, Davidovich-Rikanati R, Ibdah M, Shachtier A, Eyal Y, Lewinsohn E, Ibdah M (2017) Characterization of three chalcone synthase-like genes from apple (Malus x domestica Borkh.). Phytochemistry **140:** 125-133

Yemshanov D, McKenney D (2008) Fast-growing poplar plantations as a bioenergy supply source for Canada. Biomass and Bioenergy **32:** 185-197

Yi Chou E, Schuetz M, Hoffmann N, Watanabe Y, Sibout R, Samuels AL (2018) Distribution, mobility, and anchoring of lignin-related oxidative enzymes in Arabidopsis secondary cell walls. Journal of Experimental Botany **69:** 1849-1859

Yin R, Han K, Heller W, Albert A, Dobrev PI, Zažímalová E, Schäffner AR (2014) Kaempferol 3-O-rhamnoside-7-O-rhamnoside is an endogenous flavonol inhibitor of polar auxin transport in Arabidopsis shoots. New Phytologist **201:** 466-475

Yonekura-Sakakibara K, Higashi Y, Nakabayashi R (2019) The origin and evolution of plant flavonoid metabolism. Frontiers in Plant Science **10**

Yu M, Liu K, Liu S, Chen H, Zhou L, Liu Y (2017) Effect of exogenous IAA on tension wood formation by facilitating polar auxin transport and cellulose biosynthesis in hybrid poplar (Populus deltoids× Populus nigra) wood. Holzforschung **41:** 179-188

Zavala K, Opazo JC (2015) Lineage-Specific Expansion of the Chalcone Synthase Gene Family in Rosids. PLoS One **10:** e0133400

Zhang T, Liu C, Huang X, Zhang H, Yuan Z (2019) Land-plant phylogenomic and pomegranate transcriptomic analyses reveal an evolutionary scenario of CYP75 genes subsequent to whole genome duplications. Journal of Plant Biology **62:** 48-60

Zhang X, Huang X, Li Y, Tao F, Zhao Q, Li W (2021) Polar auxin transport may be responsive to specific features of flavonoid structure. Phytochemistry **185:** 112702

Zhao J, Dixon RA (2010) The 'ins' and 'outs' of flavonoid transport. Trends in Plant Science **15:** 72-80

Zhao J (2015) Flavonoid transport mechanisms: how to go, and with whom. Trends Plant Science **20:** 576-585

Zhou JM, Gold ND, Martin VJ, Wollenweber E, Ibrahim RK (2006) Sequential *O*-methylation of tricetin by a single gene product in wheat. Biochimica et Biophysica Acta **1760:** 1115-1124

Zhou JM, Lee E, Kanapathy-Sinnaiaha F, Park Y, Kornblatt JA, Lim Y, Ibrahim RK (2010) Structure-function relationships of wheat flavone *O*-methyltransferase: Homology modeling and site-directed mutagenesis. BMC Plant Biol **10:** 156

Zhou S, Runge T, Karlen SD, Ralph J, Gonzales-Vigil E, Mansfield SD (2017) Chemical Pulping Advantages of Zip-lignin Hybrid Poplar. ChemSusChem **10:** 3565-3573